Geological and Petrological Studies of the Mikabu Greenstones in Eastern Shikoku, Southwest Japan*

By

Kenji TAKEDA

With 10 Tables, 27 Text-figures and 2 Plates

(Received January 31, 1980)

ABSTRACT: This paper presents geological and petrological studies on the Mikabu greenstones and their associated rocks in three areas in eastern Shikoku, i.e., Kamiyama (Myozai-gun, Tokushima Pref.), Higashiiya (Miyoshi-gun, Tokushima Pref.) — Toyonaga (Otoyo-cho, Nagaoka-gun, Kochi Pref.) and and Jizoji (Tosa-cho, Tosa-gun, Kochi Pref.) areas. An emphasis is placed on the analysis of geological structures of the Mikabu belt and its relation to the Sambagawa belt in the north and to the Chichibu belt in the south. Petrological and petrochemical characteristics of the Mikabu greenstones are analyzed and examined in order to compare them with those of typical ophiolites and with those of similar rocks of various origins. The major results are listed below.

1) The Mikabu belt is a large-scale nappe (Mikabu nappe) which is covered by the sedimentary sequences of the Chichibu belt and overlies the Sambagawa crystalline schists across a thrust. The Mikabu nappe appears to have been thrust over the Sambagawa belt during the Late Triassic.

2) Folding in a large scale occurred in two distinct stages in the Mikabu belt, and they correspond to the Nagahama-Ozu phase and the Hijikawa phase (the Latest Jurassic or the Early Cretaceous) of deformation in the Sambagawa belt.

3) The Mikabu greenstones consist of pillow lava — hyalocalastite sequence interbedded with thin layers of sediments (chert, pelite and limestone), diabase dikes and gabbro sills intruded into the volcanic sequence, and peridotite-gabbro complexes. The peridotite-gabbro complexes occur as small lenses (less than about 500 m in major axis) mostly aligned in rows parallel to the thrusts within the Mikabu belt, and they seem to have been taken tectonically into the Mikabu belt in a solid state nearly contemporaneously with the movement of the Mikabu nappe. The Mikabu greenstones do not show the complete sequence of typical ophiolites.

4) Petrochemical analysis of the volcanic rocks reveals that picrite-basalts, tholeiitic basalts and alkali basalts coexist within the Mikabu greenstones. This is in marked contrast with typical ophiolites which consist of abyssal tholeiites. The origin of the Mikabu greenstones can not be explained as being derived from a single magma.

5) The tholeiitic basalts in the Mikabu greenstones are similar to abyssal tholeiites which have been depleted in incompatible elements. But the Mikabu tholeiites are poorer in Al_2O_3 than are the abyssal tholeiites, and in this respect they are similar to oceanic-island tholeiites.

6) Based mainly on the petrochemical data of the Mikabu tholeiites combined with geological data on the Mikabu belt and its surrounding areas, it is argued that the Mikabu greenstones probably formed during the Early Pennsylvanian or slightly before in a marginal basin. This conclusion is still somewhat speculative and complete understanding of the origin of the Mikabu greenstones must await future studies.

CONTENTS

* Doctoral thesis (Science) presented to the Hiroshima University in 1980

I. INTRODUCTION

The Mikabu greenstones, which consist of mafic to ultramafic rocks associated with chert, pelite and limestone, are an ophiolite suite in the Late-Paleozoic to Early-Mesozoic eugeosynclinal sequence [=Honshu (Chichibu) geosyncline] of Japan. As shown in Fig. 1, the Mikabu greenstones are distributed in a narrow belt between the Sambagawa belt and the Chichibu belt which both belong to the terrane of glaucophanitic metamorphism in Late Mesozoic age. The narrow belt has been called the Mikabu belt.

The origin of the Mikabu greenstones has long been a source of controversies and discussions among Japanese geologists for nearly a century. The Mikabu greenstones had first been geologically studied by KOTO (1888) in the Kanto mountains. He pointed out that the Mikabu greenstones consist of tuff, gabbro, diorite and serpentinite and represent a specified stratigraphic unit that unconformably overlies the crystalline schists of the Sambagawa belt and unconformably underlies weakly metamorphosed rocks of the Chichibu belt. Since then, there have been numerous disputes on mutual relationships between these three rock units from viewpoints of stratigraphy, structure, igneous activity and metamorphism.

KOJIMA (1950) claimed that the Mikabu greenstones are intrusives in a zone of intensive disturbance (the Mikabu tectonic zone) developing along the boundary between the Sambagawa belt and the Chichibu belt. While, SEKI (1958) interpreted that the Mikabu greenstones are a formation conformably intercalated between the rocks of the Sambagawa and the Chichibu belts and originated from extrusion and differentiation of basaltic magma in geosynclinal environments. After SEKI (1958), analogous interpretations on them have been given by SUZUKI (1964a, 1967), UCHIDA (1967), IWASAKI (1969) and NAKAMURA (1971). SUZUKI and his coworkers (SUZUKI et al., 1971, 1972; SUZUKI, 1977) have recognized ophiolite-like character of the Mikabu greenstones (ophiolite stratiggraphy), but they were impressed by autochthonous nature of the ophiolite. They proposed a model that lavas were extruded along fissures of a geanticlinal ridge, gabbro was later intruded within the volcanic sequence and ultramafic rocks formed in a magma chamber were brought up to the level beneath the volcanic sequence in a solid state or crystal-mush state.

However, an interpretation that the Mikabu greenstones represent the Permian oceanic crust juxtaposed along the continental margin during a period of active lithospheric convergence was given by ERNST (1972). Later IWASAKI (1979) postulated the oceanic crustal origin of the Mikabu greenstones.

On the other hand, a rapid accumulation of petrochemical data during the last decade has made it possible to infer the origin and tectonic setting of the Mikabu greenstones. It has been found that a large chemical diversity exists in the Mikabu greenstones and that picritic, tholeiitic and alkali basalts coexist in the Mikabu belt (UCHIDA, 1967; HASHIMOTO et al., 1970; NAKAMURA, 1971; SUZUKI et al., 1971. 1972; WATANABE et al., 1978). SUGISAKI et al. (1972) found a depleted characteristic of incompatible elements in the Mikabu tholeiitic basalts and interpreted that the Mikabu greenstones were erupted

along the major axial zone of a rift system such as the present-day Red Sea. While, MIYASHIRO (1975) precluded the possibility of mid-oceanic ridge, marginal basin or island arc origin of the Mikabu greenstones, because tholeiitic basalts and alkali basalts coexist in the Mikabu greenstones and furthermore the tholeiitic basalts are desimilar in their chemistry to abyssal tholeiites.

Thus, despite wealth of geological, petrological and petrochemical data, the origin and tectonic setting of the Mikabu greenstones are still in the realm of speculation. In the author's opinion, this is mainly due to (1) lack of detailed geological mapping and (2) the lack of integrated studies based on geological evidences and petrological and petrochemical data. Previous petrological and petrochemical studies have been performed for their own sake and they rarely have been combined with geological data to infer the origin of the Mikabu greenstones. Thus the interpretations of the petrological and petrochemical data have never revealed the tectonic setting of the Mikabu greenstones clearly.

In view of this situation, the author has carried out geological, petrological and petrochemical studies on the Mikabu greenstones in three areas (Kamiyama, Higashiiya-Toyonaga and Jizoji) in eastern Shikoku during the past seven years. These areas were chosen, because the Mikabu greenstones are well exposed there and also the Sambagawa, Mikabu and Chichibu belts are aligned in sequence so that their relations should be understood clearly there. This paper describes and discusses separately the geological structure, occurrences and petrography, whole-rock and mineral chemistry of the Mikabu greenstones, the relations between the Mikabu greenstones and the Sambagawa and the Chichibu belts. Then all of these data are integrated to infer the origin of the Mikabu greenstones.

This paper is a summary of the Ph. D. thesis of the Hiroshima University. The original thesis is deposited in the same university.

Acknowledgements: The author wishes to express his sincere thanks to Emeritus Prof. G. KOJIMA of the Hiroshima University for his valuable suggestion. He also gratefully acknowledges Prof. I. HARA of the same university for his continuing guidance and discussions throughout the course of this work and for critical reading of the manuscript. He is also indebted to Prof. K. HIDE of the same university for his instructive suggestion. Thanks are also due to Prof. A. HASE, Prof. S. KAKITANI, Prof. H. YOSHIDA, Dr. M. SUZUKI and Dr. T. SHIMAMOTO of the same university for their helpful advice and encouragement. The author is also indebted to Dr. T. SHIBATA of the Okayama University for his criticism and helpful advice. He is also grateful to Mr. A. MINAMI of the Hiroshima University for his kind help with techniques in the laboratory and microprobe analysis of some minerals, and to Dr. T. SHIOTA of the Tokushima University and to Mr. E. TSUKUDA of the Geological Survey of Japan for their discussions and capable assistance in the field. He is also due to Mr. H. TAKAHASHI and Mr. A. MAGAI for preparing thin sections. He would like to thank to Miss. K. YAMANAKA, Mr. T. IMAOKA and Mr. R. TOMINAGA for their kind assistances during the preparation of the manuscript.

II. GEOLOGY

A. GEOLOGICAL SITUATION

The Mikabu greenstones are better exposed in Shikoku than anywhere else (Fig. 1).

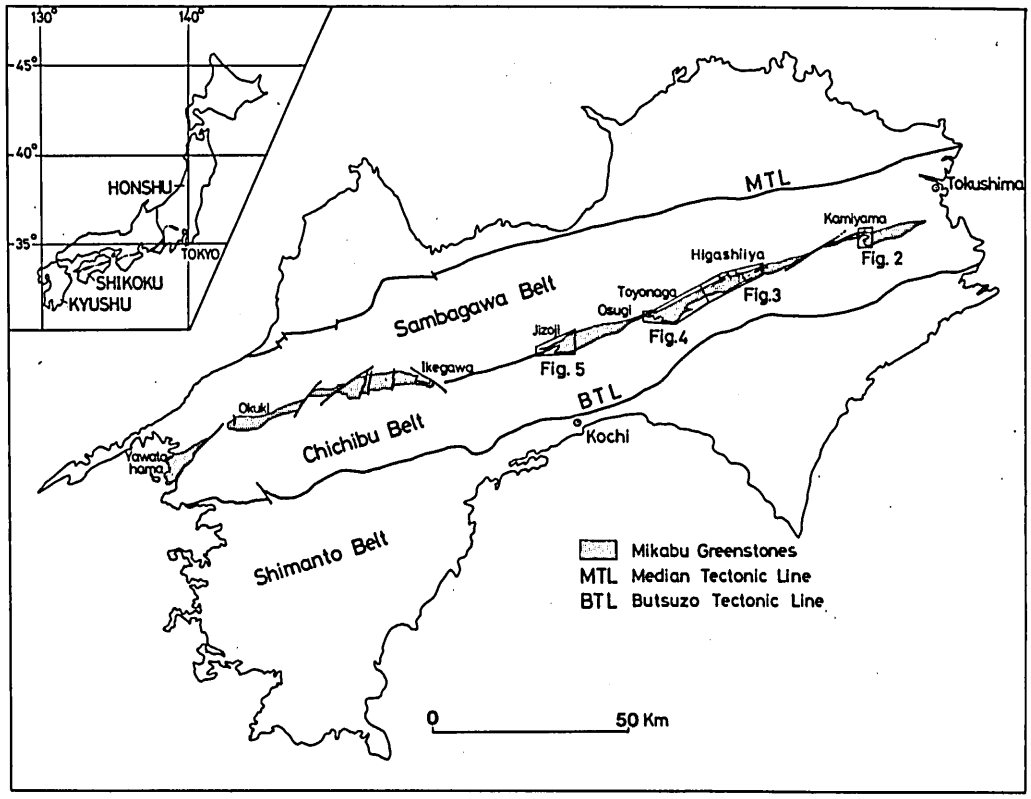

FIG. 1. Distribution map of the Mikabu greenstones in Shikoku. Outlined areas are shown in Figs. 2, 3, 4 and 5. Inset: index map (the Mikabu belt shown as heavy line).

They extends with strike of ENE–WSW and width of 1 to 5 km. In Shikoku develop crystalline schists of the Sambagawa belt on the north of the Mikabu greenstones. Recent discovery of conodont fossils from calcareous schists placed immediately on the north of the Mikabu greenstones indicated that some of original rocks of the Sambagawa crystalline schists are of Middle to Late Triassic age (MATSUDA, 1978; SUYARI et al., 1979, 1980).

The Chichibu belt is situated just on the south of the Mikabu greenstones. The rock sequence of the Chichibu belt, immediately south of the Mikabu greenstones in eastern Shikoku, is referred to the Kenzan Group (HIRAYAMA et al., 1956). Its corresponding rock sequence in central Shikoku is named the Kamiyakawa Formation (SAWAMURA et al., 1961). The rocks of these group and formation are of Late Carboniferous to Late Triassic age (SUYARI et al., 1979, 1980). These, as well as the Mikabu greenstones, suffered the Sambagawa metamorphism of pumpellyite-actinolite facies to glaucophane schist facies (IWASAKI, 1963; BANNO, 1964; ERNST et al., 1970; NAKAJIMA et al., 1977).

The Mikabu belt in Shikoku is divided into two segments, eastern segment and western segment. The eastern segment extends from Sanagochi to Jizoji over a distance of about 80 km. Three areas in the eastern segment, Kamiyama, Higashiiya-Toyonaga and Jizoji (Fig. 1), have been investigated in detail by the present author. The geological

maps of the three areas are shown in Figs. 2, 3, 4 and 5.

B. Geological Structure

The Mikabu greenstones and their surrounding rocks have been intensely folded in a similar fashion. In Fig. 6 are summarized schematically the major folds of the Mikabu greenstones in the Kamiyama, Higashiiya-Toyonaga and Jizoji areas (Takeda et al., 1977).

1. Kamiyama area

Until now geology of the Kamiyama area has been investigated by many workers (Hirayama et al., 1956; Kenzan Research Group, 1963; Iwasaki, 1969, 1979; Suyari et al., 1969; Kaji et al., 1973; Ogawa, 1974). However, geological structure of the Mikabu greenstones has been interpreted differently among these workers.

On the north the Mikabu greenstones are in fault contact with crystalline schists of the Sambagawa belt, as already pointed out by many geologists; i.e., the fault is a high-angle fault (Fig. 2). The bedding schistosity of the crystalline schists, which is nearly parallel to original bedding plane, trends ENE–WSW and dips to the north at a moderate angle.

The structure exhibited by the Mikabu greenstones is more complicated than that hitherto considered. The Mikabu greenstones form an upright antiform in the northern part and a synform with axial surface dipping to the south in the southern part (Fig. 6A). The two folds run approximately parallel each other with trend of ENE–WSW. It should be noted that the rock sequence of the Kenzan Group is also participated in the folding of the Mikabu greenstones.

A steeply north-dipping strike fault with trend of ENE–WSW develops near the axial part of the antiform. In the west of Okubo, the fault marks the boundary between the Mikabu greenstones and the rock sequence of the Kenzan Group. The Mikabu greenstones north of the fault, which might have constituted the northern limb of the antiform, dip to the north at a moderate angle.

The synformally folded Mikabu greenstones are distributed in a rather irregular manner; i.e., they protrude toward the southwest. When the author started mapping of this area, there had been a divergence in opinions on the structural and stratigraphical relations between the synfomally folded Mikabu greenstones and the rock sequence of the Kenzan Group (Suyari et al., 1969; Kaji et al., 1973; Ogawa, 1974). The author's mapping shows no sign of gradual transition of lithofacies between the both rock groups. The boundary between the two is sharp and this suggests that they are not of contemporaneous facies. Moreover, marked difference in pertological features between the volcanic rocks of the Mikabu greenstones and those of the Kenzan Group, as will be described in the following chapter, supports such a view. In addition to these data, distribution pattern of each lithofacies of the rock sequence of the Kenzan Group leads to a suggestion that the synformally folded Mikabu greenstones lie in fault contact with the rock sequence of the Kenzan Group as shown in Fig. 2.

Therefore, it is conceivable that the synformally folded Mikabu greenstones apparently overlie the rock sequence of the Kenzan Group with a thrust fault. The fact that the Mikabu greenstones and the rock sequence of the Kenzan Group consist of a common

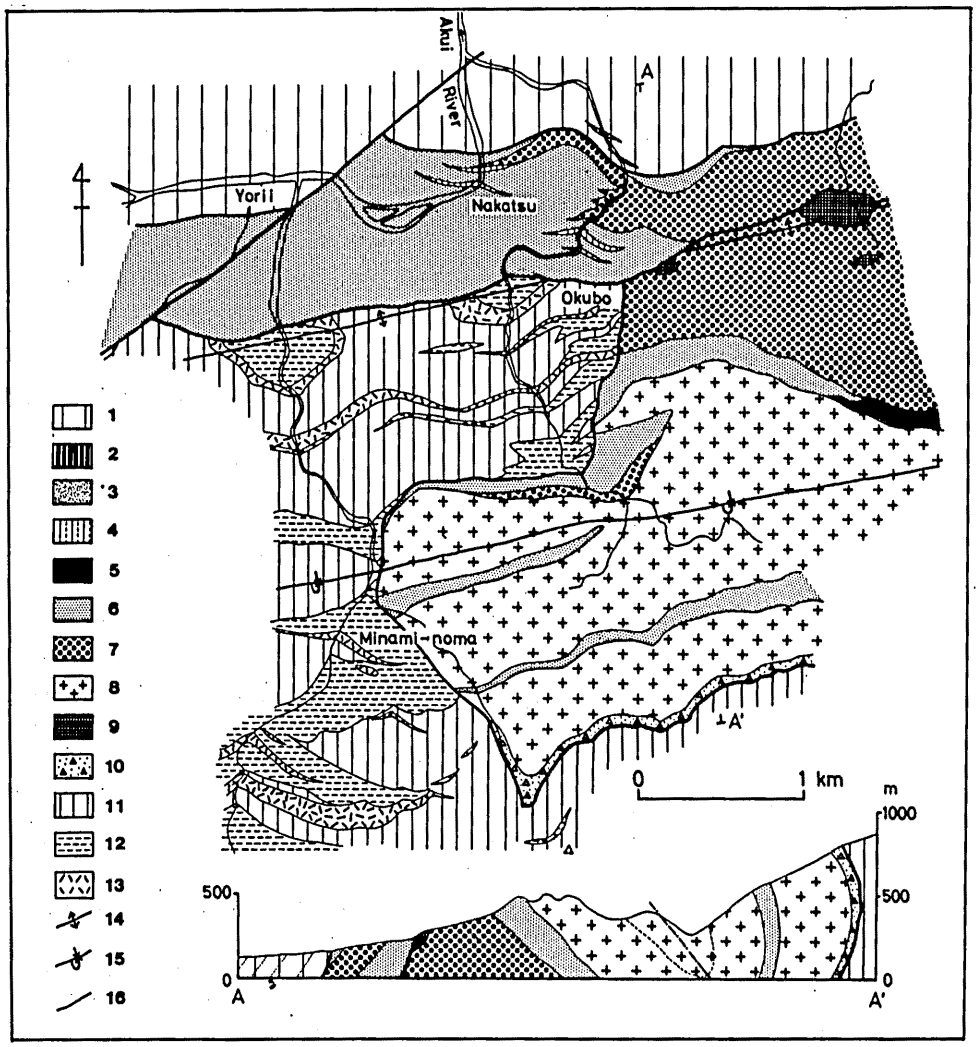

FIG. 2. Geological map of the Kamiyama area. Key to symbols used is as follows.
Sambagawa crystalline schists: 1. pelitic schist, 2. siliceous schist, 3. basic schist.
Mikabu greenstones: 4. pelite, 5. tuffaceous pelite, 6. hyaloclastic sandstone and siltstone with diabase dike, 7. hyaloclastic breccia and pillow lava and diabase dike, 8. gabbro, 9. peridotite-gabbro complex.
Kenzan Group (Chichibu belt): 10. basaltic tuff with ophiolitic breccia, pelite and chert, 11. chert, 12. pelite, 13. basaltic rocks (tuff and lava) and gabbro sheet. 14. antiform, 15. synform with "Vergenz" to the south, 16. fault.

synform indicates that the formation of the thrust fault was prior to the regional folding.

2. Higashiiya-Toyonaga area

As a whole, the Mikabu greenstones in the Higashiiya area show isoclinal structure

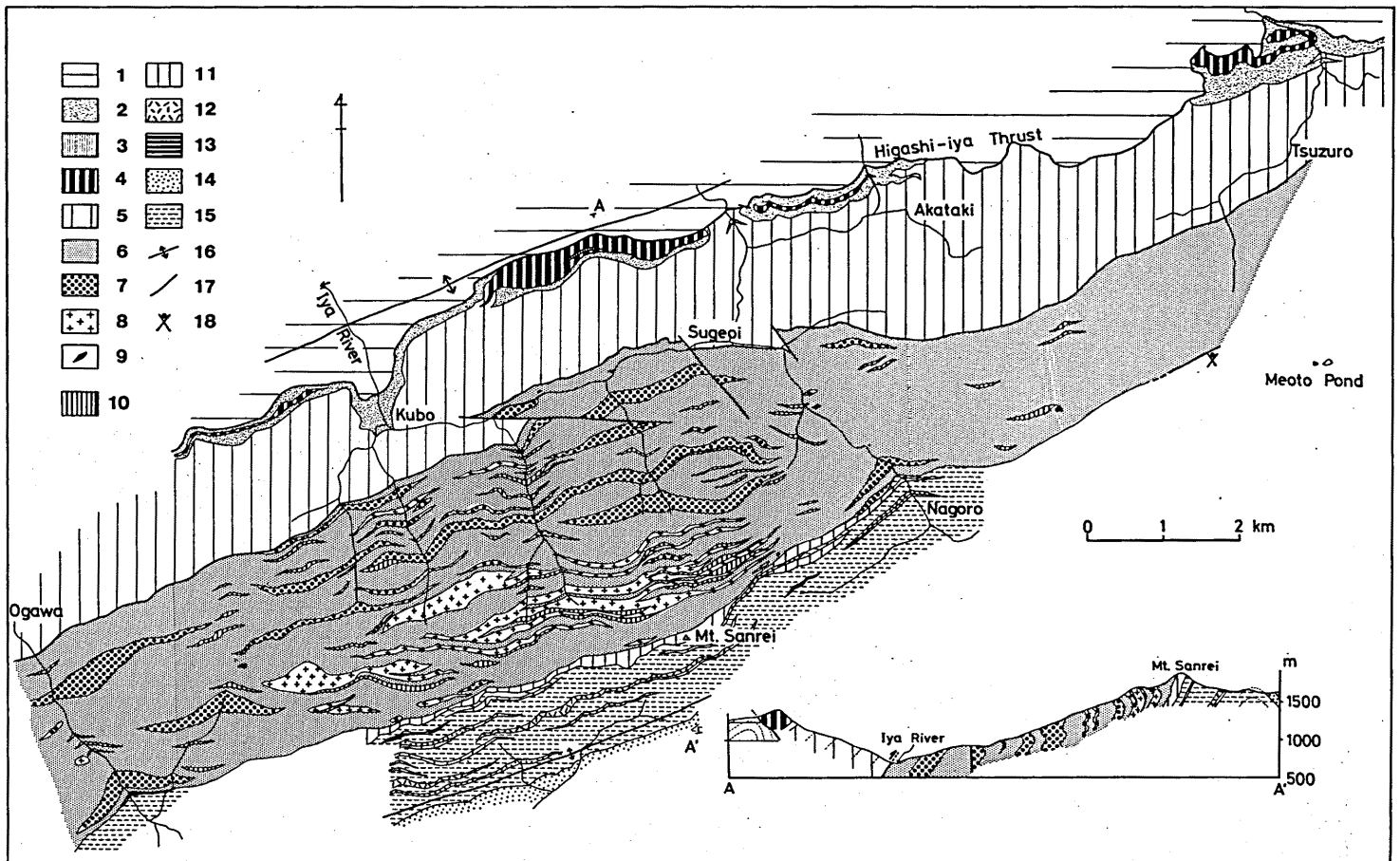

FIG. 3. Geological map of the Higashiiya area. Key to symbols used is as follows.

Sambagawa crystalline schists: 1. mainly pelitic schist, 2–4. Kubo Formation; 2. hyaloclastite with blocks of gabbro and serpentinite, 3. calcareous schist, 4. siliceous schist, 5. Sugeoi Formation; pelitic schist.

Mikabu greenstones: 6. hyaloclastic sandstone, siltstone and tuff with massive lava and diabase dike, 7. hyaloclastic breccia and volcanic breccia with pillow lava and diabase dike, 8. gabbro, 9. serpentinite and peridotite, 10. chert.

Kenzan Group (Chichibu belt): 11. chert, 12. basaltic tuff, 13. limestone, 14. greywacke, 15. pelite. 16. antiform, 17. fault, 18. fossil locality after SUYARI et al. (1979).

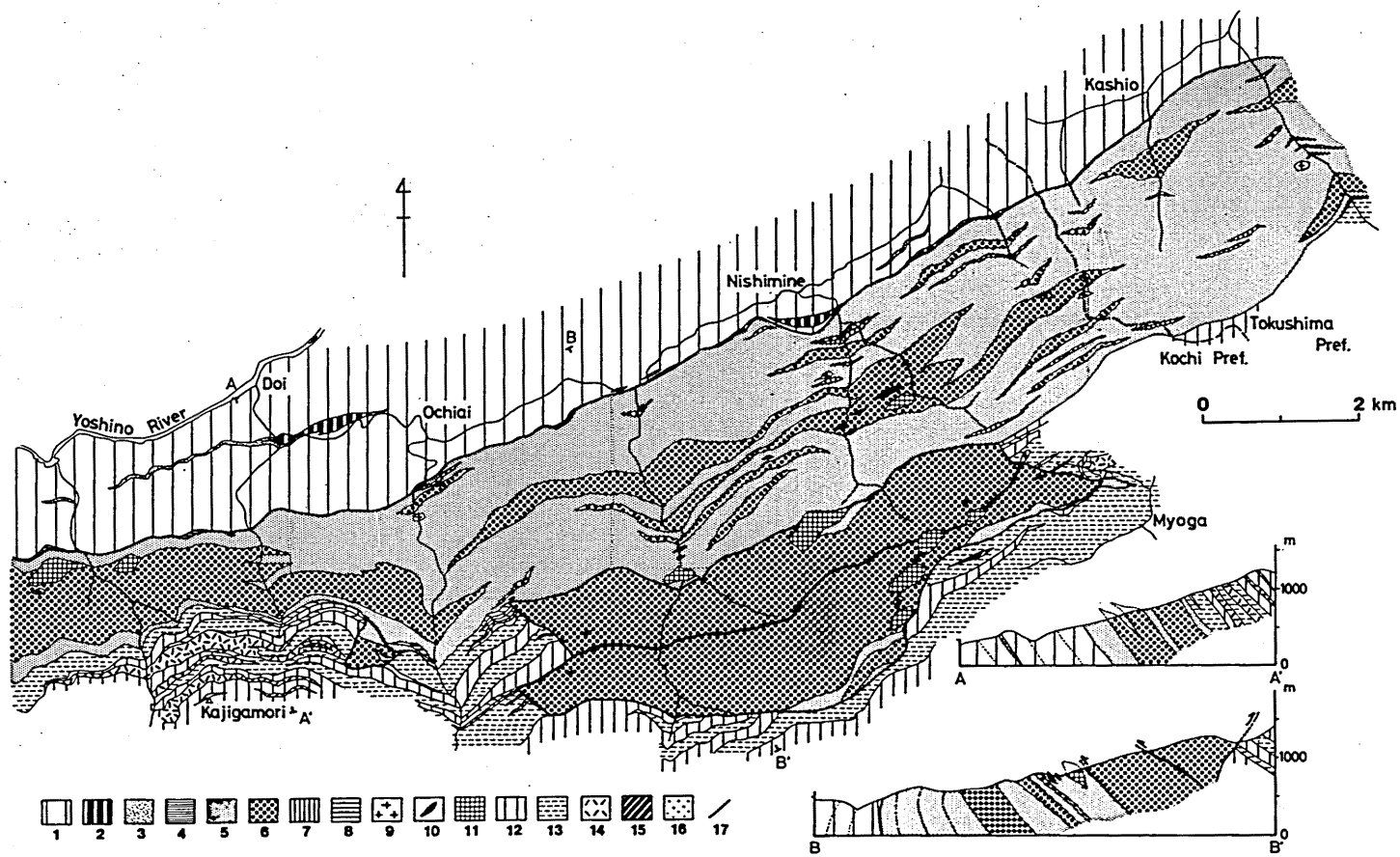

FIG. 4. Geological map of the Toyonaga area. Key to symbols used is as follows.

Sambagawa crystalline schists: 1. pelitic schist, 2. siliceous schist, 3. basic schist, 4. calcareous schist.
Mikabu greenstones: 5. hyaloclastic sandstone, siltstone with massive lava and diabase dike, 6. hyaloclastic breccia and pillow lava with diabase dike, 7. chert, 8. limestone, 9. gabbro, 10. serpentinite, peridotite and hornblendite, 11. peridotite-gabbro complex.
Kamiyakawa Formation (Chichibu belt): 12. chert, 13. pelite, 14. basaltic tuff, 15. limestone, 16. greywacke. 17. fault.

dipping to the north at a moderate angle (KOJIMA and MITSUNO, 1966). Nevertheless, the internal structure is rather complicated. This is ascribed to the development of a number of recumbent folds with dominant wavelength of 150 to 200 m and gently north-dipping axial surface (see geological profile of Fig. 3). To the south of the Mikabu greenstones, rock sequence of the Kenzan Group makes up an antiform whose fold axis is situated about 1 km south of the southern margin of the Mikabu greenstones, running ENE–WSW, apparently underlying the Mikabu greenstones. The crystalline schists of the Sambagawa belt dip to the north as a whole and overlie the Mikabu greenstones.

While, the Mikabu greenstones in the Toyonaga area are underlain by the crystalline schists of the Sambagawa belt and are overlain by the rock sequence of the Kamiyakawa Formation, all of which showing general strike of ENE–WSW and dip to the south at moderate angles as a whole (Fig. 4). The order of superposition of these rock units in this area is opposite to that of those in the Higashiiya area. In the area situated between the Higashiiya and Toyonaga areas they have almost vertical dip. This structural change along the strike has been interpreted by TAKEDA et al. (1977) as representing a large-scale recumbent fold opened toward the south with gently north-dipping axial surface and ENE-plunging axis at a low angle (ca. 10°), judging from the predominant pattern of minor-folds which were probably originated in relation with the formation of major structure (Fig. 6B). Probably the upper and lower limbs of the recumbent fold expose at the Higashiiya and Toyonaga areas, respectively.

In the southern portion between Ochiai and Nishimine of the Toyonaga area, the Mikabu greenstones become thicker compared to those in the eastern and western extensions. Careful mapping of this portion revealed that this thickening resulted from tectonic stacking of the Mikabu greenstones, where three thrust sheets comprise the Mikabu greenstones. The internal bedding of the thrust sheets is nearly parallel to the bedding of the surrounding rock sequence of the Chichibu belt. The formation of thrust sheets was prior to regional folding, because they have been folded with the surrounding rocks in a similar fashion.

A thrust fault dipping to the north at low to middle angles develops at the contact between the Mikabu greenstones and the crystalline schists of the Sambagawa belt in the Higashiiya area. Near the contact, the trend of bedding schistosity of both the Mikabu greenstones and the crystalline schists strikes parallel to the contact. A thin imbricated zone up to a few meters in width is found along the thrust fault. The thrust fault extends westward, changing its inclination from the north-dipping, through vertical, to the southerly dip and can be traced until the Toyonaga area. The thrust plane is in harmony with the form of the recumbent fold described in the above.

3. Jizoji area

A distinct high-angle fault, termed the Kamiyakawa-Ikegawa tectonic line (KOJIMA et al., 1956), runs through the central part of the mapped area (Fig. 5). Rocks along the tectonic line are remarkably sheared with width of several tens of meters. Numerous dikes of quartz-porphry occur along the fault; the intrusion is considered to be of the Miocene (ISHII et al., 1957).

SUZUKI (1964b, 1965) showed that the Mikabu greenstones constitute an anticline and its inliers are exposed from Jizoji to Higashi-ishihara of the central part of the mapped area. Detailed mapping by the present author, however, shows that the Mikabu green-

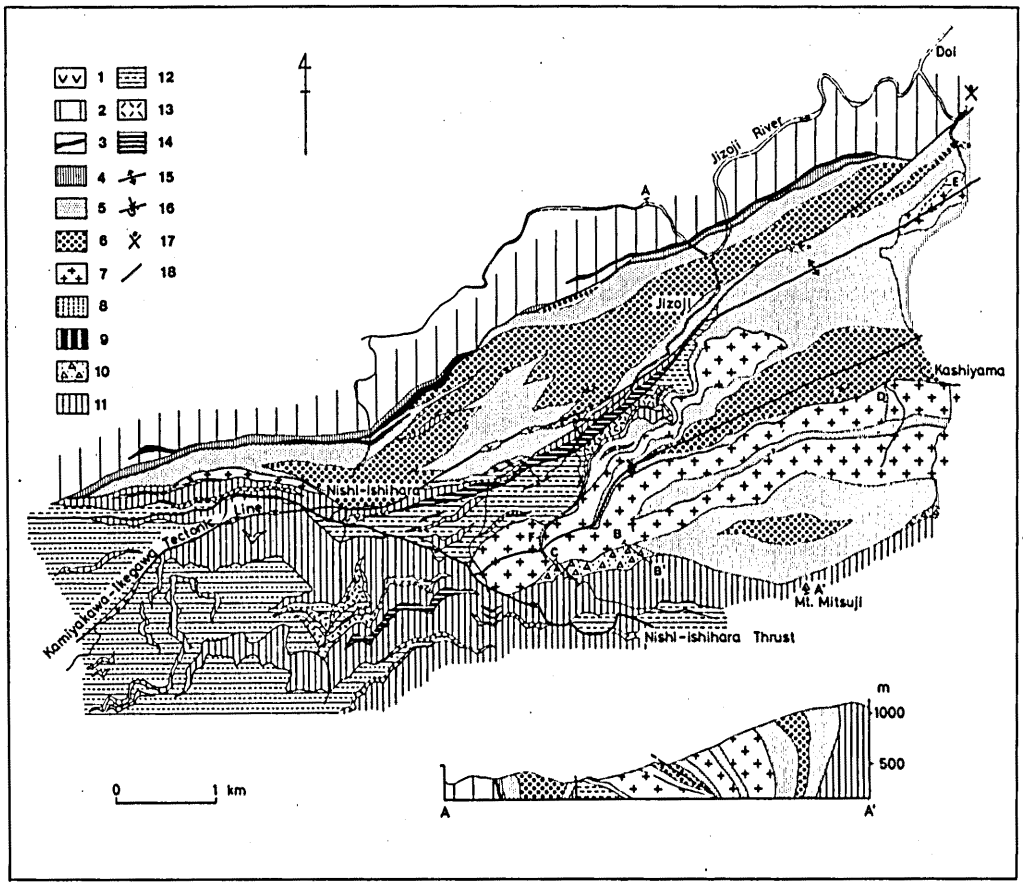

FIG. 5. Geological map of the Jizoji area. Key to symbols used is as follows.

1. Quartz porphyry (Miocene).

Sambagawa crystalline schists: 2. pelitic schist, 3. calcareous schist, 4. siliceous schist.

Mikabu greenstones: 5. hyaloclastic sandstone and siltstone with taffaceous pelite and diabase dike, 6. hyaloclastic breccia with pillow lava and diabase dike, 7. gabbro, 8. pelite, 9. chert.

Kamiyakawa Formation (Chichibu belt): 10. ophiolitic breccia and gabbro breccia, 11. chert, 12. pelite, 13. basaltic tuff, 14. limestone. 15. antiform, 16. synform with "Vergenz" to the south. 17. fossil locality after SUYARI et al. (1979), 18. fault.

Locations of stratigraphic columns B–B′ and C–C′ (Fig. 9) and gabbro sill sections investigated, Kashiyama (D), Aikawa (E) and Higashi-ishihara (F), are marked.

stones constitute two parallel ENE–WSW trending folds, an upright antiform in the north and a tight synform with gently south-dipping axial surface in the south (Fig. 6C). The axial part of the antiform is disturbed by the Kamiyakawa-Ikegawa tectonic line. The Mikabu greenstones extending from Jizoji to Nishi-ishihara constitute the northern limb of the antiform. Both the Mikabu greenstones comprising the northern limb and the crystalline schists of the Sambagawa belt dip to the north at moderate to high angles in general. They are in contact with nearly planer boundaries and the contact seems to be

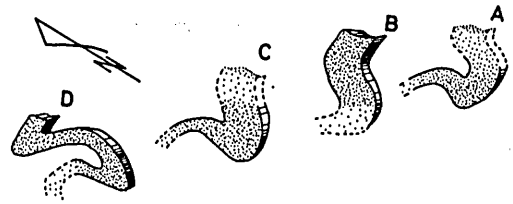

FIG. 6. Patterns of major folds of the Mikabu greenstones in the Kamiyama (A), Higashiiya-Toyonaga (B), Jizoji (C) and Ikegawa (D) areas (after TAKEDA et al., 1977).

in fault contact. Near the contact, particularly on the north of Nishi-ishihara, thin wedge-shaped layers of pelitic, siliceous and calcareous schists of the Sambagawa belt are protruded into the hyaloclastites of the Mikabu greenstones.

Sedimentological evidences, as will be presented in the following chapter, indicate that the rock sequence of the Chichibu belt surrounding the synformally folded Mikabu greenstones are essentially sedimentary cover on the Mikabu greenstones. Accordingly, the rock sequence exposed in the area from Jizoji to Higashi-ishihara do not represent true inliers of the Mikabu greenstones as supposed by SUZUKI.

The synformally folded Mikabu greenstones together with the surrounding rock sequence of the Chichibu belt are trunctuated on the southwest by a ESE-striking and moderately north-dipping thrust, named the Nishi-ishihara thrust (TAKEDA et al., 1977). A narrow fault-bounded strip of gabbro occurs along the thrust fault. The rock sequence of the Chichibu belt below the thrust gently dips southward.

It should be noted that the antiform extends westward across the Nishi-ishihara thrust. This indicates the thrusting to be prior to the folding formed the antiform and posterior to the folding of synform.

C. LITHOLOGIES AND OCCURRENCES

Petrologically the Mikabu greenstones in the investigated areas can be divided into five rock units, volcanic rocks, diabase dike, gabbro sill swarm, peridotite-gabbro complex and sedimentary rocks. Diabase dike, peridotite-gabbro complex and sediments are small in amount. Fig. 7 summarizes schematically the stratigraphic sequence of the Mikabu greenstones in the investigated areas. The mode of occurrences and lithologies of individual rock units of the Mikabu greenstones and also their surrounding rock units are described in the following sections.

1. Volcanic rocks

Volcanic rocks of the Mikabu greenstones in the investigated areas consist of hyaloclastite and basaltic lava which is either pillowed or massive, associating volcanic breccia and tuff. Pillow lava develops in forms such as bulbous, elongate and flattened (Fig. 1 in Plate 21). Pronounced laminar flow layering is observed in massive lavas of some places. These lavas are subordinate in volume to hyaloclastite. The hyaloalstite, whose matrix is now entirely altered by the Sambagawa metamorphism, is variable in lithology, showing a variation of fine-grained hyaloclastic siltstone and sandstone to coarse-grained hyaloclastic breccia [based on the classification scheme of KAWACHI et al. (1976)]. The hyaloclastic breccia with poor or abundant matrix is generally massive and non-stratified

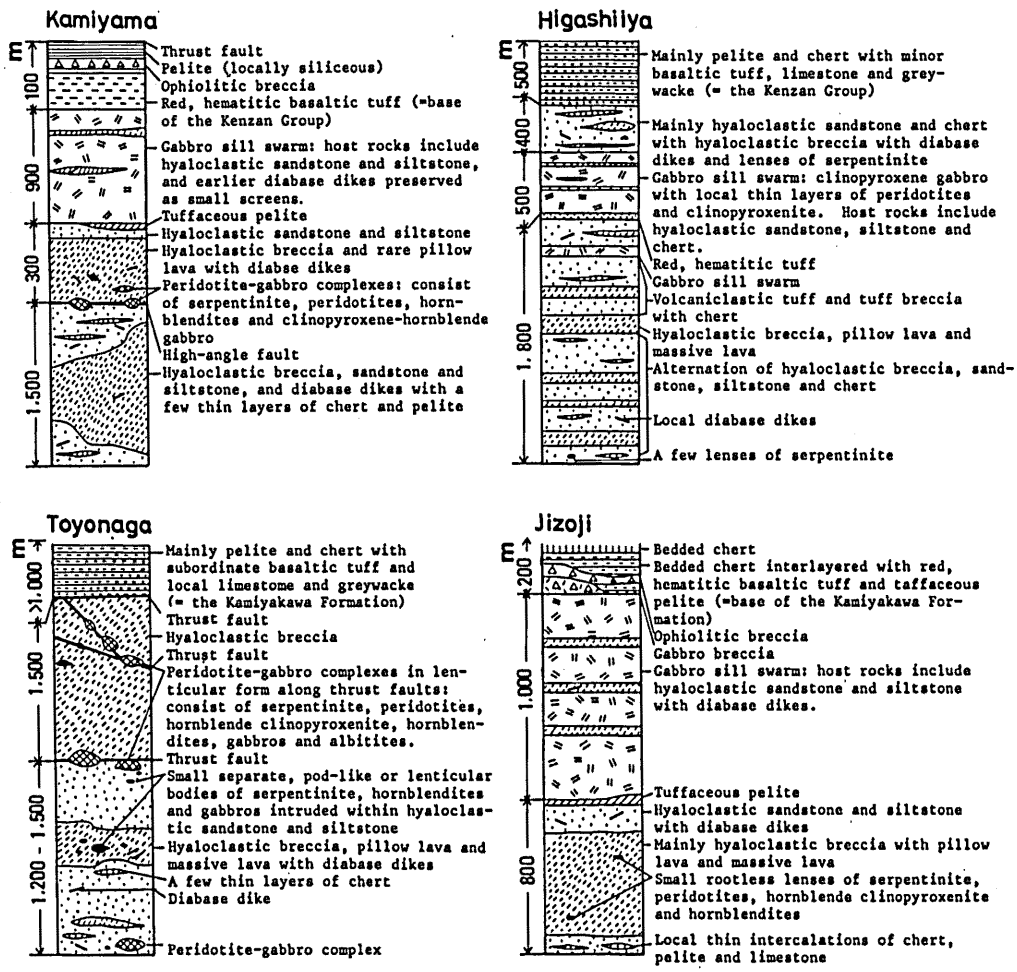

FIG. 7. Diagrammatic stratigraphic sections of the Mikabu greenstones in the Kamiyama, Higashiiya, Toyonaga and Jizoji areas.

(Fig. 2 in Plate 21), but rarely stratified with graded bedding, suggesting its reworked origin.

The volcanic breccia, characteristically occurring in the Higashiiya area, contains many fragments of basaltic lavas with various colors (dark-green, deep-green and pale-green) and with fabrics such as chilled rim, non-chilled rim, well- to poorly-developed vesicles and pronounced laminar flow layering (Fig. 3 in Plate 21). Large rafts of basalts with conspicuous laminar flow layering, which are up to 1 m in length and 25 cm in width, have been observed in some volcanic breccias. Some tuffs contain abundant relict clinopyroxene, but others are entirely free from it. Reddish-colored hematitic tuffs are sometimes found. These volcaniclastic rocks are commonly unsorted, but show occasionally stratification and grading. The presence of such the volcaniclastic rocks suggests that, during some stages of formation of the Mikabu greenstones, explosive erution oc-

curred under shallow water less than about 500 m below sea level (cf. McBIRNEY, 1963).

2. Diabase dike

Diabase is sometimes found in the volcanic rocks described above. It occurs commonly as lenticular or ellipsoidal shape which appears to be less than 10 m in its largest axis (Fig. 4 in Plate 21). Chilled contact against country volcanic rocks, generally less than a few centimeters in width, proves that the diabase lenses are of intrusive origin. The diabase lenses are generally sporadically present. But they rarely occur in small-scale swarm, though not in regular sheets. Their occurrence is not confined to a definite stratigraphic horizon (Fig. 7).

3. Gabbro sill swarm

Gabbro occurs in two modes in the volcanic rocks, small lenticular body and well-extending sill. The latter appears in swarm. The gabbro sill swarm is well exposed in the Kamiyama, Jizoji and Higashiiya areas (Fig. 7).

The Kamiyama gabbro sill swarm is emplaced in the upper stratigraphic horizon of the volcanic sequence (Fig. 2). The total thickness of the sill swarm is about 900 m. The gabbros in the sill swarm are of typically tholeiitic nature represented by two-pyroxene assemblage (NAKAYAMA et al., 1973). They show frequently flow layer defined by dimensional orientation of plagioclase crystals that is approximately parallel to the sill form.

The Jizoji gabbro sill swarm is found in the middle to upper stratigraphic horizon of the volcanic sequence (Fig. 5). Individual sills have thickness of several meters to about 360 m.

In the Higashiiya area develops a small-scale gabbro sill swarm (Fig. 3). It is about 5 km in length and 400 m in thickness and occurs in the middle to upper stratigraphic horizon of the volcanic sequence. Minor ultramafic rocks (serpentinized peridotite and clinopyroxenite) with pod-like form are found in some gabbro sills.

In order to understand petrological characteristics of the gabbro developed in sill swarm, gabbro sills in the Jizoji area have been studied along three cross-sections, the Kashiyama, Aikawa and Higashi-ishihara sections. The location of these sections is given in Fig. 5. The obtained results will be described in the following paragraphs.

The sill in the Kashiyama section is about 360 m in thickness. The petrographical characteristics change through the section as schematically shown in Fig. 8. The chilled marginal rock, generally less than 2 m in thickness, develops at the base of the sill. It changes rapidly upward into ophitic-subophitic gabbro. The ophitic-subophitic gabbro has thickness of about 200 m and is overlain by the layer of weakly laminated ferrogabbro which is placed at the upper zone of the sill. Chilled marginal rock, presumably was present, seems to be missing at the top of the sill. Gabbro, whose texture is comparable with that of cumulate, appears to be absent in the bottom of the sill.

The gabbro sills exposed along the Aikawa section and the Higashi-ishihara section are involved in the inner core of an antiformal syncline and a synformal anticline, respectively, showing their upturning. These sections are incomplete, and exposed part of the sections is estimated to be about 50 m in the Aikawa section and 220 m in the Higashi-ishihara section. Although the distribution of rock types in these sections appears to be essentially the same as that in the Kashiyama section, ferrogabbro develops more extensively in the

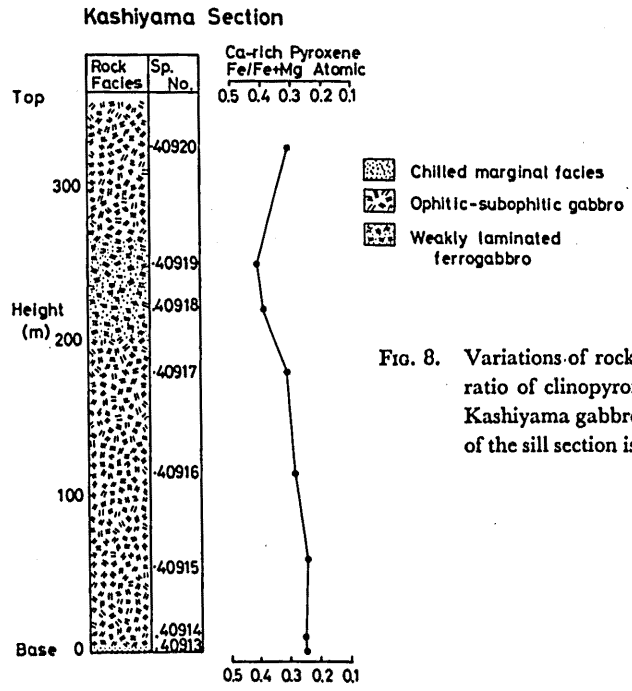

FIG. 8. Variations of rock facies and Fe/Fe+Mg ratio of clinopyroxene with height in the Kashiyama gabbro sill section. Location of the sill section is shown in Fig. 5.

former. The ferrogabbro often shows weakly igneous lamination defined by parallel arrangement of platy crystals of plagioclase, associating plagioclase-rich layer in thickness of less than 30 cm in some places. The igneous lamination is oriented approximately parallel to the wall of the gabbro sill. Gabbro pegmatite and plagiogranite also develop as latest differentiates in form such as patches, schlierens or bands in the ferrogabbro. The plagiogranite bands, which are less than 70 cm and usually about 10 cm in width, are oriented nearly parallel to the igneous lamination of wall ferrogabbro (Fig. 5 in Plate 21). Interestingly, the latest differentiates are located at about two-third to three-quarter of the way from the base to the top of the sills, as often observed in the continetal tholeiitic gabbro intrusions (e.g., WALKER, 1953; WAGER and BROWN, 1968).

4. Peridotite-gabbro complex

Ultramafic rocks occur in small amounts in the Mikabu greenstones, occupying only a few percent of their total exposure. They consist of peridotites (more or less serpentinized), clinopyroxenites and hornblendites. They occur generally as small sheet-like or lenticular bodies, less than several meters in length, in the volcanic rocks. The direction of their long axes follows the general trend of surrounding volcanic rocks. As a whole, the distribution of ultramafic rocks does not seem to be confined to a specified stratigraphic horizon in the Mikabu greenstones (Fig. 7).

In some places the ultramafic rocks are associated with gabbros and albitites (a collective name for leucocratic rocks consisting mostly of albite), forming peridotite-gabbro complexes. It is noted that the gabbros in the peridotite-gabbro complexes are characteristically hornblende-rich varieties such as clinopyroxene-hornblende gabbro, hornblende

gabbro and its pegmatoid, markedly contrasting to those in the well-differentiated gabbro sills described in the preceding section. The complexes are exposed in the Kamiyama and Toyonaga areas.

The peridotite-gabbro complexes in the Toyonaga area show lenticular form (Fig. 4). The largest complex is about 1 km in length and 400 in width. The complexes tend to be aligned along the contact surfaces, i.e., thrusting surfaces, of tectonic slices developed in the Mikabu greenstones. Although the contact between the peridotite-gabbro complexes and their surrounding volcanic rocks is not always observed, there appears to be no evidence of contact metamorphism on the latter given by the former. The peridotite-gabbro complexes seem to have been tectonically brought up to the present level (i.e., horizon of volcanic rocks) as tectonic slices.

There are many variations in combination of rock types among the peridotite-gabbro complexes. The mutual relationships among rock types in the complexes of the Toyonaga area would be explained as follows.

(1) Peridotites and clinopyroxenite are frequently interlayered, but both do not intergrade. The planes of interlayers are randomly oriented in individual complexes.

(2) Peridotites and clinopyroxenite are intruded by gabbros.

(3) The relationships of hornblendites to other types of ultramafic rocks and to gabbros can not be observed in any outcrop.

(4) Albitites occur in two different modes of occurrence. One is dike and lens. The dike ranges from 30 cm to several meters in width and occurs in hornblende clinopyroxenite, while the lens is up to a few meters in long dimension and occurs in hornblendites. Cross cutting relationship between albitites and hornblendites is found in some places. The other mode of occurrence is defined by gradational contact between hornblende gabbro, ususally its pegmatoid, and albitite.

5. Sedimentary rocks

Sedimentary rocks are interbedded with volcanic rocks in many places, though in minor amount. Their intercalation seems to be not confined to any definite stratigraphic horizon (Fig. 7). The sedimentary rocks consist of chert, pelite and limestone, among which chert is most common. Some pelites are highly ferruginous, and other are siliceous or tuffaceous.

In the Higashiiya area a fairly large amount of bedded chert is intercalated with the volcanic rocks (Fig. 3). The bedded cherts, showing pale-green to red in color, are commonly less than 10 m in thickness and are distributed throughout whole stratigraphic horizon. Some red cherts yield flattened and elongated radiolarians. It is interesting that the bedded chert is much more frequently found in the central part of the Higashiiya area than in the eastern and the western parts and in the other investigated areas of the Mikabu belt of eastern Shikoku.

6. Surrounding rock units

The sedimentary sequence of the Chichibu belt, which is the Kenzan Group in Tokushima Pref. (HIRAYAMA et al., 1956) and the Kamiyakawa Formation in Kochi Pref. (SAWAMURA et al., 1961), develops immediately on the south of the Mikabu greenstones. It consists mainly of phyllitic rocks derived from pelite, chert and mafic volcanic rocks with intercalations of limestone and greywacke of flysh-type. The rocks are metamor-

phosed in lower grade during the Sambagawa metamorphism (IWASAKI, 1963; BANNO, 1964; NAKAJIMA et al., 1977).

Chert is massive and bedded. Most of volcanic rocks are well laminated tuff. Massive basalt and gabbro sheet are also observed. Titanaugite, titaniferous phlogopite and kaersutite are ubiquitous as relict minerals in them of the Kamiyama area, indicating that magma for them was silica-undersaturated (KAJI et al., 1973; INOMATA and KAJI, 1977). Greywacke has been found in the Higashiiya-Toyonaga area (Figs. 3 & 4). Limestone is rather uncommon and is extremely thin, commonly less than several meters in thickness.

Other sedimentary deposit, here named ophiolitic breccia, has been also observed (TAKEDA et al., 1977). It occurs intermittently along the southern margin of the Mikabu greenstones in the Kamiyama and Jizoji areas (Figs. 2 & 5). It is an unbedded sedimentary breccia consisting of angular to subrounded clasts of commonly pebble- to cobble-size and of red shaly or reddish-purple volcanic cement which is now converted into mesostasis (Fig. 6 in Plate 21). Rock types present as clasts include basalt, diabase, gabbro, plagiogranite and rare chert. The petrographical characteristics of the clasts are essentially same as those of rocks of the underlying Mikabu greenstones. But, many of coarse-grained clasts are particularly abundant in hematite and are cataclastic in various degree.

In the Jizoji area there is another sedimentary breccia in close association with the ophiolitic breccia. The breccia is gabbroic in appearance, but its detailed observation reveals that it consists mainly of clasts of gabbro, accompanied with clasts of plagiogranite and of a matrix of hematite-stained basic mesostasis in which abundant fragments of clinopyroxene (and sometimes quartz) are included. The gabbro clasts are generally of granule- to boulder-size and angular to subrounded. But large blocks of quartz gabbro of up to several meters in length have been also found. The clasts are similar in petrographical aspects to gabbros of the Mikabu greenstones, although they are commonly characterized by cataclastic texture and strong weathering, giving rise to hydrous iron-oxides.

Fig. 9 illustrates the representative stratigraphic columns showing the position of the ophiolitic breccia and gabbroic breccia in the south of Higashi-ishihara of the Jizoji area. These breccias are placed at the lower most stratigraphic horizon of the Kamiyakawa Formation and overlie the gabbro sill of the Mikabu greenstones. It is noted that the gabbro breccia occurs only in close vicinity of the gabbro sill.

The ophiolitic breecia in the Kamiyama area is intercalated within the sequence consisting of red hematitic tuff and pelite (locally siliceous). The sequence belongs to the Kenzan Group and overlies in depositional contact with the gabbro sills of the Mikabu greenstones.

Recently SUYARI et al. (1979, 1980) have collected conodont fossils from limestone and chert of the rock sequence of the Chichibu belt, adjacent to the Mikabu greenstones, in the Kamiyama, Higashiiya and Jizoji areas. The discovered conodonts are of the Late Carboniferous (Early Pennsylvanian) and the Middle-Late Triassic age. However, the comprehensive picture of distribution of the rock sequence of the Late Carboniferous age and that of the Middle-Late Triassic age in the Chichibu belt adjacent to the Mikabu greenstones is not yet clarified. And relationships between the two dated sequences is also unknown.

The crystalline schists of the Sambagawa belt in the investigated areas are composed

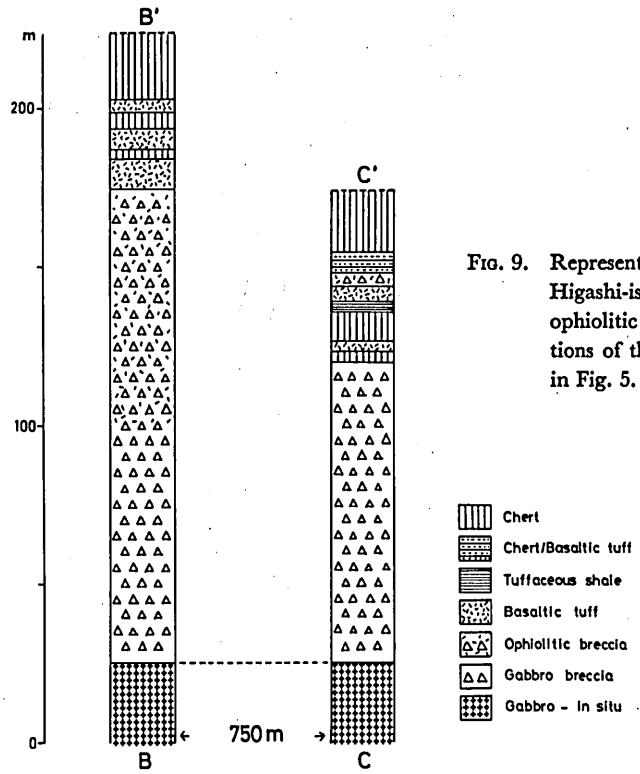

FIG. 9. Representative stratigraphic columns of the Higashi-ishihara area showing the position of ophiolitic breccia and gabbro breccia. Locations of the stratigraphic columns are shown in Fig. 5.

mainly of pelitic schists along with minor siliceous, calcareous and basic schists. They also include a distinct lithology. That is greenstone sequences (the Kubo Formation, TAKEDA, 1976) which crop out intermittently in the Higashiiya area (Fig. 3). The greenstone sequences are made up mainly of well-stratified reworked hyaloclastites with interlayers of siliceous, calcareous and pelitic schists. Also small blocks of gabbro and serpentinite (less than a few meters in length) are rarely observed in the hyaloclastic matrix. The lithological and petrological characters of basaltic fragments in the reworked hyaloclastites, gabbro and serpentinite are quite similar to those of rocks from the Mikabu greenstones. In view of occurrence of the greenstone sequences, it is highly probable that they are olistostromal origin and that their provenance was the Mikabu greenstones. Similar greenstone sequence has also been found at Koyadaira-mura, the eastern extension of the Higashiiya area (see the geological map of the Tokushima Pref., scale: 1/150,000, NAKAGAWA et al., 1972).

Conodont fossils of Late Triassic age were found by SUYARI et al. (1979) in a thin layer of calcareous schist close to the Mikabu greenstones at Shireishi, Tosa-cho, Kochi Pref. (see Fig. 5 for the fossil locality). Similarly, conodont fossils of Middle to Late Triassic age have been found from several thin layers of calcareous schist north of the Mikabu greenstones of the Ikegawa-Oda area, western Shikoku (MATSUDA, 1978; SUYARI et al., 1979, 1980).

III. IGNEOUS PETROLOGY

A. ANALYTICAL METHODS

Minerals have been analyzed by using the three channel JEOL X-ray microprobe analyzer (JXA-5A) with 40° take-off angle. Instrumunt conditions are: 15 Kv accelerating voltage, about 0.02 μA specimen current, 2–3 μ beam diameter. Five countings of 10 seconds integration time were averaged for a single complete analysis. Natural and synthetic minerals were used as standards. The correction procedure used is that of BENCE and ALBEE (1968) with alpha factors of NAKAMURA and KUSHIRO (1970).

Major element abundance for whole-rock has been determined by the microprobe analysis of unfluxed glasses fused directly from compressed rock powder pellets. Fusion is done by using the plasma-torch. The detail of this method is reported by SUZUKI et al. (1977). Analytical conditions of silicate rock glasses are the same as those for mineral analysis, except for beam diameter of 20 μm. Glass samples are moved slowly (100 μm/min.) under the electron beam during analysis in order to minimize alkali loss. Accuracy and precision of the method determined by repeated analyses of U. S. G. S. and G. S. J. standard rocks are discussed by SUZUKI et al. (1977). Practical application of this method gave fairly satisfactory results. Average analysis of U. S. G. S. -W-1 is listed in Table 1 in comparison with the recommended values of FLANAGAN (1973).

The Fe_2O_3 in whole-rock is calculated by the following procedure: 1) analyze the total iron content by means of electron microprobe and express it in the form of FeO (designated here as FeO*), 2) determine the true FeO content by potassium permanganate titrimetry and 3) calculate Fe_2O_3 by use of $1.1 \times (FeO^*-FeO)$.

B. PETROGRAPHY

The Mikabu greenstones are metamorphosed, but their original texture and minerals are frequently detected. The following petrographical description is hoped to give information about the original rocks. Detailed study of the Sambagawa metamorphism is beyond the scope of this work.

1. Basalts

Although basaltic lavas and lava fragments in hyaloclastic breccias and volcanic breccias are metamorphosed as a whole, relict minerals and texture are frequently well preserved in them. Their original petrographical characteristics have been studied on the basis of analysis of these relict minerals and fabrics. According to the obtained results, the basalts in the investigated areas appear to be divided into three groups with reference to mineralogy, Group I, Group II and Group III. Original petrographical characteristics of representative rocks of each rock group are as follows.

Group I:

Basalts of this group occur commonly in form of pillow lava. They are composed essentially of olivine, clinopyroxene, chromian spinel and glass. Plagioclase is not found, and this is characteristic of basalts of this group. The basalts are either porphyritic or aphyric. The porphyritic basalts contain phenocrysts of olivine set in a groundmass composed of clinopyroxene, glass (altered to chlorite, fibrous tremolite and minor

leucoxene) with small amount of chromian spinel (up to 0.15 mm in diameter). Microphenocrystic clinopyroxene also occurs as isolated euhedral grain or glomeroporphyritic aggregates in some samples. Modal analysis indicates that some samples (e.g., KJ–1 and N–2) are rich in olivine phenocrysts (10–20 percent). The olivine phenocrysts (1–2 mm in diameter), which are now completely replaced by chlorite and minor tremolite, are commonly euhedral and sometimes display embayed or hollow crystal form. They sometimes include tiny grains of chromian spinel and/or small globules filled with undetermined brown-tinted mineral. There is a distinct contrast on morphology of groundmass clinopyroxene between core and rim of a single pillow. The clinopyroxene in the core is generally euhedral and equant (0.2 mm in average size), whereas that in the rim is skeletal, dendritic or feathery (Figs. 1 & 2 in Plate 22). Calcite and magnetite are also present as metamorphic minerals.

Group II:

Basalts of this group occur in two forms, pillow and massive lavas. They are composed of olivine, clinopyroxene, plagioclase, glass and opaque mineral as primary minerals. The basalts are either aphyric or contain olivine phenocrysts altered to chlorite. Microphenocrystic clinopyroxene and plagioclase which is replaced by albite also occur. Epidote, actinolite, leucoxene, magnetite and hematite are other metamorphic minerals.

Generally pillow basalts of this group appear to be divided into three parts on the basis of texture, outermost rim, inner rim and core. The outermost rim, generally less than 1 cm in width, is glassy and consists of brown-tinted devitrified glass with irregular cracks. Hexagonal cracks develop occasionally, showing tortoise-shell structure. The areas bounded by the hexagonal cracks are about 0.5 mm in diameter. While, variolitic texture is characteristic of the inner rim. Many brown spherulitic aggregates of clinopyroxene intergrown with acicular plagioclase (now albite) in a devitrified glassy matrix (Fig. 3 in Plate 22). The varioles are generally less than 0.4 mm in size. Swallow-tailed clinopyroxene often forms the core of varioles. In the inner rim, clinopyroxene exhibiting quenched crystal morphology such as sheaf-like, curled or feathery form is also observed. The core is generally intersertal, and consists of crystalline growth of clinopyroxene and plagioclase. Such the textural variation is due to change of cooling rate of magma and has recently also described in ocean-floor pillow lavas (e.g., BRYAN, 1972).

Group III:

Basalts of this group, which dominantly occur as massive lavas, are mineralogically defined by presence of pink-tinted titaniferous clinopyroxene. They are porphyritic or doleritic. The porphyritic basalts consist of euhedral clinopyroxene phenocrysts (up to 1 cm in length) and microphenocrysts, which are often concentrically zoned, and a groundmass composed of plagioclase, clinopyroxene, magnetite and dark mesostasis. Clinopyroxene in the groundmass is frequently sector-zoned. Some porphyritic basalts (e.g., MD–1) are highly enriched in megacrysts (uo to 1 cm in length) and phenocrysts of clinopyroxene, attaining modal value of about 30 percent (Fig. 4 in Plate 22). The doleritic basalts consist of interlocking crystal of clinopyroxene and plagioclase which is wholly replaced by albite. Epidote, pumpellyite, aegirine-augite, stilpnomelane, muscovite, leucoxene and hematite are also found as metamorphic minerals.

2. Diabase dike

Though the constituent minerals of the diabases show a wide range in degree of meta-

morphic recrystallization, generally, original igneous texture is well preserved. They are fine-to medium-grained and their typical texture is ophitic. Relict clinopyroxene is frequently retained, but partial replacement by chlorite and/or actinolite is common. Primary plagioclase, which appears to have shown lath shape, is now completely broken down to assemblage of albite, pumpellyite and epidote with minor muscovite. Magnetite as a primary mineral has been found in some samples, though small in amount.

3. Gabbro sill swarm

Petrographical characteristics of the Jizoji gabbro sills will be described below.

Chilled marginal rocks: The chilled marginal rocks are distinctly finer-grained than the ophitic-subophitic gabbro. They are commonly aphyric, but rarely contain phenocrystic clinopyroxene set in a groundmass composed of plagioclase, clinopyroxene and minor brown hornblende. Metamorphic minerals such as albite, chlorite, pumpellyite and leucoxene are observed.

Ophitic-subophitic gabbros: The rocks are massive and their constituent minerals are medium- to coarse-grained. The texture is ophitic-subophitic. Their initial constituent minerals appear to be plagioclase and clinopyroxene with minor amounts of brown hornblende and magnetite. The plagioclase is turbid and occasionally has been saussuritized to an aggregate of albite, epidote, pumpellyite and actinolite. The clinopyroxene is well preserved, but partly replaced by chlorite and actinolite.

Ferrogabbros: Ferrogabbros appear dark brown with unaided eye. They are divided into two main rock types on the basis of fabric, i.e., weakly laminated type and massive type, although there is no significant difference in mineral composition between them. The laminated ferrogabbro is characterized by plagioclase laths (2–3 mm in length) showing dimensional orientation (Fig. 5 in Plate 22). Hence they can be regarded as cumulus phase. Ferroaugite, green hornblende, ilmenite, titanomagnetite, quartz and apatite are present as intercumulus minerals. The plagioclase is clouded or saussuritized. The ferroaugite is often partly replaced by actinolite together with chlorite and stilpnomelane. On the other hand, the massive ferrogabbro shows ophitic texture, showing no parallel alignment of plagioclase crystals. The modal value of iron-titanium oxides in these gabbros is variable, ranging from 5 to 10 percent.

Gabbro pegmatites: Gabbro pegmatites typically contain clinopyroxene crystals of 3 cm in maximum length and plagioclase up to 3 cm. Quartz, apatite and opaque minerals (titanomagnetite and ilmenite) are also common as primary accessory minerals. Partial decomposition of clinopyroxene to actinolite, chlorite and stilpnomelane is common. The plagioclase laths have been saussuritized or replaced by dusty minerals.

Plagiogranites: The rocks are pale-green in color, consisting mainly of fine- to medium-grained quartz and plagioclase with minor apatite as initial minerals (Fig. 6 in Plate 22). Mineralogically they are characterized by virtual absence of potassium feldspar. The texture is granophyric. The plagioclase has been albitized or pumpellyized.

Ferroaugite plagiogranite is one of transitional rock types between ferrogabbro and plagiogranite. It contains quartz, plagioclase and ferroaugite with minor ilmenite and apatite as primary phases.

4. Peridotite-gabbro complex

Petrological studies on the peridotite-gabbro complexes have mainly been performed on

those of the Toyonaga area, but lenticular peridotite bodies in the volcanic rocks of the Higashiiya and Jizoji areas have also been studied. The rocks in the complexes are more or less metamorphosed, and hence it is often difficult to know their original mineral constituents. The examined ultramafic rocks are essentially composed of olivine, clinopyroxene, brown hornblende and opaque minerals. No orthopyroxene and plagioclase are found. Modal characteristics of some representative ultramafic rocks, which are most weakly metamorphosed, are shown in Fig. 10. The original modal compositions of these rocks have been estimated from both relict and metamorphic minerals assuming the following reactions took place: olivine into serpentine and dusty magnetite, part of clinopyroxene into chlorite and actinolite, brown hornblende into actinolite.

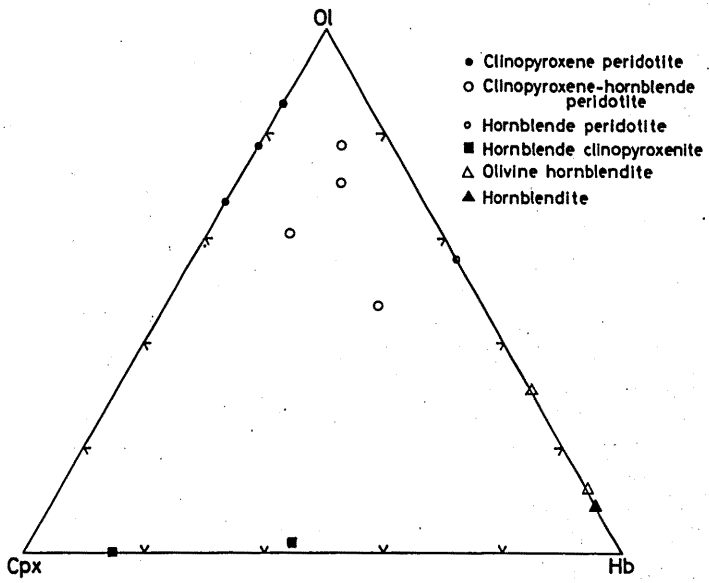

Fig. 10. Modal characteristics of some ultramafic rocks. Classification of IUGS (1973) is used with a slight modification. Ol=olivine, Cpx=clinopyroxene, Hb=hornblende.

Peridotites: The rocks consist commonly of olivine associating clinopyroxene and brown hornblende in variable proportion. So, they can be divided into following three types in increasing order of brown hornblende, clinopyroxene peridotite, clinopyroxene-hornblende peridotite and hornblende peridotite. Olivine grains in these peridotites are completely replaced by serpentine and magnetite which occurs as strings or trains of grains outlining olivine pseudomorphs and/or as dense aggregates within olivine pseudomorphs. They are euhedarl and 0.5 to 2 mm in size. Chromian spinel (0.2 mm in maximum size) occurs in and/or around settled grains of olivine and so it can be also regarded as a cumulus phase precipitated from liquid before or at the same time olivine. It dose not exceed 2 percent in modal value. The cumulus phases, olivine and chromian spinel, are cemented by interstitial clinopyroxene and/or brown hornblende, which are often coarse-grained enough to embrace poikilitically the cumuls phases (Fig. 7

in Plate 22). In clinopyroxene-hornblende peridotites, brown hornblende sometimes encloses cumulus clinopyroxene crystals, suggesting that the former postdates the latter. Occasionally phlogopite occurs also interstitially as minute grain in some peridotites. Sphene, calcite, chlorite and tremolite are also found as secondary minerals.

Hornblende clinopyroxenites: The rocks consist chiefly of clinopyroxene accompanied with brown hornblende and opaque minerals. Euhedral grains of clinopyroxene, generally having size of 0.6 to 1.3 mm, are surrounded by intercumulus brown hornblende. Minute olivine replaced by chlorite is sometimes found only in small amount. Titanomagnetite as primary opaque phase occurs as small crystals, being less than 0.2 mm in size, and is usually present in accessory amount. It occurs as inclusions in brown hornblende, though generally occurring in interstices between large silicate crystals. Alteration of clinopyroxene and brown hornblende to actinolite and chlorite is a common feature.

Olivine hornblendites and hornblendites: These rocks consist mainly of brown hornblende accompanying olivine in highly variable amount. In the present paper, the term olivine hornblendite is for hornblendite containing olivine of 10 to 40 volume percent (Fig. 10). Brown hornblende forms small euhedral crystals which are commonly less than 0.5 mm in length. It is often mantled by actinolite and sometimes is completely replaced by it. Olivine which is entirely changed to chlorite and magnetite, is generally up to 1 mm in length, and occurs as porphyritic or glomeroporphyritic crystals. Large porphyritic clinopyroxene is rarely found in hornblendites. Titanomagnetite as primary opaque phase is also found in some olivine hornblendites and hornblendites. A small amount of leucoxene is invariably present as a secondary mineral.

Gabbros: Gabbros are commonly massive and are made up chiefly of clinopyroxene, brown hornblende and plagioclase with accessory opaque minerals (iron oxide and titanium oxide) as primary minerals. No olivine and orthopyroxene are seen. The gabbros are divided into three rock types in increasing order of brown hornblende, hornblende-clinopyroxene gabbro, clinopyroxene-hornblende gabbro and hornblende gabbro. Gabbro pegmatite, which contains brown hornblende and plagioclase with accessory apatite and iron oxides, is found in the hornblende gabbro. Clinopyroxene in these gabbros, in general, has mantle of brown hornblende which commonly grades outward through bluish-green amphibole belonging to hastingsite-ferrohastingsite series to actinolite. Probably the bluish-green amphibole is a product of late magmatic stage and the actinolite is of regional metamorphism. Plagioclase in all types of gabbro is wholly saussuritized.

Albitites: Albitites have been distinguished into six main types on the basis of mineral assemblage, albitite proper, stilpnomelane-quartz albitite, stilpnomelane-chlorite albitite, pyrite albitite, actinolite albitite and hornblende albitite. X-ray and electron microprobe analyses show that plagioclase in these albitites is of low temperature type ($2\theta_{1\bar{3}1}-2\theta_{131}=1.1°$ on CuK_α on the average) and has composition of $An_{0-1.7}$. Twinning is generally of Albite law.

Albitite proper consists almostly of albite (up to 2 mm in length) with negligible amounts (usually less than 5 percent) of actinolite, stilpnomelane and sphene. The texture is generally granular, sometimes showing fragmentation by mylonitization or cataclasis.

Stilpnomelane-quartz albitite is porphyritic with phenocrysts of quartz (up to 5 percent in modal value) set in a groundmass composed mainly of albite and stilpnomelane. Sphene, apatite, muscovite and opaques are accessories.

Stilpnomelane-chlorite albitite consists predominantly of albite with subordinate

amounts of chlorite and stilpnomelane. Apatite, epidote, allanite and muscovite are present as accessories. The texture is variable and is distinguished into three fundamental types: 1) granular aggregate of albite grains with average size of 2 mm, 2) porphyritic type shown by albite phenocrysts in a fine-grained groundmass consisting mainly of tiny untwinned albite crystals and 3) mylonitized type showing single set of well-defined schistosity. There are gradational types among three types. The porphyritic type can be called albitophyre (Fig. 8 in Plate 22).

Pyrite albitite is granular and is composed of albite and pyrite. The pyrite is euhedral and occurs both as discrete crystals and aggregates. It makes up nearly 50 percent of the rock. Some pyrite albitites are porous and show brown-yellowish tint, indicating that the rocks may be referred to a kind of gossan.

Actinolite albitite is fine-grained and consists of interlocked crystals of albite and actinolite.

Hornblende albitite is composed mainly of albite, brown hornblende, chlorite and actinolite with minor amounts of epidote, pumpellyite, crossite, stilpnomelane, sphene, muscovite and opaque minerals, frequently showing gabbroic texture. The hornblende albitite often grades into hornblende gabbro and its pegmatite.

Albitites in the Mikabu greenstones closely resemble to those in the Kamuikotan belt (Suzuki, 1953) with reference to mineralogy and texture.

C. Whole-Rock Compositions

Major elements of a total thirty-two samples have been analyzed with the microprobe. They consist of eleven basalts, four diabases and seventeen rocks from the Jizoji gabbro sills. Representative analyses are shown in Tables 1 and 2.

It is now recognized that elements might have been redistributed extensively in some metabasites owing to ocean-floor weathering and/or regional metamorphism (see discussion by Miyashiaro, 1975). The Na_2O/K_2O versus Na_2O+K_2O diagram after Miyashiro (1975) is of some help in clarifying the nature and extent of alkali migration in metabasites. A considerable number of the present analyses is plotted above the curve V–V in the Na_2O/K_2O versus Na_2O+K_2O diagram in Fig. 11. Miyashiro showed that all fresh Quaternary volcanic rocks of basic and intermediate compositions in widely varied modes of occurrences and regions are plotted above the curve V–V in this diagram and rocks plotted above the curve would have been affected by some post-igneous changes. The rocks plotted above the curve correspond to all the Group II basalts and diabases and to some of gabbros. Therefore it is suggested that post-igneous alteration in terms of alikali component is particularly intensive for these rocks.

It is noted that the rocks having high Na_2O/K_2O ratio, in general, are also accompanied with siginificant depletion in CaO content (e.g., Nos. 6 & 15 in Table 1, and Nos. 1, 6 & 7 in Table 2). High Na_2O/K_2O ratio and low CaO content are typical of spilitic rocks (Vallance, 1960; Cann, 1969). Accordingly the Group II basalts, diabases and some of gabbros appear to have been more or less spilitized.

Although secondary change in whole-rock compositions is recognized in some samples, each rock groups have distinct chemeical characteristics, as will be described in the following.

The Group I basalts are picrite-basaltic and are characterized by high MgO, low SiO_2 and low Al_2O_3 contents and high CaO/Al_2O_3 ratio (0.87–1.30). Their TiO_2 content is

TABLE 1. CHEMICAL COMPOSITIONS OF BASALTS AND DIABASES FROM THE MIKABU GREENSTONES IN EASTERN SHIKOKU (ON A WATER-FREE BASIS).

	Basalts							
	Group I					Group II		
	1	2	3	4	5	6	7	8
SiO_2	44.8	47.8	45.9	47.2	46.8	54.0	51.1	48.1
TiO_2	1.86	1.75	1.42	1.66	2.34	0.82	0.90	1.02
Al_2O_3	7.75	8.75	9.67	10.1	11.0	11.6	12.8	14.5
FeO*	13.6	11.8	13.5	11.9	12.8	8.77	9.19	11.4
MnO	0.25	0.28	0.31	0.26	0.32	0.21	0.25	0.27
MgO	19.8	17.2	18.8	16.4	15.7	9.96	8.89	9.69
CaO	10.1	9.94	9.28	10.3	9.62	9.27	12.1	11.9
Na_2O	1.92	2.34	1.26	2.27	1.77	5.19	4.17	3.10
K_2O	0.02	0.06	0.05	0.05	0.13	0.03	0.31	0.04
Total	100.10	99.92	100.19	100.14	100.48	99.85	99.71	100.02
FeO*/MgO	0.69	0.69	0.72	0.73	0.82	0.88	1.03	1.18

	Group III			Diabases				W-1**	
	9	10	11	12	13	14	15		
SiO_2	47.0	45.8	48.1	50.5	47.2	46.5	48.8	52.89	(53.05)
TiO_2	2.07	3.28	4.24	1.03	1.53	1.64	1.55	1.20	(1.07)
Al_2O_3	9.22	16.1	14.6	14.2	15.4	16.1	14.3	15.23	(15.12)
FeO*	9.74	11.2	12.6	10.2	11.3	10.9	13.2	10.22	(10.06)
MnO	0.27	0.25	0.28	0.25	0.24	0.25	0.38	0.17	(0.17)
MgO	13.4	6.49	6.40	9.41	7.78	7.29	7.22	6.58	(6.67)
CaO	16.4	12.6	8.18	11.3	11.9	14.0	9.30	11.05	(11.05)
Na_2O	1.72	3.45	4.57	3.86	3.68	3.01	4.94	2.10	(2.17)
K_2O	0.25	0.49	1.13	0.09	0.10	0.04	0.04	0.62	(0.64)
Total	100.07	99.96	100.10	100.84	99.13	99.73	99.73	100.06	
FeO*/MgO	0.73	1.73	1.97	1.08	1.45	1.50	1.83		

* Total iron as FeO. ** unpublished data by A. MINAMI. Recommended values of FLANAGAN (1973) are bracketed.

1. Aphyric picrite-basalt, T3103, Toyonaga, 2. Olivine porphyritic picrite-basalt, KJ-2, Jizoji, 3. Olivine porphyritic picrite-basalt, N-2, Jizoji, 4. Olivine porphyritic picrite-basalt, KJ-1, Jizoji, 5. Olivine porphyritic picrite-basalt, T2606, Toyonaga, 6. Aphyric basalt, Hp-5, Higashiiya, 7. Olivine moderately phyric basalt, Hp-4, Higashiiya, 8. Aphyric basalt, H2801, Higashiiya, 9. Clinopyroxene porphyritic basalt, MD-1, Toyonaga, 10. Aphyric (doleritic) basalt, H1405, Higashiiya, 11. Clinopyroxene sparsely phyric basalt, H2109, Higashiiya, 12. Clinopyroxene diabase, H1309, Higashiiya, 13. Porphyritic olivine-bearing clinopyroxene diabase, J607, Jizoji, 14. Clinopyroxene diabase (microgabbroic), H1804, Higashiiya, 15. Clinopyroxene diabase, H1910, Higashiiya. Analyzed by K. TAKEDA.

moderately high, ranging from 1.42 to 2.34 percent. These picrite-basalts tend to have low total alkali, and on the Na_2O+K_2O versus SiO_2 diagram in Fig. 12 they fall in the low Na_2O+K_2O and low SiO_2 side of the tholeiitic basalt field of Hawaiian volcanic rock series after MACDONALD and KATSURA (1964).

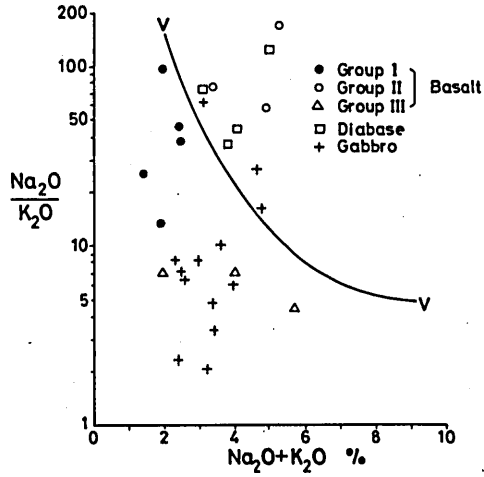

FIG. 11. Na_2O/K_2O vs. Na_2O+K_2O diagram for basalts, diabases and the Jizoji gabbros. Line V–V indicates the upper limit of Na_2O/K_2O for all fresh Quaternary volcanic rocks of basic and intermediate compositions after MIYASHIRO (1975).

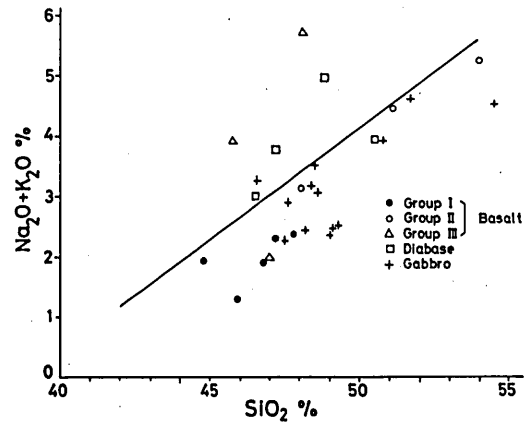

FIG. 12. Na_2O+K_2O vs. SiO_2 diagram for basalts, diabases and the Jizoji gabbros. MACDONALD & KATSURA's (1964) boundary between tholeiitic and alkalic series for the Hawaiian volcanic rocks is shown as a straight line.

Chemical analyses indicate some overlap between the Group II basalts and diabases in terms of major element compositions. They are spilitic, as mentioned in the above. Their TiO_2 and Al_2O_3 contents are rather low, ranging from 0.82 to 1.05 percent and from 11.6 to 14.5 percent, respectively, but the diabases tend to have higher Al_2O_3 and TiO_2 contents than have the Group II basalts. The Group II basalts fall in the tholeiitic field somewhat below the dividing line in the Na_2O+K_2O versus SiO_2 diagram, and the diabases do in both the alkali and tholeiitic basalt fields (Fig. 12). Although magmatic parentage for these rocks can not be determined by using whole-rock major element parameters such as Na_2O+K_2O versus SiO_2 diagram because of alkali migration in them, relict clinopyroxene analyses, as described in the following section, confirm that they are tholeiitic.

Two samples from the Group III basalts, nos. H1405 and H2109, are characterized by their distinctly high potassic and titanian nature and relatively low SiO_2 content. The high TiO_2 content is consistent with the presence of titaniferous clinopyroxene. Sample MD-1 is exceptionally high in CaO and moderately high in MgO. That results from the presence of abundant megacryst and phenocryst of highly calcic clinopyroxene. The basalts of this group, with one exception of clinopyroxene-enriched sample, fall in the alkali basalt field in the Na_2O+K_2O versus SiO_2 diagram (Fig. 12). These composi-

TABLE 2. CHEMICAL COMPOSITIONS OF REPRESENTATIVE ROCKS FROM THE JIZOJI GABBRO SILLS (ON A WATER-FREE BASIS).

	1	2	3	4	5	6	7	8	9	10
SiO_2	48.6	47.5	48.2	49.3	49.1	51.7	54.5	50.8	59.1	72.3
TiO_2	0.93	0.47	0.52	0.65	0.66	1.96	2.25	3.45	1.95	0.68
Al_2O_3	15.3	18.2	18.3	15.2	17.2	12.6	11.8	10.6	11.8	12.6
FeO*	10.4	7.52	7.67	9.99	9.45	15.5	15.1	19.9	16.8	4.86
MnO	0.27	0.17	0.28	0.35	0.41	0.41	0.32	0.54	0.43	0.13
MgO	8.47	7.46	7.21	7.86	7.27	5.51	4.18	2.77	1.78	0.69
CaO	12.3	15.9	14.7	13.5	12.4	6.80	7.94	7.61	3.03	3.65
Na_2O	3.02	2.04	2.16	2.17	2.61	4.37	4.32	3.36	4.65	4.57
K_2O	0.05	0.24	0.29	0.34	0.76	0.26	0.16	0.56	0.41	0.24
Total	99.34	99.50	99.33	99.36	99.86	99.11	100.57	99.59	99.95	99.72
Fe_2O_3**	1.56	2.16	2.24	2.08	3.26	4.67	6.30	3.45	8.35	1.57
FeO***	9.00	5.58	5.65	8.12	6.52	11.3	9.40	16.8	9.29	3.45
SI****	37.9	42.3	40.4	37.6	34.9	20.8	16.9	10.1	7.1	6.5

* Total iron as FeO. ** Fe_2O_3 calculated by use of $1.1 \times (FeO^* - FeO^{***})$. *** FeO determined by potassium permanganate titrimetry. **** Solidification index $(MgO \times 100/MgO + FeO^{***} + Fe_2O_3^{**} + Na_2O + K_2O)$.

1–6. Specimens from the Kashiyama sill section (360 m thick). Refer to Fig. 8 for relative height of the specimens. 1. Chilled marginal facies, J913, 2. Hornblende-clinopyroxene gabbro, J914, 3. Clinopyroxene gabbro, J915, 4. Hornblende-clinopyroxene gabbro, J916, 5. Hornblende-clinopyroxene gabbro, J917, 6. Ferrogabbro, J918. 7–10. Specimens from the other two sections (Aikawa and Higashi-ishihara). 7. Gabbro pegmatite, J1003, 8. Ferrogabbro, J902, 9. Ferroaugite plagiogranite, J1009, 10. Plagiogranite, J909. Analyzed by K. TAKEDA.

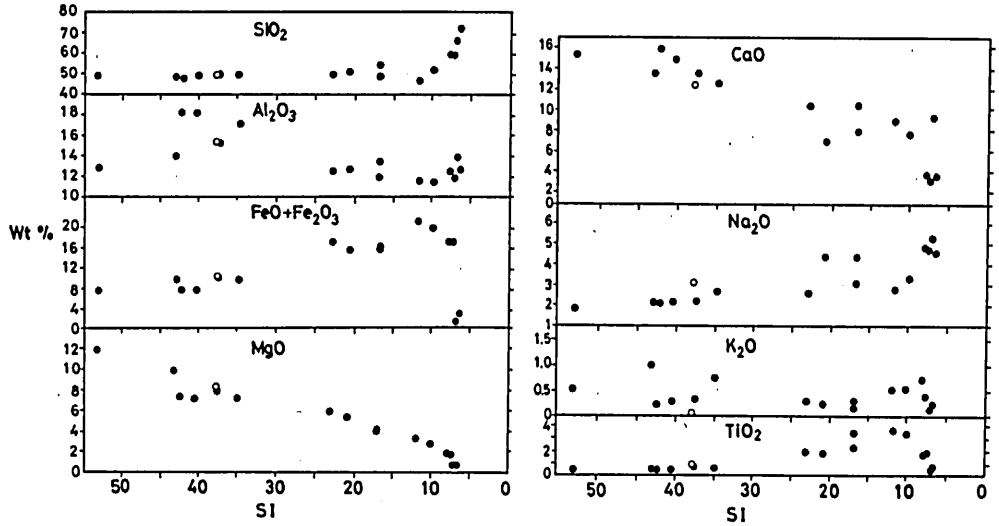

FIG. 13. SI variation diagram for rocks from the Jizoji gabbro sills. Open circle: chilled marginal rock, closed circles; gabbros and plagiogranites.

tional characteristics are typical of alkali olivine basalts (e.g., KUNO, 1968) and are consistent with their petrography.

Plots of oxides composition for rocks from the Jizoji gabbro sills in function of the solidification index ($SI=MgO\times100/MgO+FeO+Fe_2O_3+Na_2O+K_2O$) are shown in Fig. 13. The range of SI of analyzed samples is wide, indicating marked fractionation. In Fig. 13, all analyses from the three sill sections are plotted together. All oxides, except for K_2O, fall on sharply defined trend line. SiO_2 increases very slowly until the late stage where SI becomes about 10 and thereafter rises rapidly. Al_2O_3 shows first a slight increase, and decreases at the later stage. Total iron increases until it attains about 20 percent at $SI=10$ and decreases abruptly. A similar curve is obtained for TiO_2. This fact indicates that the abrupt change of slope of these two curves is due to the appearance of titaniferous magnetite and/or ilmenite as crystalline phases at this stage. MgO decreases monotonously during fractionation. CaO decreases, whereas Na_2O shows an increase with decreasing SI. These variations confirm that the fractionation trend is essentially tholeiitic and not calc-alkaline (KUNO, 1959).

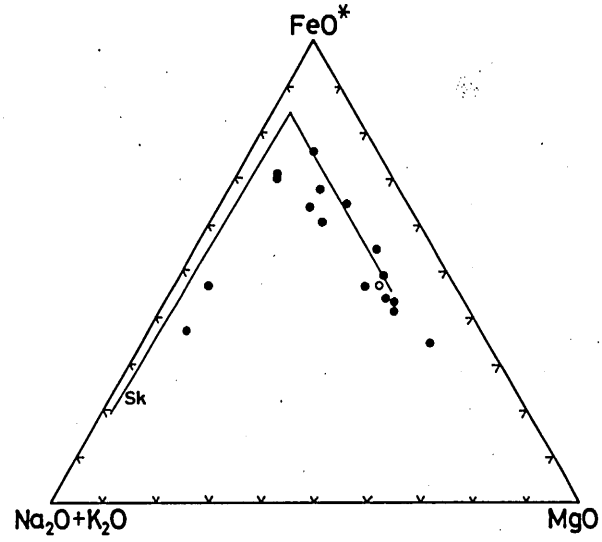

FIG. 14. MgO—FeO*—(Na_2O+K_2O) diagram for rocks from the Jizoji gabbro sills. Solid line (Sk) indicates the trend of successive liquids of the Skaergaard intrusion (WAGER, 1960). Symbols used are the same as those in Fig. 13.

The tholeiitic fractionation trend of the Jizoji gabbros is also expressed in the AFM diagram (Fig. 14). The trend is nearly parallel to the FeO*–MgO edge of the triangular diagram until the ferrogabbro stage, and it turns sharply toward the Na_2O+K_2O corner when the plagiogranite stage is attained.

It is noticeable that the plagiogranite is characteristically low in K_2O content. The low K_2O nature of the plagiogranite is well marked in the virtual absence of potassium-feldspar in the rock. On the basis of major element chemistry, the plagiogranite is of the "oceanic plagiogranite" type, which has been recognized by COLEMAN and PETERMAN

(1975) as a distinct group of leucocratic rocks in ophiolites.

Judging from the Na_2O/K_2O versus Na_2O+K_2O diagram, the chilled marginal rock of the Jizoji gabbro sills appears to have been spilitized. Therefore, it can not be taken as a reliable guide to the parent magmatic composition, particularly, in terms of alkali content. The parent magma of the Jizoji gabbro sills is probably low-K tholeiite which fractionated to be enriched in SiO_2 at the late stage of fractionation.

D. MINERAL CHEMISTRY

1. Clinopyroxene

Clinopyroxene can be frequently found as a relict mineral in each rock units (except for sedimentary rocks) of the Mikabu greenstones. Compositional characteristics of the relict clinopyroxene in each rock units will be given in the following.

TABLE 3. REPRESENTATIVE MICROPROBE ANALYSES OF CLINOPYROXENE IN BASALTS.

	Group I							
	T2606		N-2	KJ-2			KJ-1	T3103
	Mph	G	G	Mph	G	G	G	G
SiO_2	52.4	51.0	51.1	51.1	46.4	46.3	49.7	51.1
TiO_2	0.56	0.71	0.71	0.90	2.22	2.29	1.45	1.15
Al_2O_3	1.69	3.62	2.90	3.40	6.72	7.65	4.61	3.54
Cr_2O_3	0.81	0.44	1.25	1.02	0.14	0.11	0.74	0.23
FeO*	6.25	7.33	5.99	6.56	9.29	12.0	7.74	7.21
MnO	0.20	0.20	0.20	0.23	0.22	0.31	0.24	0.26
MgO	17.9	17.8	16.3	17.2	14.6	14.0	19.8	15.9
CaO	20.3	18.7	20.5	20.2	19.5	18.0	15.9	20.7
Na_2O	0.23	0.27	0.27	0.25	0.30	0.33	0.35	0.26
Total	100.34	100.07	99.22	100.86	99.39	100.99	100.53	100.35
O=6								
Si	1.923	1.878	1.899	1.870	1.759	1.732	1.836	1.885
Al^{IV}	0.073	0.122	0.101	0.130	0.241	0.268	0.164	0.115
Al^{VI}	—	—	0.026	0.017	0.056	0.069	0.037	0.039
Ti	0.015	0.034	0.020	0.025	0.063	0.064	0.040	0.032
Cr	0.023	0.020	0.037	0.030	0.004	0.003	0.022	0.007
Fe	0.191	0.225	0.186	0.200	0.291	0.374	0.238	0.222
Mn	0.006	0.006	0.006	0.007	0.007	0.010	0.007	0.008
Mg	0.978	0.973	0.899	0.939	0.814	0.781	0.874	0.871
Ca	0.795	0.737	0.816	0.791	0.782	0.720	0.782	0.816
Na	0.016	0.019	0.020	0.018	0.022	0.024	0.025	0.018
Total	4.020	4.014	4.010	4.027	4.039	4.045	4.025	4.013
Atomic %								
Ca	40.4	38.1	42.9	41.0	41.5	38.4	41.3	42.8
Mg	49.9	50.3	47.3	48.7	43.1	41.7	46.1	45.6
Fe	9.7	11.6	9.8	10.3	15.4	19.9	12.6	11.6

Table 3 (Continued)

	Group II				Group III			
	Hp-5	T703	Hp-4	H2801	MD-1		H1405	H2109
	G	Mph	G	G	Ph	G	G	G
SiO_2	48.7	51.5	46.6	48.0	52.3	48.0	43.1	44.2
TiO_2	0.42	0.88	1.25	0.65	0.43	2.11	4.09	3.88
Al_2O_3	4.56	2.87	7.03	2.71	1.69	5.74	7.60	6.70
Cr_2O_3	0.89	0.52	0.09	0.18	0.80	0.23	0.15	0.06
FeO*	6.29	6.48	10.9	15.2	4.00	6.66	9.00	9.28
MnO	0.26	0.23	0.38	0.38	0.11	0.23	0.22	0.31
MgO	16.4	17.1	14.6	12.1	15.9	13.2	12.1	12.1
CaO	22.1	20.4	19.3	20.9	22.8	23.2	22.9	23.4
Na_2O	0.24	0.26	0.46	0.34	0.32	0.45	0.52	0.50
Total	99.86	100.24	100.61	100.46	98.35	99.82	99.68	100.43
O=6								
Si	1.816	1.896	1.748	1.849	1.948	1.797	1.650	1.682
Al^{IV}	0.184	0.104	0.252	0.123	0.052	0.203	0.343	0.301
Al^{VI}	0.016	0.019	0.059	—	0.022	0.050	—	—
Ti	0.012	0.024	0.035	0.019	0.012	0.059	0.118	0.111
Cr	0.026	0.015	0.003	0.006	0.024	0.007	0.005	0.002
Fe	0.196	0.198	0.341	0.488	0.124	0.208	0.288	0.295
Mn	0.008	0.007	0.012	0.012	0.003	0.007	0.007	0.010
Mg	0.908	0.936	0.818	0.696	0.884	0.738	0.687	0.684
Ca	0.884	0.801	0.774	0.862	0.910	0.929	0.941	0.952
Na	0.017	0.018	0.033	0.025	0.023	0.032	0.038	0.037
Total	4.067	4.019	4.075	4.080	4.002	4.030	4.077	4.074
Atomic %								
Ca	44.4	41.4	40.1	42.1	47.4	49.5	49.1	49.3
Mg	45.7	48.4	42.3	34.0	46.1	39.4	35.9	35.4
Fe	9.9	10.2	17.6	23.9	6.5	11.1	15.0	15.3

* Total iron as FeO.

T703: Olivine moderately phyric glassy basalt, Toyonaga. Other specimens are the same as those in Table 1. Abbreviations are as follows: Ph=phenocryst, Mph=microphenocryst, G=groundmass. Analyzed by K. TAKEDA.

a. Basalts and diabases

Representative analyses of clinopyroxenes in basalts and diabases are listed in Tables 3 and 4. It is well-recognized that the diagnostic criteria in distinguishing between clinopyroxenes from alkali basalts and those from tholeiitic basalts are Ca/Mg+Fe ratio and Al_2O_3 and TiO_2 concentrations; i.e., clinopyroxenes from alkali basalts have higher Ca/Mg+Fe ratio and higher Al_2O_3 and TiO_2 than those from tholeiitic basalts (KUSHIRO, 1960; LEBAS, 1962; COOMBS, 1963). Therefore, nature of clinopyroxene as relict phase provides a strong clue to evaluate the nature of magmatic parentage of metabasites. In

Table 4. MICROPROBE ANALYSES OF CLINOPYROXENE IN DIABASES.

	K2601	H1309	J2704	H1701	H1910	H3102	J607
SiO_2	51.5	51.0	52.3	49.9	49.9	51.3	50.8
TiO_2	0.32	0.37	0.44	0.59	0.54	0.39	0.78
Al_2O_3	3.14	3.60	2.28	5.71	3.37	2.59	2.06
Cr_2O_3	0.80	0.44	0.38	0.73	0.14	0.24	0.06
FeO*	5.67	5.60	6.10	6.34	8.57	8.43	10.2
MnO	0.07	0.21	0.21	0.21	0.27	0.30	0.32
MgO	17.6	17.1	17.6	15.5	16.0	15.4	15.0
CaO	21.3	21.8	21.3	21.4	20.6	20.3	20.0
Na_2O	0.18	0.24	0.20	0.26	0.27	0.22	0.28
Total	100.58	100.36	100.81	100.64	99.66	99.17	99.50
O=6							
Si	1.886	1.874	1.911	1.833	1.869	1.921	1.915
Al^{IV}	0.114	0.126	0.089	0.167	0.131	0.079	0.085
Al^{VI}	0.021	0.030	0.009	0.080	0.018	0.035	0.006
Ti	0.009	0.010	0.012	0.016	0.015	0.011	0.022
Cr	0.023	0.013	0.011	0.021	0.004	0.007	0.002
Fe	0.173	0.172	0.186	0.194	0.268	0.263	0.319
Mn	0.002	0.007	0.007	0.007	0.009	0.010	0.010
Mg	0.956	0.935	0.958	0.849	0.892	0.861	0.840
Ca	0.835	0.858	0.833	0.841	0.824	0.813	0.808
Na	0.013	0.017	0.014	0.019	0.019	0.016	0.020
Total	4.032	4.042	4.030	4.027	4.049	4.016	4.027
Atomic %							
Ca	42.5	43.7	42.1	44.6	41.5	42.0	41.1
Mg	48.7	47.5	48.5	45.1	45.0	44.4	42.7
Fe	8.8	8.8	9.4	10.3	13.5	13.6	16.2

* Total iron as FeO.

K2601: Clinopyroxene diabase, Kamiyama. J2704: Porphyritic olivine-bearing clinopyroxene diabase, Jizoji. H1701: Clinopyroxene-enriched diabase, Higashiiya. H3102: Poikilitic clinopyroxene diabase, Higashiiya. H1309, H1910 and J607: See footnotes of Table 1. Analyzed by K. TAKEDA.

the following, the analytical results of clinopyroxene are discussed with special reference to magmatic parentage.

Compositional variation of clinopyroxenes in basalts and diabases in terms of atomic percent Ca, Mg and Fe is shown in Fig. 15. There is no significant difference in abundance of major elements between clinopyroxenes in the Group I basalts and those in the Group II basalts. The clinopyroxenes are mostly augitic. Many analyses of these augites lie within the field of clinopyroxenes from the Hawaiian tholeiitic basalts (EVANS and MOORE, 1968; FODOR et al., 1975).

On the other hand, pink-tinted clinopyroxenes in the Group III basalts have higher CaO content than those in the other two groups of basalts, mostly belonging to salite

(Fig. 15). Although compositional variation in these salites in terms of atomic percent Ca, Mg and Fe is largely different among each samples, most of the salites define an overall trend line of increasing Ca with increasing Fe, which is roughly similar to the trend defined by clinopyroxenes from the Hawaiian nephelinitic suite (FODOR et al., 1975).

Most of clinopyroxenes from diabases are augite. Ca content of the augites decreases gradually with increasing iron and is approximately in accord with that of early precipitating Ca-rich pyroxene from slowly cooled tholeiitic intrusions such as in the Skaergaard (BROWN, 1957).

Fig. 16 shows Ti–Al relation in clinopyroxenes in basalts and diabases. Ti and Al distribution is slightly but significantly different between augites in the Group I basalts

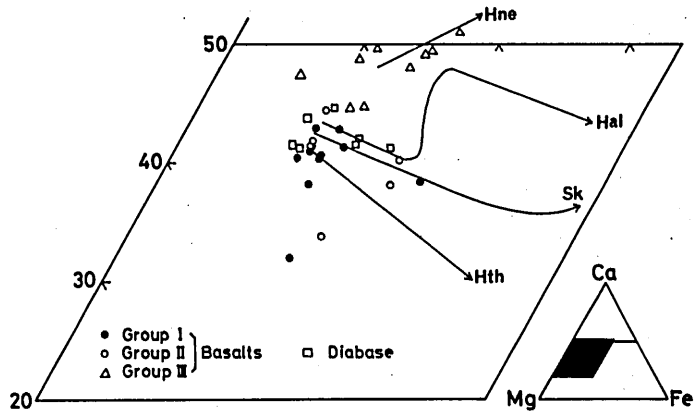

FIG. 15. Ca—Mg—Fe diagram for clinopyroxene from basalts and diabases. Overall crystallization trends of clinopyroxenes from the Hawaiian volcanic rocks of tholeiitic (Hth), alkalic (Hal) and nephelinitic (Hne) suites (FODOR et al., 1975) and the early part of the Skaergaard Ca-rich pyroxene trend (Sk) (BROWN, 1957) are included for comparison.

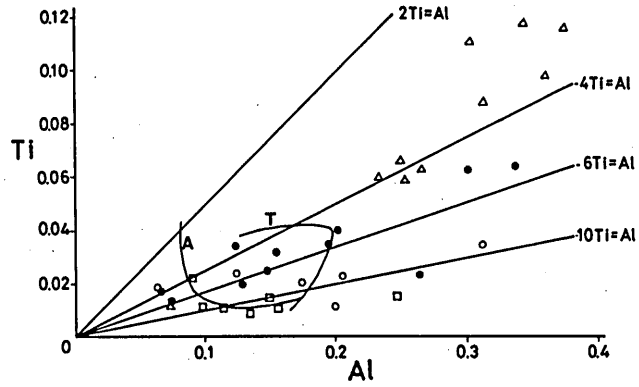

FIG. 16. Ti–Al relation in clinopyroxene from basalts and diabases. Symbols used are the same as those in Fig. 15. The curves A and T indicate, respectively, the lower limit of alkali basalt field and the upper limit of tholeiitic basalt field after MARUYAMA (1976).

and those in the Group II basalts. Most of augites in the former have Ti/Al ratio between 1/4 and 1/6, whereas those in the latter, for the most part, have Ti/Al ratio smaller than 1/6. While, salites in the Group III basalts are generally enriched in Al and Ti compared to clinopyroxenes in the other two groups of basalts. They mostly lie within the field of Ti/Al ratio between 1/2 and 1/4. Comparing with clinopyroxenes in these basalts the amounts of Ti and Al in clinopyroxenes in diabases are low.

In Fig. 16 are also shown the fields of tholeiitic and alkali basalts after MARUYAMA (1976). Most of analyses of clinopyroxenes from the Group III basalts and diabases are plotted in the alkali basalt field and the tholeiitic basalt field, respectively. While, majority of the analyses of clinopyroxenes from the Group I basalts and the Group II basalts is plotted in both alkali and tholeiitic basalt fields. Minor element chemistry of pyroxene can not always be used to identify magma type. Work on terrestrial basalt

TABLE 5. REPRESENTATIVE MICROPROBE ANALYSES OF CLINOPYROXENE IN ROCKS FROM THE JIZOJI GABBRO SILLS.

	1	2	3	4	5	6	7	8
	J913	J914	J915	J916	J917	J918	J919	J920
SiO_2	52.2	51.2	52.2	52.1	52.7	51.6	51.5	52.0
TiO_2	0.50	0.59	0.38	0.16	0.11	0.09	0.23	0.28
Al_2O_3	1.93	2.21	1.52	0.79	0.62	0.43	0.64	1.10
Cr_2O_3	0.11	0.07	0.07	0.04	0.05	0.02	0.06	0.05
FeO*	9.10	8.77	8.53	9.95	10.5	13.5	14.2	11.0
MnO	0.42	0.29	0.39	0.49	0.41	0.52	0.59	0.36
MgO	15.3	14.4	14.7	13.9	12.9	11.7	11.4	13.4
CaO	20.5	22.1	22.5	22.7	22.3	21.2	20.9	21.8
Na_2O	0.34	0.33	0.28	0.16	0.17	0.15	0.15	0.26
Total	100.40	99.96	100.57	100.29	99.76	99.21	99.67	100.25
O=6								
Si	1.923	1.916	1.940	1.956	1.988	1.982	1.967	1.956
Al^{IV}	0.077	0.084	0.060	0.035	0.012	0.018	0.029	0.044
Al^{VI}	0.007	0.014	0.007	—	0.016	0.001	—	0.005
Ti	0.014	0.017	0.011	0.005	0.003	0.003	0.007	0.008
Cr	0.031	0.002	0.002	0.001	0.001	0.001	0.002	0.001
Fe	0.280	0.274	0.265	0.312	0.331	0.433	0.454	0.346
Mn	0.013	0.009	0.012	0.016	0.013	0.017	0.019	0.012
Mg	0.840	0.803	0.814	0.777	0.726	0.673	0.649	0.751
Ca	0.809	0.886	0.895	0.913	0.899	0.872	0.855	0.878
Na	0.024	0.024	0.020	0.012	0.012	0.011	0.011	0.019
Total	4.018	4.029	4.026	4.027	4.001	4.011	3.993	4.020
Atomic %								
Ca	41.9	45.1	45.4	45.6	46.0	44.1	43.7	44.5
Mg	43.6	40.9	41.2	38.8	37.1	34.0	33.1	38.0
Fe	14.5	14.0	13.4	15.6	16.9	21.9	23.2	17.5

Table 5 (Continued)

	9	10	11	12	13	14	15	16
	J901	J902	J910	J818	J822	J1002	J1003	J1009
SiO_2	52.2	49.9	49.7	51.5	51.8	52.2	51.0	49.8
TiO_2	0.08	0.09	0.13	0.37	0.42	0.19	0.23	0.06
Al_2O_3	0.28	0.22	0.33	1.43	2.04	0.48	0.73	0.28
Cr_2O_3	0.06	0.06	0.05	0.15	0.05	0.04	0.04	0.01
FeO*	14.5	21.3	21.7	9.34	8.75	11.8	17.7	21.8
MnO	0.54	0.66	0.81	0.55	0.44	0.63	0.68	1.08
MgO	10.3	6.63	7.11	13.9	15.2	12.6	9.56	5.88
CaO	21.9	20.4	19.8	21.6	21.0	21.1	19.9	20.3
Na_2O	0.29	0.32	0.37	0.17	0.36	0.26	0.62	0.55
Total	100.15	99.58	100.00	99.01	100.06	99.30	100.46	99.76
O=6								
Si	1.999	1.987	1.973	1.949	1.930	1.987	1.972	1.987
Al^{IV}	0.001	0.010	0.015	0.051	0.070	0.013	0.028	0.013
Al^{VI}	0.012	—	—	0.013	0.019	0.008	0.005	—
Ti	0.002	0.003	0.004	0.010	0.012	0.005	0.007	0.002
Cr	0.002	0.002	0.002	0.005	0.002	0.001	0.001	0.000
Fe	0.464	0.707	0.719	0.295	0.273	0.376	0.572	0.727
Mn	0.018	0.022	0.027	0.018	0.014	0.020	0.022	0.036
Mg	0.589	0.393	0.420	0.783	0.843	0.715	0.550	0.349
Ca	0.895	0.869	0.840	0.876	0.838	0.860	0.824	0.867
Na	0.022	0.025	0.028	0.013	0.026	0.019	0.046	0.042
Total	4.004	4.018	4.028	4.013	4.027	4.004	4.027	4.023
Atomic %								
Ca	45.9	44.1	42.5	44.8	42.9	44.1	42.3	44.6
Mg	30.3	20.0	21.2	40.1	43.1	36.6	28.3	18.0
Fe	23.8	35.9	36.3	15.1	14.0	19.3	29.4	37.4

* Total iron as FeO.

1–8, 9–11 and 12–16 are clinopyroxenes from the Kashiyama, Aikawa and Higashi-ishihara sill sections, respectively. Cryptic variation in composition of the clinopyroxenes from the Kashiyama section is illustrated in Fig. 8. J901–J910 and J1002: Ferrogabbro, J818 and J822: Clinopyroxene gabbro. Other specimens are the same as those in Table 2. Analyzed by K. TAKEDA.

samples (e.g., COISH and TAYLOR, 1979) and experimental work on lunar picrite-basalt samples (e.g., WALKER et al., 1976) have shown that cooling rate affects significantly the contents of Al and Ti in pyroxene; i.e., Al and Ti in pyroxene increase with increasing cooling rate. This is especially important in the present case, because the analyzed clinopyroxenes in the Group I and Group II basalts are of microphenocryst and groundmass. In fact, there is a tendency that the groundmass clinopyroxenes showing quenched morphology tend to have high Al and Ti contents and are plotted in the alkali

basalt field in Ti–Al diagram. Such Al- and Ti-rich clinopyroxenes are considered to be products of disequlibrium crystallization, and therefore it can not be regarded as diagnostic of parent magma type.

Judging collectively from Ca/Mg+Fe ratio and concentrations of Al_2O_3 and TiO_2 of clinopyroxenes, it is concluded that the Group II basalts and diabases belong to tholeiitic affinity and the Group III basalts do to the alkaline affinity.

b. Gabbro sills

Representative analyses of clinopyroxenes from rocks of the Jizoji gabbro sills are listed in Table 5. In order to test fractionation model, change of clinopyroxene composition throughout sill section in terms of major elements has been examined in the Kashiyama section above all, because the section is nearly complete. Results are shown in Fig. 8. Regular change of Fe/Fe+Mg ratio of clinopyroxene, as an indicator of fractionation, is well established. The Fe/Fe+Mg ratio is nearly constant from the base to about 60 m above the base (specimens 40913–40915), and then gradually increases upward. After a maximum value of Fe/Fe+Mg ratio (0.41) has been reached for clinopyroxene (specimen 40919) from near two-third of the way from the base to the top of the sill, there is a decrease in Fe/Fe+Mg ratio of clinopyroxene upward. This fact can be interpreted that the fractionation is most advanced at near the two-third of the way from the base to the top of the sill.

All the analyses of clinopyroxenes from the Jizoji gabbro sills is plotted on the Ca—Mg—Fe diagram in Fig. 17. The figure indicates that the pyroxene compositions vary considerably among sill sections, with principally Fe—Mg substitution, an overall trend is characterized by a moderate iron-enrichment with gradual slight decrease in Ca content. Average trend of the clinopyroxenes from the three sill sections ranges approximately from $Ca_{46}Mg_{41}Fe_{13}$ to $Ca_{44}Mg_{17}Fe_{39}$. The clinopyroxenes from the Jizoji gabbro sills are more calcic than Ca-rich pyroxenes from well-documented tholeiitic intrusions such as Skaergaard (BROWN, 1957; BROWN and VINCET, 1963), Bushveld (ATKINS, 1969) and Palisades (WALKER et al., 1973), and especially Ca content of the Jizoji clinopyroxenes

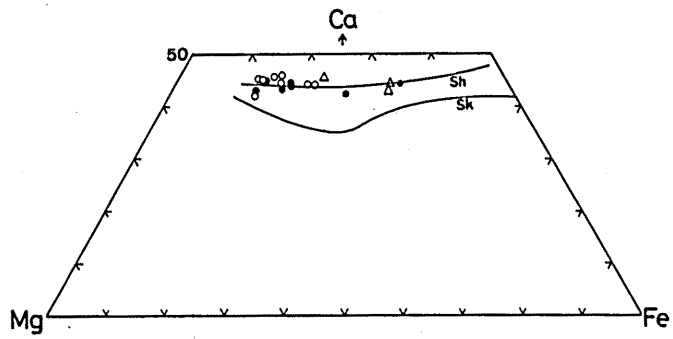

FIG. 17. Ca—Mg—Fe diagram for clinopyroxene from the Jizoji gabbro sills. Data for the Jizoji sills are plotted for individual sill section (open circle: Kashiyama section, closed circle: Aikawa section, triangle: Higashi-ishihara section). The solid lines Sk and Sh indicate, respectively, the crystallization trends for Ca-rich pyroxene from the Skaergaard intrusion (BROWN, 1957; BROWN and VINCET, 1963) and from the Shiant Isles sill (GIBB, 1973).

is rather comparable with that of clinopyroxenes crystallized from mildly alkaline magma, as in the Shiant Isles sill (GIBB, 1973).

Variation in major element cations, Ca, Mg and Fe, is accompanied by changes in minor elements. Distribution of Al and Ti in the Jizoji clinopyroxenes is somewhat random, but there are overall trends toward lower Al and Ti contents with increasing Fe/Fe+Mg ratio, as in the Skaergaard Ca-rich pyroxenes. Na seems to increase slightly with fractionation, although there is a considerable scatter in the data. Mn increases with fractionation. Cr content is low and decreases rapidly. Al and Ti contents of the Jizoji clinopyroxenes are characteristically low (Fig. 18), and are consistent with the properties of tholeiitic pyroxenes crystallized at crustal level.

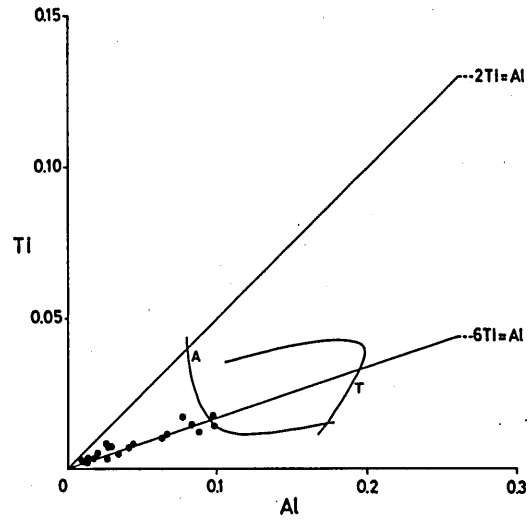

FIG. 18. Ti–Al relation for clinopyroxene from the Jizoji gabbro sills. The solid curves A and T are the same as those in Fig. 16.

c. Peridotite-gabbro complexes

Results of microprobe analyses of clinopyroxenes from various rock types in the peridotite-gabbro complexes are shown in Table 6. The variation in major element compositions of the clinopyroxenes is shown in the Ca—Mg—Fe diagram in Fig. 19. Ca content, in general, increases from 41 to 46 atomic percent, while Fe content varies from 8 to 15 atomic percent as host rock changes from ultramafic rocks to gabbros. This suggests a genetic link between the ultramafic rocks and their associated gabbros.

The clinopyroxenes contain relatively small amount of Al_2O_3 (2.14–4.19 percent) and TiO_2 (0.31–1.09 percent). No systematic variation of Al_2O_3 and TiO_2 contents in the clinopyroxenes with increasing Fe content is found. Some of clinopyroxenes from peridotites contain high amount of Cr_2O_3 more than 1 percent, therefore they belong to the category of chromian endiopside.

The Ca-increasing trend with iron enrichment of the clinopyroxenes from the peridotite-gabbro complexes in question differs markedly from the trend of clinopyroxenes from the Jizoji gabbro sills, as shown in the preceding section. This fact suggests that both the two rock groups are not genetically related and are hardly produced from a common magma and physical conditions.

In Fig. 19 chemical data of clinopyroxenes from ultramafic complexes in other areas of the Mikabu belt are also plotted for comparison. The present clinopyroxenes are most similar to those from the northern Kanto mountains (TAZAKI and INOMATA, 1974) and Ufu-san, central Japan (INOMATA and TAZAKI, 1974) in regard to content of the major elements and to the crystallization trend. Similar Ca-increasing trend of clinopyroxene is also observed in clinopyroxene from some ultramafic complexes, for example, Union Bay (RUCKMICK and NOBLE, 1959), which is one of the best example of zoned ultramafic complexes, Greenhills in New Zealand (MOSSMAN, 1973), Hayachine in the Kitakami

TABLE 6. REPRESENTATIVE MICROPROBE ANALYSES OF CLINOPYROXENE IN ULTRAMAFIC ROCKS AND ASSOCIATED GABBROS.

	PIII	PII	PI	H	C	PII	GI	GII
	T2914	J1	H2602	T2502	T2906	H2013	T2916	T305
SiO_2	52.3	50.9	50.8	51.6	50.7	51.7	50.2	51.3
TiO_2	0.59	0.69	0.69	0.81	0.51	1.01	0.80	0.41
Al_2O_3	2.26	3.17	3.32	2.40	4.19	2.81	3.98	2.14
Cr_2O_3	1.11	1.08	1.06	0.93	0.89	0.67	0.21	0.08
FeO*	5.26	5.40	5.37	5.98	5.76	6.33	7.73	8.50
MnO	0.22	0.21	0.16	0.26	0.19	0.28	0.24	0.33
MgO	18.0	16.4	16.2	17.4	15.8	16.3	15.0	14.9
CaO	20.8	21.5	21.9	20.3	20.7	21.0	21.0	21.7
Na_2O	0.28	0.37	0.32	0.28	0.32	0.39	0.35	0.36
Total	100.82	99.72	99.82	99.96	99.06	99.79	99.51	99.72
O=6								
Si	1.905	1.882	1.878	1.900	1.873	1.889	1.873	1.921
Al^{IV}	0.095	0.118	0.122	0.100	0.127	0.111	0.127	0.079
Al^{VI}	0.002	0.020	0.023	0.006	0.057	0.012	0.048	0.016
Ti	0.016	0.019	0.019	0.022	0.013	0.028	0.022	0.012
Cr	0.032	0.032	0.031	0.027	0.027	0.020	0.005	0.002
Fe	0.160	0.167	0.166	0.183	0.180	0.195	0.242	0.265
Mn	0.007	0.007	0.005	0.009	0.007	0.009	0.009	0.010
Mg	0.978	0.906	0.893	0.954	0.882	0.901	0.837	0.832
Ca	0.810	0.852	0.867	0.780	0.830	0.834	0.839	0.869
Na	0.020	0.027	0.023	0.022	0.022	0.029	0.027	0.026
Total	4.025	0.030	4.027	4.003	4.018	4.028	4.029	4.032
Atomic %								
Ca	41.6	44.3	45.0	40.7	43.9	43.2	43.8	44.2
Mg	50.2	47.0	46.4	49.8	46.6	46.7	43.6	42.3
Fe	8.2	8.7	8.6	9.5	9.5	10.1	12.6	13.5

* Total iron as FeO.

PI: Clinopyroxene peridotite, PII: Clinopyroxene-hornblende peridotite, PIII: Hornblende peridotite, C: Hornblende clinopyroxenite, H: Hornblendite, GI: Clinopyroxene-hornblende gabbro, GII: Hornblende-clinopyroxene gabbro. Analyzed by K. TAKEDA.

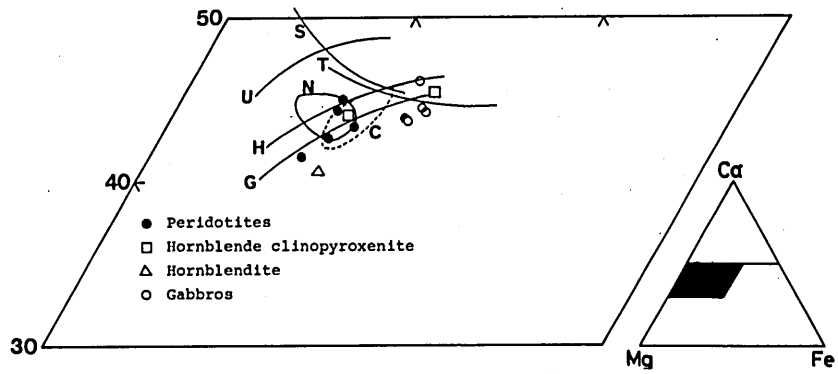

FIG. 19. Ca—Mg—Fe diagram for clinopyroxene from peridotite-gabbro complexes. Included for comparison are the trends and fields of clinopyroxenes from ultramafic complexes at other localities in the Mikabu belt and from well-known ultramafic complexes in the world. Abbreviations used are: N=northern Kanto mountains (TAZAKI & INOMATA, 1974), S=Shiokawa, central Japan (MAKIMOTO, 1978), C=Ufu-san and Tonmaku-yama, central Japan (INOMATA & TAZAKI, 1974), T=Toba, Kii peninsula (NAKAMURA, 1971), U=Union Bay (RUCKMICK & NOBLE, 1959), G=Greenhills (MOSSMAN, 1973), H=Hayachine (ONUKI, 1963).

mountains, northeast Japan (ONUKI, 1963). These trends are nearly parallel to each other and also to the Mikabu trend in question, but lie more calcic and magnesian side than in the Mikabu (Fig. 19).

It is noteworthy that ultramafic complexes, in which clinopyroxene shows the Ca-increasing trend with increasing iron, are characteristically accompanied with plentiful primary hornblende. MURRAY (1972) suggested that the Ca-increasing trend of clinopyroxene from the zoned ultramafic complexes is due to high water pressure which would inhibit the crystallization of plagioclase, and all Ca available in the magma enters into pyroxene. This explanation appears to be applicable to the Ca-increasing trend of the clinopyroxene in question. High water pressure is perhaps responsible for the restricted iron-enrichment of the clinopyroxene compared with that from the Jizoji gabbro sills.

2. Brown hornblende

Widespread appearance of brown hornblende is a characteristic of rocks in the peridotite-gabbro complexes. Table 7 lists representative microprobe analyses of brown hornblende from rocks of various rock types. The hornblende is calciferous and its Al_2O_3 content ranges from 7.61 to 12.1 percent. K_2O content is rather low (less than 0.53 percent). CaO content is almost constant (11 to 12 percent) with MgO and FeO being variable. The plot of all analyses on the Al^{IV}—Na+K diagram (Fig. 20) shows that the amphibole composition is rather close to the pargasite composition together with molecules of hornblende and edenite. Much of the amphibole belong to pargasite in the classification of LEAKE (1968). This pargasite is rich in TiO_2 (2.66 to 5.30 percent), so that it is Ti-pargasite. Kaersutite is defined as Ti-rich amphibole with Ti content of 0.5 to 1.0 atoms per formula unit or approximately 5 percent or more by weight (WILKINSON, 1961, AOKI, 1963; LEAKE, 1968). Accordingly, some of Ti-amphiboles

TABLE 7. REPRESENTATIVE MICROPROBE ANALYSES OF BROWN HORNBLENDE IN ULTRAMAFIC ROCKS AND ASSOCIATED GABBROS.

	PI	PII	HI	PII	C	PIII	GI	GIII
	H2602	H2013	T1205	J1	T2906	T2914	T2916	T1102
SiO_2	45.5	44.6	42.0	40.4	41.4	41.4	43.2	44.0
TiO_2	3.74	4.13	5.01	5.30	3.68	3.86	3.04	2.66
Al_2O_3	7.61	8.39	11.7	11.4	11.3	10.9	9.16	10.2
FeO*	6.65	7.90	8.74	8.96	12.0	12.3	16.1	16.3
MnO	0.23	0.14	0.17	0.24	0.23	0.25	0.48	0.54
MgO	17.8	17.5	14.6	15.0	14.3	14.1	12.2	11.0
CaO	11.1	11.3	11.8	11.7	11.3	11.1	10.3	9.03
Na_2O	3.54	3.24	2.53	3.26	2.84	2.95	2.60	3.32
K_2O	0.47	0.53	0.18	0.42	0.19	0.50	0.22	0.35
Total	96.64	97.73	96.73	96.68	97.24	97.36	97.30	97.40
O=23								
Si	6.615	6.475	6.174	6.001	6.156	6.176	6.506	6.593
Al^{IV}	1.303	1.433	1.826	1.998	1.844	1.824	1.494	1.407
Al^{VI}	—	—	0.193	—	0.137	0.086	0.130	0.392
Ti	0.409	0.450	0.552	0.591	0.410	0.432	0.344	0.298
Fe	0.833	0.955	1.070	1.180	1.486	1.523	2.017	2.032
Mn	0.029	0.017	0.021	0.030	0.029	0.032	0.061	0.069
Mg	3.862	3.769	3.201	3.305	3.159	3.131	2.732	2.460
Ca	1.731	1.758	1.851	1.855	1.794	1.761	1.656	1.446
Na	0.997	0.910	0.720	0.965	0.817	0.852	0.757	0.962
K	0.088	0.098	0.033	0.080	0.037	0.094	0.042	0.067
Total	15.867	15.865	15.641	15.933	15.869	15.911	15.739	15.726
mg**	81.8	79.5	74.6	74.4	67.6	66.8	56.8	53.6

* Total iron as FeO. ** mg=100Mg/Mg+Fe+Mn.
Rock types PI, PII, PIII, C, GI and GII are the same as those in Table 6. Others, HI: olivine hornblendite, GIII: Hornblende gabbro. Analyzed by K. TAKEDA.

from peridotites and olivine hornblendites correspond to kaersutite.

The composition of the Ti-rich amphiboles changes as the host rock does. That implies the compositional variation of the amphiboles with fractionation. The 100Mg/Mg+Fe+Mn ratio, as a best measure of fractionation, shows a range of 81.8 to 53.9 and is, generally, higher in peridotites (81.8–66.8) and hornblendites (76.0–66.0) and lower in hornblende clinopyroxenites (67.5–62.5) and gabbros (67.5–53.9). Fig. 21 shows the plots of Si, Al and Ti against 100Mg/Mg+Fe+Mn ratio. The points in the figure are rather scattered, but overall trends can be drown. Si decreases with increasing Fe until the 100Mg/Mg+Fe+Mn ratio reaches about 70, and then increases gradually with further increase in Fe. Al shows the reciprocal relationship to Si, indicating Si–Al substitution in the tetrahedral site, while Ti shows the sympathetic relationship to Al. Total alkali appears to exhibit no systematic variation trend against 100Mg/Mg+Fe+Mn ratio.

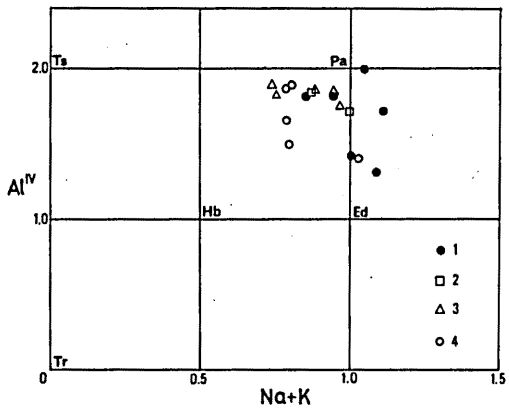

FIG. 20. Al^{IV} vs. Na+K diagram for brown hornblende from (1) peridotites, (2) hornblende clinopyroxenite, (3) olivine hornblendite and hornblendite, and (4) gabbros. Ed=edenite, Hb=hornblende, Tr=tremolite, Ts=tschermakite, Pa=pargasite.

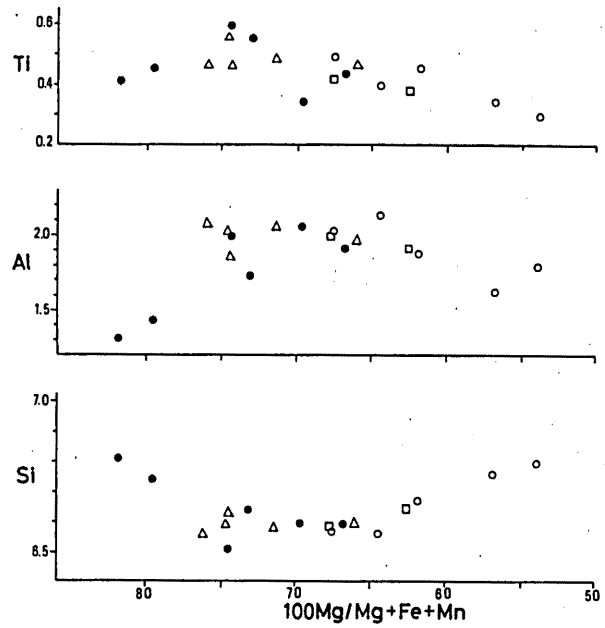

FIG. 21. Variation of Si, Al and Ti with 100Mg/Mg+Fe+Mn for brwon hornblende. Symbols used are the same as those in Fig. 20.

The occurrence of Ti-pargasite and kaersutite has also been reported from ultrmafic rocks in the Mikabu belt in the northern Kanto mountains (TAZAKI and INOMATA, 1974) and central Japan (INOMATA and TAZAKI, 1974).

3. Phlogopite

Occasionally, phlogopite occurs interstitially in some peridotites. Apparently fresh phlogopite shows reddish-brown pleochroic color. The electron microprobe analysis has revealed that it is titaniferous phlogopite containing 5.47 to 7.62 percent TiO_2 (Table

TABLE 8. MICROPROBE ANALYSES OF PHLOGOPITE IN CLINOPYROXENE PERIDOTITE.

	1	2	O=23	1	2
SiO_2	36.7	37.2	Si	5.343	5.391
TiO_2	7.62	5.47	Al^{IV}	2.309	2.289
Al_2O_3	13.5	13.4	Al^{VI}	—	—
FeO*	7.91	9.06	Ti	0.833	0.597
MnO	0.20	0.23	Fe	0.962	1.100
MgO	20.1	21.7	Mn	0.025	0.028
CaO	0.04	0.04	Mg	4.354	4.694
Na_2O	1.18	1.08	Ca	0.007	0.006
K_2O	7.22	6.59	Na	0.332	0.304
			K	1.341	1.220
Total	94.47	94.77	Total	15.506	15.629

* Total iron as FeO. Columns 1 and 2: data for two different grains from a specimen H2602. Analyzed by K. TAKEDA.

TABLE 9. MICROPROBE ANALYSES OF CHROMIAN SPINEL IN PICRITE-BASALT.

	1	2	3
TiO_2	2.80	2.90	3.09
Al_2O_3	10.8	11.0	15.3
Cr_2O_3	42.9	41.9	35.9
Fe_2O_3*	10.1	10.4	11.5
FeO*	24.9	25.1	26.1
MnO	0.36	0.37	0.38
MgO	6.83	6.75	6.75
Total	98.69	98.42	99.02
O=32			
Ti	0.577	0.599	0.623
Al	3.480	3.563	4.824
Cr	9.290	9.092	7.611
Fe^{3+}	2.075	2.148	2.318
Fe^{2+}	5.706	5.753	5.840
Mn	0.084	0.086	0.087
Mg	2.787	2.760	2.696

* Fe_2O_3 and FeO computed from total iron assuming perfect spinel stoichiometry. Columns 1, 2 and 3: data for three different grains of chromian spinel in a groundmass from a specimen T2606. Analyzed by A. MINAMI.

8). Its Na_2O content is fairly high. Accordingly, it is possible that Na ion replaces the octahedral K ion in the phlogopite.

4. Chromian spinel

Chromian spinel is commonly found in picrite-basalts and peridotites. Chromian

TABLE 10. MICROPROBE ANALYSES OF CHROMIAN SPINEL IN PERIDOTITE.

	H1303B-2						
	1	2	3	4	5	6	7
TiO_2	4.64	2.89	0.69	0.71	1.05	6.49	7.82
Al_2O_3	12.2	14.6	31.3	31.4	29.1	9.05	2.10
Cr_2O_3	17.0	22.3	24.5	25.3	24.5	19.4	8.81
Fe_2O_3*	26.7	25.5	12.3	10.8	12.8	25.2	40.1
FeO*	32.4	28.2	19.8	19.4	20.9	34.4	34.9
MnO	2.61	1.20	0.51	0.47	0.60	3.44	2.26
MnO	1.05	4.50	11.3	11.4	10.2	0.37	0.30
Total	96.6	99.19	100.40	99.48	99.15	98.35	96.29
O=32							
Ti	1.019	0.596	0.125	0.129	0.195	1.427	1.832
Al	4.179	4.708	8.864	8.952	8.452	3.121	0.772
Cr	3.917	4.826	4.659	4.833	4.776	4.481	2.171
Fe^{3+}	5.867	5.274	2.227	1.957	2.383	5.543	9.392
Fe^{2+}	7.915	6.475	3.979	3.929	4.307	8.412	9.096
Mn	0.644	0.279	0.104	0.095	0.125	0.853	0.596
Mg	0.459	1.842	4.043	4.105	3.763	0.162	0.141

	H1303A-1					
	8	9	10	11	12	13
TiO_2	0.72	0.99	3.03	4.79	5.09	0.24
Al_2O_3	31.2	27.6	19.7	13.4	11.4	3.19
Cr_2O_3	26.3	26.4	24.8	21.3	18.8	12.6
Fe_2O_3*	10.3	13.8	16.6	23.7	26.3	52.3
FeO*	19.3	20.5	28.0	32.1	33.5	28.1
MnO	0.47	0.52	1.29	1.94	2.55	0.48
MgO	11.6	10.6	5.16	2.67	1.01	1.98
Total	99.89	100.41	98.58	99.90	98.65	98.89
O=32						
Ti	0.130	0.183	0.609	0.999	1.099	0.055
Al	8.855	7.982	6.200	4.390	3.854	1.127
Cr	5.013	5.113	5.246	4.672	4.260	2.984
Fe^{3+}	1.872	2.539	3.336	4.940	5.689	11.779
Fe^{2+}	3.886	4.198	6.259	7.440	8.048	7.047
Mn	0.096	0.108	0.293	0.455	0.619	0.122
Mg	4.148	3.877	2.057	1.105	0.432	0.885

* Fe_2O_3 and FeO computed from total iron assuming perfect spinel stoichiometry.
H1303B-2: Spinel with chemical zoning, illustrated in Fig. 22.
H1303A-1: Spinel with chemical zoning, 8 and 9=core, 10=outer zone of core, 11–13=rim.
Analyzed by K. TAKEDA.

spinel grains in picrite-basalts are euhedral and optically homogeneous. Three microprobe analyses of groundmass chromian spinel have been made for the sample T2606 of picrite-basalt, and the analytical results are given in Table 9. FeO and Fe_2O_3 values are calculated from total iron by assuming the spinels are stoichiometric with 3 cations per 4 oxygens. The chromian spinels show no chemical zoning and range in $Mg/Mg+Fe^{2+}$ ratio from 0.32 to 0.33 and in $Cr/Cr+Al$ ratio from 0.61 to 0.73. They are fairly enriched in Ti (more than 2.8 percent TiO_2).

The ore microscopic observation on polished thin sections revealed that most of chromian spinel grains from peridotites have more or less rounded shape and are armored with magnetite. The chromian spinel grains are commonly optically homogeneous, but show occasionally zoning which is visible due to reflectivity difference. The chromian spinel with optical zoning consists of a dark grey core surrounded by a rim of chromian spinel of low reflectivity. At the contact the core and the rim of chromian spinel is sharply bounded.

In Fig. 22 are summarized the microprobe data (Table 10) of compositional variation across a spinel grain with typical optical zoning (H1303B-2) from a clinopyroxene peridotite. The spinel grain with optical zoning is chemically divided into three parts, core, outer zone of core and rim. The boundary between the outer zone of core and the rim of chemical zoning corresponds to that between the core and the rim of optical zoning. The core of the chromian spinel is nearly homogeneous with a slight increase in iron oxides, minor decerase in Al_2O_3 and MgO, and constant or slightly decreasing Cr_2O_3 toward its margin. While, the outer zone of core is distinguished from the core by abrupt decrease in Al_2O_3 and MgO, abrupt increase in iron oxides, TiO_2 and MnO and

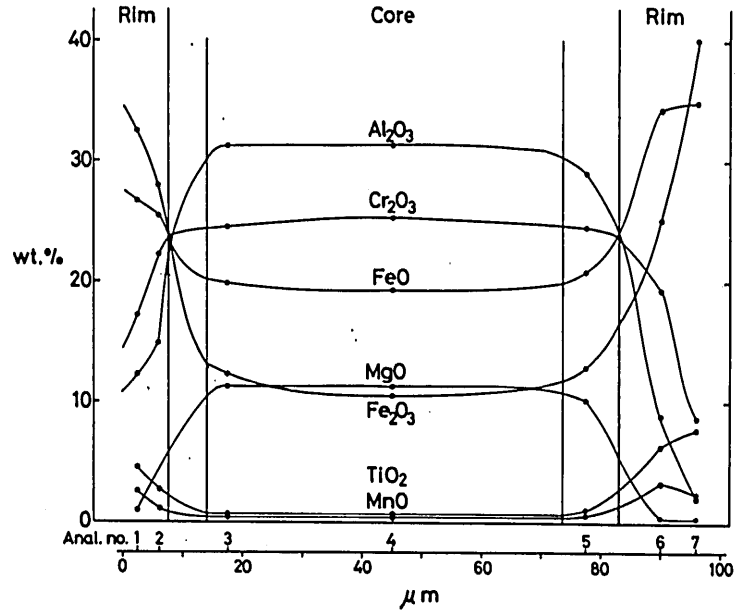

FIG. 22. Compositional variation across a spinel grain with typical zoning (H1303B-2). Analysis numbers (Anal. no.) above abscissa are the same as those in Table 10.

slight decrease in Cr_2O_3. Sharp decrease in Cr_2O_3 as compared with the outer zone of core, followed by further gradual decrease, is characteristic of the rim. Iron oxides, TiO_2 and MnO continue to increase and Al_2O_3 and MgO decrease gradually and reach negligible amounts in the outermost rim. In the outermost rim of certain zoned chromian spinel grains (e.g., H1303A–1 in Table 10) from the same sample of clinopyroxene peridotite depletion in TiO_2 is observed. The microscopic observation shows that intergrowth of magnetite and sphene is invariably seen around such Ti-depleted chromian spinel grains.

The chromian spinels from the peridotite are ferritchromites, ranging in Cr/Cr+Al ratio from 0.34 to 0.39 in the core (Fig. 23). They are also enriched in TiO_2 and its value varies largely in function of Fe^{3+}/Al+Cr+Fe^{3+} ratio, and increases generally with increasing Fe^{3+} content, to the maximum of approximately 7.8 weight percent (Fig. 24). This variation can be expressed, in molecular terms, by increase of ulvöspinel with increasing magnetite. Interestingly, the chemical data for chromian spinels from the Mikabu peridotite do not fall within the compositional fields of chromian spinel from alpine-type peridotites and stratiform intrusions (Figs. 23 & 24). The chromian spinels from the Mikabu peridotite have higher TiO_2 content and lower Cr/Cr+Al ratio, higher and variable Fe^{3+}/Al+Cr+Fe^{3+} ratio than those from the latter two (cf. Dickey, 1975), and in this respect they are more akin to chromian spinels from volcanic rocks (e.g., Leg

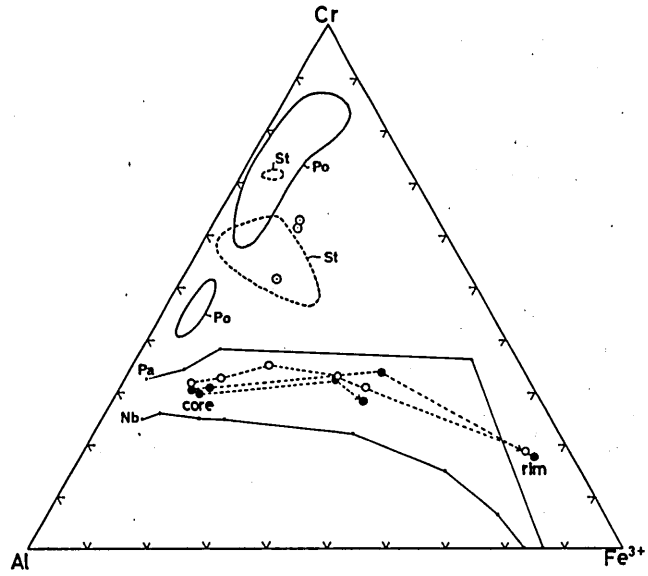

Fig. 23. Cr—Al—Fe^{3+} diagram for chromian spinels from picrite-basalt (open circle with dot) and clinopyroxene peridotite (open circle: H1303A–1, closed circle: H1303B–2). The fields Po and St are for chromian spinels from "podiform chromite deposits" in alpine-type peridotites and from layered stratiform intrusions, respectively (data from Dickey, 1975). The solid lines Pa and Nb indicate the compositional changes of spinels from Leg 6 basalts in the Parace Vela Basin of Philippine Sea (Ridley et al., 1974) and Nanzaki basanitoid (Shiraki et al., 1979), respectively.

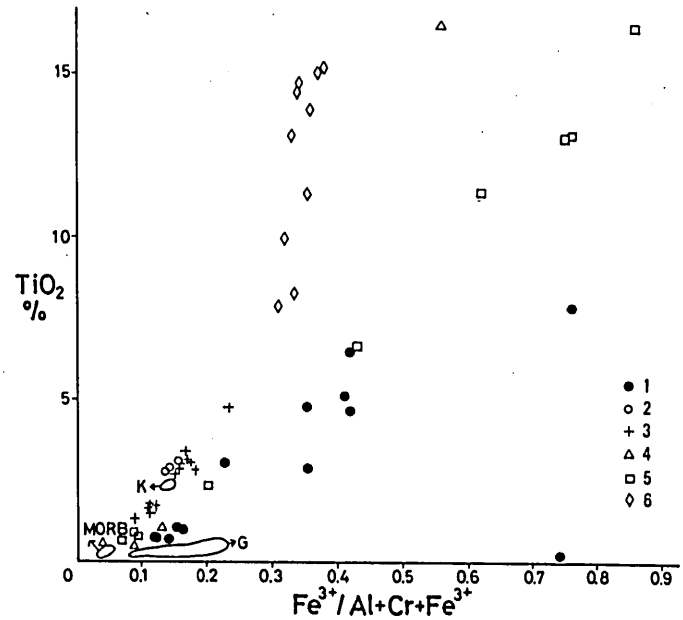

FIG. 24. Weight percent of TiO_2 plotted against $Fe^{3+}/Al+Cr+Fe^{3+}$ for chromian spinels from picrite-basalt and clinopyroxene peridotite. Data for spinels from some volcanic rocks are also included for comparison: 1=clinopyroxene peridotite (this work), 2=picrite-basalt (this work), 3=Mineoka picrite-basalt (TAZAKI, 1975), 4=Leg 6 basalts (RIDLEY et al., 1974), 5=Nanzaki basanitoid (SHIRAKI et al., 1979), 6=Snake River Plain basalt (THOMPSON, 1973). MORB, K and G indicate the fields for spinels from Mid-Atlantic Ridge basalts (SIGURDSSON & SCHILLING, 1976), Hawaiian tholeiites (Kilauea Iki, EVANS & WRIGHT, 1972), and tholeiitic and calc-alkali basalts of Guam (SHIRAKI et al., 1977), respectively.

6 basalts of Philippine Sea, RIDLEY et al., 1974; Nanzaki basanitoid, SHIRAKI et al., 1979), in which chromian spinel of intermediate composition between chromite and titanomagnetite is commonly found.

Ferritchromite has often been found at the rim around chromite core in serpentinites from alpine-type peridotites and stratiform intrusions (BEESON and JACKSON, 1969; ULMER, 1974). The formation of ferritchromite has been variously attributed, such as to serpentinization, regional metamorphism and magmatic alteration (see duscussion by BLISS and MACLEAN, 1975). Although there is no clear evidence, the ferritchromite core in the Mikabu peridotite might have been formed by direct precipitation from magma. It is highly possible that the formation of magnetite rim around the ferritchromite core is attributed to serpentinization or regional (Sambagawa) metamorphism or both. The compositional variation of the zoned chromian spinels probably corresponds to falling temperature and increasing crystallization of chromian spinel, presumably accompanied by an increase in fO_2. The Ti-depleted rim of certain grains is probably due to alteration of originally Ti-enriched one by a secondary process. Oxygen fugacities increased presumably during this process and with sufficient increase in fO_2 after accumulation, so that TiO_2 have exsolved by oxidation of Fe_2TiO_4, a component in chromian spinel, and

used to form sphene.

It is to be noted that a significant difference of composition between the chromian spinels from the picrite-basalt and those from the peridotite can be found (Figs. 23 & 24); i.e., Cr/Cr+Al ratio and TiO_2 content at a given value of $Fe^{3+}/Al+Cr+Fe^{3+}$ ratio are higher for chromian spinels from the picrite-basalt than are for those from the peridotite. This difference in composition of chromian spinels might have been affected by the difference in magma compositions from which the spinels crystallized and physical environments.

IV. Discussions and Conclusions

A. Genetic Relationship Among Volcanic Rocks and Between Volcanic Rocks and Intrusive Rocks

The mineralogical and petrochemical data presented in the preceding chapters provided much insight into the compositional charactersitics of each rock unit of the Mikabu greenstones and demonstrated chemical diversity among them. Here, genetic relationship among volcanic rocks and between volcanic rocks and intrusive rocks are discussed based on the difference in chemical composition and on the geological occurrence.

In Fig. 25, weight percent of TiO_2 of basalts, diabases and a chilled marginal rock of gabbro sill is plotted against the FeO*/MgO ratio. Significant difference of TiO_2 content is observed between the picrite-basalts and the tholeiitic basalts; i.e., the former has higher TiO_2 content at equivalent FeO*/MgO ratio than has the latter. Ti is generally believed to be one of most immobile elements during processes of secondary alteration (Pearce and Cann, 1973). Hence its value probably represents the primary igneous value. A similar difference is apparent on the FeO* versus FeO*/MgO diagram in Fig. 26. The difference may be due to the presence of titanomagnetite, a cumulus phase in picrite-basalts, which may be expected to occur in rocks with high FeO*/MgO ratios. However, the microscopic observation reveals that the picrite-basalts do not contain the titanomagnetite. An alternative explanation might be that the separation of the picrite-basalts and the tholeiitic basalts on these plots was resulted from selective loss of MgO from the more altered tholeiitic basalts. But even if such a loss of MgO might have occurred, it is hardly difficult to reconcile with the observed variations in terms of TiO_2 and FeO* abundances between both basalts. Therefore, it is unlikely that the tholeiitic basalts have been derived by fractional crystallization from the magma that produced the parent picrite-basalts.

Similarly, at a given value of FeO*/MgO, alkali basalts deviate from the trends defined by the tholeiitic basalts and the picrite-basalts. Moreover, the alkali basalts do not lie along the expected fractionation trends of the tholeiitic basalts and picrite-basalts. Therefore, simple shallow-level fractionation can not account for the major element variations in the picrite-basaltic, tholeiitic and alkali basalts. It is likely that these three types of basalt were generated from the three separate parent magmas. With respect to amount, the tholeiitic basalts appear to predominate over the picrite-basalts and the alkali basalts. It is difficult, however, at this time to explain exactly the spatial distribution of the three types of basalt and to determine the sequence of eruption of the basalts, because of lack of systematic geological and chemical data.

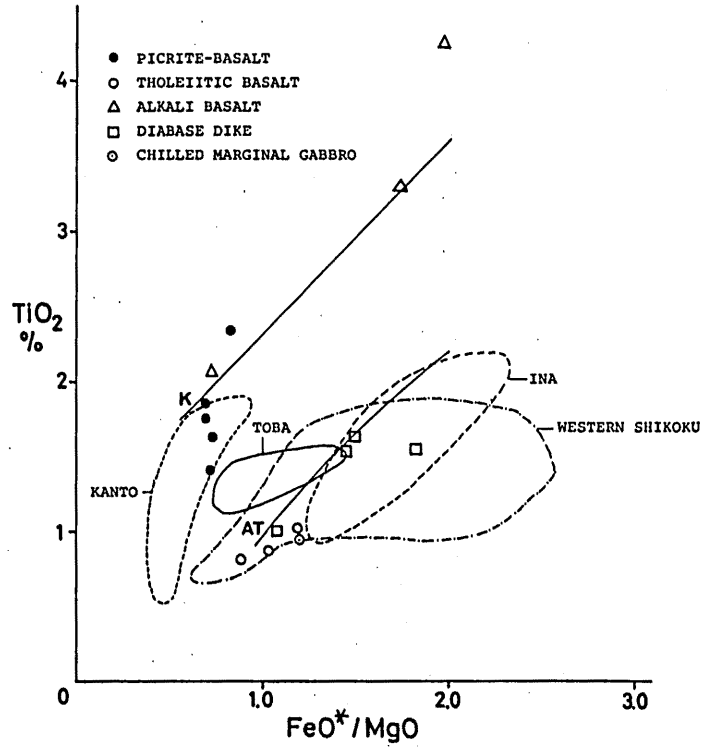

FIG. 25. Weight percent of TiO_2 plotted against FeO*/MgO for basalts, disbase dikes and chilled marginal gabbro in the Mikabu greenstones of eastern Shikoku. The compositional fields of basalts and diabases from other regions in the Mikabu belt are also shown for comparison: data sources; Kanto (UCHIDA, 1967), Ina (WATANABE et al., 1978), Toba (NAKAMURA, 1971), western Shikoku (SUZUKI et al., 1971, 1972; TANAKA, 1977). K and AT indicate, respectively, the average fractionation trends of Kilauea lavas (data sources: MUIR and TILLEY, 1957, 1963; TILLEY, 1960; MACDONALD and KATSURA, 1961, 1964; MURATA and RICHTER, 1966) and abyssal tholeiites (after MIYASHIRO, 1975).

Diabases and rocks from gabbro sills show the tholeiitic character. It is seen from the Figs. 25 and 26 that the analytical data of the diabases and the chilled marginal rock of gabbro sill lie on the presumed trend lines of the tholeiitic basalts; i.e., they show increasing TiO_2 and FeO* trends with increasing FeO*/MgO ratio. Therefore, it is reasonable to suppose that these tholeiitic rocks have been derived from a common magma. The diabases and the chilled marginal rock are slightly but significantly enriched in iron than are the tholeiitic basalts, and this suggests their formation near the surface intrusion of tholeiitic magma at advanced stages of fractional crystallization. The tholeiitic gabbros are strongly differentiatted in place, giving rise to high-iron and high-titanium gabbros and plagiogranites at later crystallization stages.

Close spatial association of ultramafic rocks with gabbroic and albititic rocks appears to indicate that they form genetically related suite. This may be supported by systematic

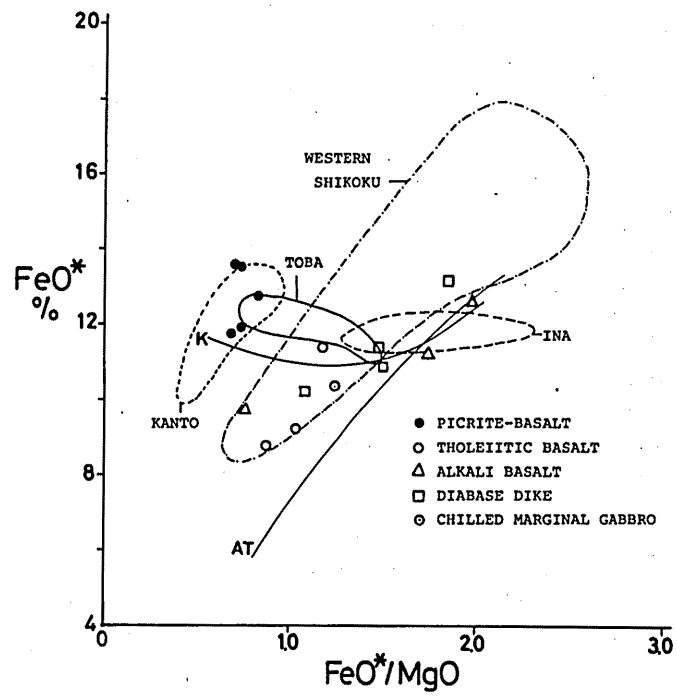

FIG. 26. Weight percent of FeO* plotted against FeO*/MgO for basalts, diabase dikes and chilled marginal gabbro in the Mikabu greenstones of eastern Shikoku. The compositional fields of basalts and diabases from Kanto, Ina, Toba and western Shikoku in the Mikabu belt are also shown for comparison (see Fig. 25 for data sources). K and At are the same as those in Fig. 25.

chemical trends of some silicate minerals such as clinopyroxene and brown hornblende among the suite; the Mg/Mg+Fe ratio of these minerals varies rather systematically among rock types, and, generally, its value is higher in minerals from olivine-bearing rocks and lower in those from plagioclase-bearing rocks. These features would suggest that the peridotite-gabbro complexes formed by magmatic differentiation processes from a single parent magma.

The minerals from the peridotite-gabbro complexes can not be used to estimate temperature and pressure conditions, because none of them are in a critical assemblage from which physical conditions may be predicted. All assemblages are relatively poor in Al_2O_3. This fact may be taken as an evidence for crystallization relatively lower, but undetermined pressures of crystallization.

The distribution of each type of rocks in the peridotite-gabbro complexes is rather chaotic and it can not be explained by differentiation process in situ. Albitites in the complexes are often subjected to granulation and mylonitization. Deformation during the emplacement might be responsible for the brittle deformation of the albitites. It is likely that the peridotite-gabbro complexes had crystallized and differentiated in a magma chamber at some depth below the volcanic sequence, and that they were emplaced into the volcanic sequence by a later orogeny as solid masses.

Although rocks that seem to represent the composition of primary magma of the peridotite-gabbro complexes are absent, their mineralogical features may be used to infer the composition of primary magma. Abundant occurrence of primary amphibole in the complexes suggests that water was an important component of the magma throughout the crystallization of rocks in them. The amphibole is Ti-rich varieties such as Ti-pargasite and kaersutite, and hence it seems that the rocks have been derived from Ti-rich magma. The Ti-rich nature of the magma is also shown by the presence of cumulus titanian chromian spinel and titaniferous phlogopite as an intercumulus precipitate in peridotites. The presence of kaersutite is indicative of crystallization from silica-undersaturated magma, because kaersutite is generally a phase known only from the precipitate of silica-undersaturated magma (WILKINSON, 1961). Judging from the above, most probably a magma of alkaline (ankaramitic) composition, enriched in water and TiO_2, is envisaged for the parent magma of the ultramafic rocks and their associated gabbros. The significantly greater Fe/Fe+Mg ratio of the early precipitating ferromagnesian minerals in these rocks implies that the rocks have been formed at a more advanced, or low temperature, stages of crystallization.

The peridotite-gabbro complexes and the picrite-basalts may be related each other genetically. The peridotites are fairly iron-enriched and may represent cumulates from the magma that produced the picrite-basalts. However, chemical difference of chromian spinel from both kinds of rocks appears to preclude its possibility. Alternatively, the peridotite-gabbro complexes may represent plutonic equivalents of the alkaline magma that gave rise to lavas of alkaline composition. This is highly probable, but the ubiquitous presence of primary amphibole in the peridotite-gabbro complexes, in particular, provides a striking contrast to the alkali basalts, which lack that phase entirely. Exceptionally hydrous condition under which the peridotite-gabbro complexes have crystallized might have been attained within the magma chamber. Although there is no clear evidence, that probably resulted from entry and mixing of introduced (ocean?) water. Soda-rich silicic rocks represented by albitites which occur as thin dikelets or large irregular bodies within the peridotite-gabbro complexes can be interpreted as products from hydrothermal solution. Small, abundant miarolitic cavities often filled with pyrite are a distinctive feature of some alibitite. Retrograde boiling is thought to be responsible for their formation; gas steaming is a probable explanation. Some gabbros have metasomatically altered by the hydrothermal soda-rich solution.

B. CHARACTERISTICS OF THE MIKABU THOLEIITIC BASALTS

The tholeiitic basalts in the Mikabu greenstones have characteristic chemical compositions. First, they are significantly depleted in TiO_2, which is correlated to the field of the abbysal tholeiites (Fig. 25). Second, their K_2O content is characteristically low. These tendencies have also been confirmed in tholeiitic basalts from other areas in the Mikabu belt. HASHIMOTO et al. (1970) and SUZUKI et al. (1971) regarded the low K_2O content as datum showing chemical similarity of the Mikabu tholeiitic basalts to abyssal tholeiites, which have low K_2O content (ENGEL et al., 1965). While, MIYASHIRO (1975) emphasized that the low K_2O content of the Mikabu tholeiitic basalts can not be used as the evidence for abyssal tholeiite origin, because alkali migration is commonly widespread during regional metamorphism. Alkali migration has been also noticed in the present tholeiitic basalts. It seems, nevertheless, that the low K_2O content of the Mikabu

tholeiitic basalts would be taken as of primary nature of the rocks, because their differentiates (plagiogranites) are distinctively low in K_2O, which is reflected in the lack of potassium feldspar.

Low Al_2O_3 content is another chemical feature of the Mikabu tholeiitic basalts, as already noted by predecessors (e.g., SUGISAKI, 1977). In Fig. 27, Al_2O_3 weight percent of basalts, diabase dikes and a chilled marginal gabbro in Tables 1 and 2 is plotted against FeO*/MgO ratio. An increasing Al_2O_3 trend with increasing FeO*/MgO ratio is recognized for the rocks of tholeiitic composition. The tholeiitic basalts and diabases from other regions of the Mikabu belt, for example, the Ina area, central Japan (WATANABE et al., 1978) and the Okuki-Tomisuyama area, western Shikoku (SUZUKI et al., 1971, 1972), also have similar Al_2O_3 variation trend. This trend of Al_2O_3 variation forms contrast to that of the abyssal tholeiites, in which Al_2O_3 content decreases invariably with increasing FeO*/MgO ratio (SHIBATA, 1976). In contrast, average Al_2O_3 variation trend of the Kilauea lavas, shown in the same figure, is nearly parallel to that of the Mikabu tholeiitic basalts and diabase dikes. The Kilauea trend up to an FeO*/MgO of about 1.5 is chiefly controlled by olivine fractionation (MACDONALD and KATURA, 1964). Common presence of olivine phenocryst in the Mikabu tholeiitic basalts in question seems to favor this model. Mineralogically, low Al_2O_3 may be partly

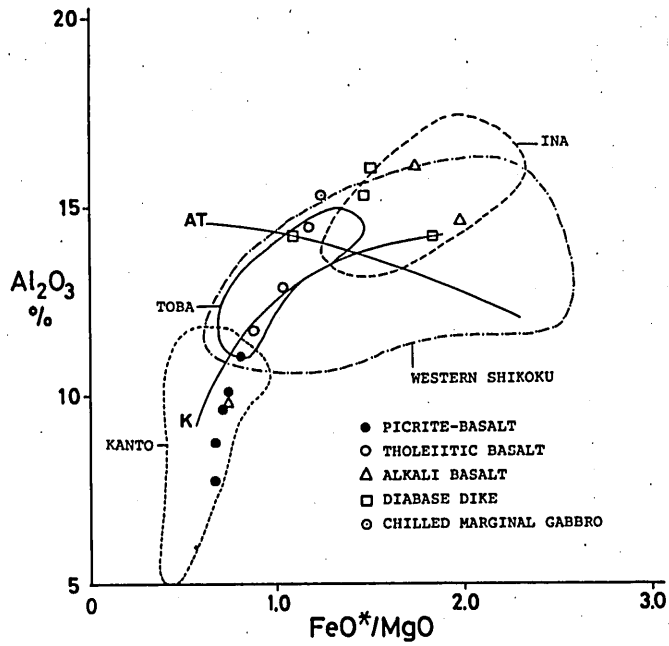

FIG. 27. Weight percent of Al_2O_3 plotted against FeO*/MgO for basalts, diabase dikes and chilled marginal gabbro in the Mikabu greenstones of eastern Shikoku. The compositional fields of basalts and diabases from Kanto, Ina, Toba and western Shikoku in the Mikabu belt are also shown for comparison (see Fig. 25 for data sources). AT indicates the lower limit of Al_2O_3 content of abyssal tholeiites after SHIBATA (1976). K indicates the average fractionation trend of Kilauea lavas (see Fig. 25 for data sources).

reflected in the failure of appearance of plagioclase as discrete phenocryst phase. This strikingly contrasts to abyssal tholeiites in which plagioclase are ubiquitous as phenocryst (e.g, SHIDO and MIYASHIRO, 1971). Even in aphyric Mikabu tholeiitic basalts, their Al_2O_3 is low. This fact, together with Al_2O_3 variation trend, suggests that low Al_2O_3 content is for the most part a primary feature of the parent liquid magma. In respect to Al_2O_3 abundance and Al_2O_3 variation trend, the Mikabu tholeiitic basalts are rather akin to Hawaiian tholeiites than abyssal tholeiites.

Trace element data for the present rock samples have not been available. HATTORI et al. (1972) showed low Rb (av. 1.8 ppm), low Sr (av. 106 ppm) contents and high K/Rb ratio for the Mikabu tholeiitic basalts in Shikoku. TANAKA (1975) determined rare earth element (REE) abundance of tholeiitic basalts and gabbros from the Mikabu greenstones and showed the light REE-depleted pattern for them, which is characteristic of abyssal tholeiites (e.g., BRYAN et al., 1976) and marginal basin tholeiites (e.g., RIDLEY et al., 1974). The class of rocks termed "island arc tholeiites" (JAKES and GILL, 1970) also has similar REE pattern as is characteristic of abyssal tholeiites and marginal basin tholeiites. Therefore, the REE data only can not distinguish these three types of tholeiites. TANAKA, however, emphasized that the low Ba/La ratio on the chondrite-normalized pattern of the Mikabu tholeiitic basalts precludes the possibility of their island arc tholeiites origin. This view is supported by high concentration of Cr and Ni in the Mikabu tholeiitic basalts (KAWABE, 1974). $^{87}Sr/^{86}Sr$ ratio has been measured on the Mikabu tholeiitic basalts from Shikoku by TANAKA et al. (1979). Low initial $^{87}Sr/^{86}Sr$ ratio (0.7034–0.7039) is compatible with mantle origin and is in the range for abyssal tholeiites.

Thus, available trace element data indicate that the Mikabu tholeiitic basalts are characteristically depleted in incompatible elements. This feature is consistent with the documented chemical features of abyssal tholeiites and marginal basin tholeiites, but the Mikabu tholeiitic basalts are essentially low in Al_2O_3 content, markedly differing form these tholeiites.

C. Relationship Between Tectonic Units

The mutual relationship between the Mikabu greenstones and their surrounding rock units is discussed based on the geological data presented in the preceding chapters. The geological age of the Mikabu greenstones will be also considered.

The stratigraphical relationship between the Mikabu greenstones to the rock sequence of the Chichibu belt appears to be obscured by later deformations in many places. Only in some places there are sedimentological data indicating the initial stratigraphical relationship between them.

In the Higashiiya area a conformable relationship between the Mikabu greenstones and the rock sequence of the Chichibu belt is inferred from the fact that the Mikabu greenstones are in contact with a thick (about 100 m), continuous layer of chert belonging to the rock sequence of the Chichibu belt, with nearly planar boundaries. But, in the area there is no sedimentological evidence to indicate the virtual stratigraphical relationship between them. While, in the Kamiyama and Jizoji areas the ophiolitic breccia is the base of the rock sequence of the Chichibu belt. The mode of occurrence and lithology of the ophiolitic breccia, as described in detail in the preceding pages, clearly indicate that the rock sequence of the Chichibu belt represents essentially sedimentary cover on the

Mikabu greenstones.

Field observations indicate that the Mikabu greenstones are in thrust fault contact with the crystalline schists of the Smabagawa belt in many places. High-angle faulting at the northern edge of the Mikabu greenstones of the Kamiyama area appears to be formed after thrusting. Although it seems to be difficult to evaluate the thrust fault on the basis of obtained field data alone, the author considers for reasons presented below that the thrust fault has important meanings on the relationship between the Mikabu greenstones and the crystalline schists and that the contact must have been more sheared.

The Mikabu greenstones overlie the crystalline schists in unfolded condition. In this situation feeder of the Mikabu greenstones should be found at their northern edge. But such feeder has not been recognized, and this suggests that a large tectonic discontinuity exists between the two rock units.

New paleontological data have shown that the rocks immediately adjacent to the Mikabu greenstones belong to two different ages, the Late Carboniferous and the Triassic. Such apparently contradictory evidence is common in mélange terranes (Hsü, 1968). As discussed later, the age of the Mikabu greenstones is considered to be of the Late Carboniferous. While, the underlying crystalline schists were derived from the Middle to Late Triassic strata at least partly. The fossil data would lead to an interpretation that the Mikabu greenstones are separated by a thrust from the crystalline schists. Otherwise arises contradictory stratigraphical relationship.

There is no discontinuity of metamorphic grade in a section from the underlying crystalline schists to the rocks overlying the Mikabu greenstones. Moreover, bedding schistosity develops in parallel disposition throughout these rocks. These facts suggest that the thrusting took place before and/or during the Sambagawa metamorphism. Possibly the trace of original sheared matrix might have been masked by overprinting related to the Sambagawa metamorphism.

Thus, it would be concluded that the Mikabu greenstones depositionally covered by the rock sequence of the Chichibu belt, here called the Mikabu nappe, rest on the crystalline schists of the Sambagawa belt across a thrust.

The age of the Mikabu greenstones has not been known, because there has not been found any fossiliferous sediments interlayered with volcanic rocks and no radiometric ages are available: the radiolarians found from cherts in the Higashiiya area are not of indicative of the age of the Mikabu greenstones because of their recrystallization and deformation. Hitherto, the age of the Mikabu greenstones has been inferred to be of the Early Permian in Shikoku (Suyari et al., 1969; Kashima, 1969; Kanmera, 1971). Recent discoveries of conodont fossils from rocks surrounding the Mikabu greenstones provide a clue to the age of the Mikabu greenstones.

The recent fossil discoveries lead to some geologists (e.g., Suyari et al., 1979) to assume that the Mikabu greenstones in Shikoku belong to two different ages, i.e., the Carboniferous and the Triassic. However, marked similarity in lithology, petrology and other geologic disposition of the Mikabu greenstones throughout Shikoku rather suggests a single episode of their formation. The relation that the rock sequence of the Chichibu belt represents essentially sedimentary cover on the Mikabu greenstones is now firmly established. Therefore it seems that the age of the Mikabu greenstones is older than that of the rock sequence of the Chichibu belt. The age of oldest rocks in the Chichibu belt adjacent to the Mikabu greenstones is of the Early Pennsylvanian. Thus, the

Mikabu greenstones appear to have originated in the Early Pennsylvanian or slightly before it.

D. Tectonic Setting, Emplacement and Subsequent Tectonic History

The Mikabu greenstones may be referred to a kind of ophiolite; the rock suite conforms to the description of ophiolite given at the G.S.A. Penrose Conference on Ophiolite (ANONYMOUS, 1972). As compared with the complete ophiolite sequence, the Mikabu phiolite suite in eastern Shikoku has the following characteristics.

1. Ultramafic rocks occur in small amount in the Mikabu greenstones, occupying only a few percent of their total exposure. They consist of cumulus peridotites and clinopyroxenites, and hornblendites, often forming small complexes grouped with gabbros and albitites. The peridotite-gabbro complexes occur sporadically within voluminous volcanic sequence and their appearance is not confined to a definite horizon. Ultramafic rocks assumed to be representatives of depleted mantle such as lherzolite and harzburgite with metamorphic fabric are entirely missing.
2. Sheeted mafic dike complex is lacking; occurrence of diabase dike is uncommon and is not concentrated in a single stratigraphic unit.
3. Only gabbro sill swarm shows a definite horizon (generally middle) in the volcanic sequence.
5. Non-volcanogenic sediments, commonly chert, pelite and limestone, are interbedded with volcanic rocks. Ophiolitic breccia mostly derived from the greenstones themselves (except for ultramafic rocks) rest on the greenstone complex in some places.

In view of occurrence, the Mikabu ophiolite suite shows no regular ophiolite sequence. The Mikabu greenstones can be described as a voluminous volcanic sequence with minor intercalations of sediments, in which diabase dikes and gabbro sills have been intruded and peridotite-gabbro complexes originated within magma chamber beneath the volcanic sequence, were tectonically transported as solid masses. As far as we note the rock suite and sequence, apart from their origin, the Mikabu greenstones may be referred to a dismembered ophiolite (COLEMAN and IRWIN, 1974) or non-sequence type ophiolite (MIYASHIRO, 1973).

In the preceding petrological discussions, it is pointed out that the Mikabu greenstones in eastern Shikoku represent igneous suite derived from multiple parent magmas, picrite-basaltic, tholeiitic and alkali magmas. This has also been demonstrated by petrochemical data for the Mikabu greenstones from other regions (UCHIDA, 1967; HASHIMOTO et al., 1970; NAKAMURA, 1971; SUZUKI et al., 1971, 1972; SUGISAKI et al., 1972; WATANABE et al., 1978). This characteristic is markedly different from that of well-documented ophiolites, because ophiolite parentage is essentially of "single magma", low-K tholeiites [e.g., COLEMAN (1977) among many others; see THAYER (1976) for a critical review of the problem associated with the single magma origin of ophiolites].

The petrology of the Mikabu greenstones does not provide definitive evidence concerning the tectonic setting in which the greenstones originated. Based mainly on the petrochemical properties of the Mikabu tholeiitic basalts as discussed before, oceanic or marginal basin environment is highly probable for the Mikabu greenstones. We have a fairly concrete evidence for the exsistence of a land or island arc on the south of the Mikabu greenstones and the northern zone of the Chichibu belt. Most recent authors consider the complex units occurring as several narrow and discontinuous strips along

the Kurosegawa tectonic belt as remnants of continental or mature island arc basement (ICHIKAWA et al., 1972; HADA et al., 1979). Some geological data obtained in the Ryoke and the Mino-Tamba belts, the Inner Zone of Southwest Japan, have provided a probability that a land composed of sialic crystalline basements existed during the pre-Triassic time in the Ryoke metamorphic belt (low-pressure/high-temperature type metamorphism) which strikes parallel to the Sambagawa belt to the north of the Median tectonic line (KOJIMA and OKAMURA, 1968; ADACHI, 1976; SHIMIZU et al., 1978). These geological data considered, it seems not unlikely to suppose that the Sambagawa-Chichibu basin in which the Mikabu greenstones are involved was a small marginal basin. Thus from the petrochemical data combined with the geological data, a marginal basin crust origin is preferred for the Mikabu greenstones, although oceanic island environment in a marginal basin is also plausible.

The absence of the pre-Onimaru (Late Mississippian), Carboniferous system in the Chichibu belt except for the Kurosegawa tectonic belt suggests that the land existed in a fairly large part of the Chichibu belt before the Late Mississippian (ICHIKAWA, 1975). The emplacement of the Mikabu ophiolitic magma, which is considered to have taken place during the Early Pennsylvanian or slightly before it, is an earlier geologic event in the evolution of the Sambagawa-Chichibu basin. Accordingly, the Late-Mississippian — Early Pennsylvanian seems to be critical time in the evolution of the Sambagawa-Chichibu belts, when ocean emerged eventually to form a marginal basin. The Mikabu greenstones might be an incipient ridge that perhaps grew into a spreading center in a marginal basin. The presence of the ophiolitic breecia and gabbro breccia resting directly on the Mikabu greenstones at several places suggests the the Mikabu greenstones were eroded to form the breccias below the submarine fault scarps at the spreading center prior to the main sedimentation of the Chichibu belt. Toward the end of the Late-Triassic eugeosynclinal sediments were laid down over a large part of the Sambagawa and the Chichibu belts.

Extensive compressional tectonism seems to have initiated during the Late-Triassic time in the Sambagawa and the Chichibu belts. The Mikabu greenstones together with the overlying rock sequence of the Chichibu belt have tectonically brought into juxtaposition with the Triassic basin of the southern marginal zone of the Sambagawa belt, resulting in the formation of a nappe (the Mikabu nappe). Within the nappe itself occurred the thrusting, forming thrust sheets (subnappes). It appears that gravity sliding at the front of the advancing nappe directed from the south to the north supplied its sedimentary slices within the autochthonous Triassic basin, forming olistostromes. The Triassic basin was then overridden by a successively advancing nappe. It is likely that the emplacement of the Mikabu nappe has occurred before and during the Sambagawa metamorphism.

Subsequent to the main phase of the Sambagawa metamorphism, the Mikabu greenstones and their surrounding rocks have been extensively deformed by folding. The style of folds of the Mikabu greenstones (Fig. 6) in eastern Shikoku, upright and recumbent folds, suggests polyphase deformation history, but there is only a little direct evidence. Two distinctive phases of folding of the Mikabu greenstones have been established in the Ikegawa-Mikawa'mura area, western Shikoku (Fig. 6D), where recumbent folds with gently to moderately north-dipping axial surfaces have clearly bent by an upright antiform (TSUKUDA, 1976; TAKEDA et al., 1977). This suggests that the two types of fold of the

Mikabu greenstones in eastern Shikoku formed in the same order as they did in the Ikegawa-Mikawa'mura area.

Tectonic movement of the Sambagawa belt proper, subsequent to the main phase of the Sambagawa metamorphism, has been distinguished largely into two main phases, i.e., the older Nagahama-Ozu phase and the younger Hijikawa phase (the Latest Jurassic or the Earliest Cretaceous age) (HIDE, 1972; HARA et al., 1977). The tectonic movement of the Nagahama-Ozu phase, showing movement direction toward the south, has produced nappes, accompanied by south-facing large recumbent folds. While, the tectonic movement of the Hijikawa phase is characterized by the formation of large-scale upright folds oriented en echelon. On the basis of movement picture, the recumbent folding and upright folding of the Mikabu greenstones are comparable with the tectonic movements of the Nagahama-Ozu and the Hijikawa phases, respectively. The present geological structure of the Mikabu greenstones appears to have been much affected by the movement of the Nagahama-Ozu phase. The upright folding was a later event that affected the already transported Mikabu greenstones.

In summary, it is pointed out that emplacement, metamorphism and subsequent deformation of the Mikabu greenstones have taken place in a rather short period of time from the Late-Triassic to the Early Cretaceous. The movement of mainly the Jurassic has resulted in the shortening of the Sambagawa-Chichibu belt.

REFERENCES

ADACHI, M. (1976): Paleogeographic aspects of the Japanese Paleozoic-Mesozoic geosyncline. *J. Earth Sci., Nagoya Univ.*, **23/24**, 13–55.

ANONYMOUS (1972): Penrose field conference on ophiolites. *Geotimes*, **17**, 24–25.

AOKI, K. (1963): The kaersutites and oxykaersutites from alkalic rocks of Japan and surrounding areas. *J. Petrol.*, **4**, 198–210.

ATKINS, F. B. (1969): Pyroxenes of the Bushveld intrusion, south Africa. *J. Petrol.*, **10**, 222–249.

BANNO, S. (1964): Petrologic studies on the Sanbagawa crystalline schists in the Bessi-Ino district, central Shikoku, Japan. *J. Fac. Sci. Univ. Tokyo*, Sec II, **15**, 203–319.

BEESON, M. H. and JACKSON, E. D. (1969): Chemical composition of altered chromites from Stilwater Complex, Montana. *Amer. Mineral.*, **54**, 1084–1100.

BENCE, A. E. and ALBEE, A. L. (1968): Empirical correction factors for the electron microanalysis of silicates and oxides. *J. Geol.*, **76**, 382–403.

BLISS, N. W. and MACLEAN, W. H. (1975): The paragenesis of zoned chromite from central Manitoba. *Geochim. Cosmochim. Acta.*, **39**, 973–990.

BROWN, G. M. (1957): Pyroxenes from the early and middle stages of fractionation of the Skaergaard intrusion, East Greenland. *Miner. Mag.*, **31**, 511–543.

——— and VINCET, E. A. (1963): Pyroxenes from the late stages of fractionation of the Skaergaard intrusion, East Greenland. *J. Petrol.*, **4**, 175–196.

BRYAN, W. B. (1972): Morphology of quenched crystals in submarine basalts. *J. Geophys. Res.*, **77**, 5812–5819.

———, THOMPSON, G., FREY, F. A. and DICKEY, J. S. (1976): Inferred geologic settings and differentiation in basalts from the deep-sea drilling project. *J. Geophys. Res.*, **81**, 4285–4304.

CANN, J. R. (1969): Spilites from the Carlsberg Ridge, Indian Ocean. *J. Petrol.*, **10**, 1–19.

COISH, R. A. and TAYLOR, L. A., (1979): The effects of cooling rate on texture and pyroxene chemistry in DSDP Leg 34 basalt: A microprobe study. *Earth Planet. Sci. Lett.*, **42**, 389–398.

COLEMAN, R. G. (1977): *Ophiolites.* Springer-Verlag, New York. 229p.

——— and IRWIN, W. P. (1974): Ophiolites and ancient continental margins. In: C. A. BURK and C. L. DRAKE (Editors), *The geology of continental margins.* Springer-Verlag, New York, 921–931.

——— and PETERMAN, Z. E. (1975): Oceanic plagiogranite. *J. Geophys. Res.*, **80**, 1099–1108.

COOMBS, D. S. (1963): Trends and affinities of basaltic magmas and pyroxenes as illustrated on the diopside-olivine-silica diagram. *Miner. Soc. Amer. Special Paper*, **1**, 227–250.

DICKEY, J. S. Jr. (1975): A hypothesis of origin of podiform chromite deposits. *Geochim. Cosmochim. Acta*, **39**, 1061–1074.

ENGEL, A. E. J., ENGEL, C. G. and HAVENS, R. G. (1965): Chemical characteristics of oceanic basalts and the upper mantle. *Geol. Soc. Amer. Bull.*, **76**, 719–734.

ERNST, W. G. (1972): Possible Permian oceanic crust and plate junction in central Shikoku, Japan. *Tectonophysics*, **15**, 233–239.

———, SEKI, Y., ONUKI, H. and GILBERT, M. C. (1970): Comparative study of low-grade metamorphism in the California Coast Ranges and the outer metamorphic belt of Japan. *Geol. Soc. Amer. Mem.*, **124**, 276 p.

EVANS, B. W. and MOORE, J. G. (1968): Mineralogy as a function of depth in the prehistoric Makaopuhi tholeiitic lava lake, Hawaii. *Contrib. Mineral. Petrol.*, **17**, 85–115.

EVANS, B. W. and WRIGHT, T. L. (1972): Composition of liquidus chromite from the 1959 (Kilauea Iki) and 1965 (Makaopuhi) eruptions of Kilauea volcano, Hawaii. *Amer. Mineral.*, **57**, 217–230.

FLANAGAN, F. J. (1973): 1972 values for international geochemical reference samples. *Geochim. Cosmochim. Acta.*, **37**, 1189–1200.

FODOR, R. V., KEIL, K. and BUNCH, T. E. (1975): Contributions to the mineral chemistry of Hawaiian rocks. IV. Pyroxenes in rocks from Haleakala and west Maui volcanoes, Maui, Hawaii. *Contrib. Mineral. Petrol.*, **50**, 173–195.

GIBB, F. G. F. (1973): The zoned clinopyroxenes of the Shiant Isles sill, Scotland. *J. Petrol.*, **14**, 203–230.

HADA, S., SUZUKI, T., YOSHIKURA, S. and TSUCHIYA, N. (1979): The Kurosegawa Tectonic Zone in Shikoku and tectonic environment of the Outer Zone of Southwest Japan (in Japanese with English abstract). In: *The basement of Japanese Islands — Prof. H. KANO Mem., Vol.*, Toko Printing, Sendai, 341–368.

HARA, I., HIDE, K., TAKEDA, K., TSUKUDA, E., TOKUDA, M. and SHIOTA, T. (1977): Tectonic movement in the Sambagawa belt (in Japanese with English abstract). In: K. HIDE (Editor), *The Sambagawa belt*, Hiroshima Univ. Press, Hiroshima, 307–390.

HASHIMOTO, M., KASHIMA, N. and SAITO, Y. (1970): Chemical composition of Paleozoic greenstones from two areas of southwest Japan. *J. Geol. Soc. Japan*, **76**, 463–476.

HATTORI, H., SUGISAKI, R. and TANAKA, T. (1972): Nature of hydration in Japanese Paleozoic geosynclinal basalt. *Earth Planet. Sci. Lett.*, **15**, 271–285.

HIDE, K. (1972): Significance of the finding of two recumbent folds in the Sambagawa metamorphic belt of the Nagahama-Ozu district, west Shikoku (in Japanese with English abstract). *Mem. Fac. Gen. Educ., Hiroshima Univ.*, III, **5**, 35–51.

HIRAYAMA, K., YAMASHITA, N., SUYARI, K. and NAKAGAWA, C. (1965): Geological map of Kenzan, scale 1: 75,000, and its explanatory text (in Japanese), Tokushima Pref., 52 p.

HSÜ, J. K. (1968): Principles of melange and their bearing on the Franciscan-Knoxville paradox. *Bull. Geol. Soc. Amer.*, **79**, 1063–1074.

ICHIKAWA, K. (1975): Honshu and Shimanto geosynclines in Southwest Japan and plate tectonics (in Japanese with English abstract). *Assoc. Geol. Collab. Japan, Monograph* **19**, 241–246.

———, MATSUMOTO, T. and IWASAKI, M. (1972): Geologic History of Japanese Islands (in Japanese). *KAGAKU (Science)*, **42**, 181–191.

INOMATA, M. and KAJI, A. (1977): Titaniferous phlogopite from the green rocks of the Paleozoic terrain of the Minami-noma area, Tokushima Prefecture, Shikoku, Japan. *J. Japan. Assoc. Mineral. Petrol. Econ. Geol.*, **72**, 322–326.

INOMATA, M. and TAZAKI, K. (1974): Phlogopite and Ti-pargasite-bearing ultramafic rocks from the Mikabu zone, central Japan. *J. Japan. Assoc. Mineral. Petrol. Econ. Geol.*, **69**, 205–214.

ISHII, K., ICHIKAWA, K., KATTO, J., YOSHIDA, H. and KOJIMA, G. (1957): Geology of the Chichibu terrain along the highway from Kamiyakawa to Ino, Shikoku (in Japanese with English abstract). *J. Geol. Soc. Japan*, **63**, 449–454.

IWASAKI, M. (1963): Metamorphic rocks of the Kotsu-Bizan area, eastern Shikoku. *J. Fac. Sci. Univ. Tokyo*, Sec. II, **15**, 1–90.

——— (1969): The basic rocks at the boundary between the Sambagawa metamorphic belt and the Chichibu unmetamorphosed Paleozoic sediments (in Japanese with English abstract). *Mem. Geol. Soc. Japan*, **4**, 41–50.

——— (1979): Gabbroic breccia (olistostrome) in the Mikabu Green Stone Belt of the eastern Shikoku. *J. Geol. Soc. Japan*, **85**, 481–487.

JAKES, P. and GILL, J. (1970): Rare earth elements and the island arc tholeiitic series. *Earth Planet. Sci. Lett.*, **9**, 17–28.

KAJI, A., OGAWA, Y. and SHIOTA, T. (1973): Green rocks from the Paleozoic terrain of the Minami-noma area, Kamiyama, Tokushima Prefecture (in Japanese with English abstract). *J. Gakugei, Tokushima Univ., Nat. Sci.*, **24**, 31–39.

KANMERA, K. (1971): Paleozoic and Early Mesozoic geosynclinal volcanicity in Japan (in Japanese with English abstract). *Mem. J. Geol. Soc. Japan*, **6**, 97–110.

KASHIMA, N. (1969): Stratigraphical studies of the Chichibu belt in western Shikoku. *Mem. Fac. Sci., Kyushu Univ., Ser. D.*, **19**, 387–436.

KAWABE, I. (1974): Transition metal contents of Paleozoic geosynclinal basalts in southwest Japan and their geological significance (in Japanese with English abstract). *J. Geol. Soc. Japan*, **80**, 539–554.

KAWACHI, Y., LANDIS, C. A. and WATANABE, T. (1976): Hyaloclastite — A critical review (in Japanese with English abstract). *J. Geol. Soc. Japan*, **82**, 355–366.

KENZAN RESEARCH GROUP (1963): Geology of the crystalline schist region of eastern Shikoku (in Japanese with English abstract). *Chikyu Kagaku (Earth Sci.)*, **69**, 16–19.

KOJIMA, G. (1950): On the so-called Mikabu system in the outer zone of south-western Japan (in Japanese with English abstract). *J. Geol. Soc. Japan*, **56**, 339–344.

——— and MITSUNO, C. (1966): Geological map of Kawaguchi, scale 1: 50,000, and its explanatory text (in Japanese with English abstract). *Geol. Surv. Japan.*

——— and OKAMURA, Y. (1968): On the Kitaoshima granite gneiss complex. *J. Sci., Hiroshima Univ., Ser. C*, **5**, 295–306.

——— and SUZUKI, T. (1958): Rock structure and quartz fabric in a thrusting shear zone: the Kiyomizu tectonic zone in Shikoku, Japan. *J. Sci., Hiroshima Univ., Ser. C*, **2**, 173–193.

———, YOSHIDA, H., KATTO, J., ICHIKAWA, K. and ISHII, K. (1956): Geology of the Sambagawa crystalline schist zone along the highway from Saijo to Kamiyakawa, Shikoku (in Japanese with English abstract). *J. Geol. Soc. Japan*, **62**, 317–326.

KOTO, B. (1888): On the so-called crystalline schist of Chichibu. *J. Coll. Sci. Tokyo Imp. Univ.*, II, 77–141.

KUNO, H. (1959): Origin of Cenozoic petrographic provinces of Japan and surrounding areas. *Bull. Volcanol., Ser. II*, **20**, 37–76.

——— (1968): Differentiation of basaltic magmas. In: H. H. HESS and A. POLDERVAART (Editor), *Basalts, Vol.* 2, Interscience, New York, 623–688.

KUSHIRO, I. (1960): Si–Al relation in clinopyroxenes from igneous rocks. *Amer. J. Sci.*, **258**, 548–554.

LEAKE, B. E. (1968): A catalog of analyzed calciferous and subcalciferous amphiboles together with their nomenclature and assoicated minerals. *Geol. Soc. Amer. Special Paper*, **98**.

LEBAS, M. J. (1962): The role of aluminium in igneous clinopyroxenes with relation to their parentage. *Amer. J. Sci.*, **260**, 267–288.

MACDONALD, G. A. and KATSURA, T. (1961): Variation in the lava of the 1959 eruption in Kilauea Iki. *Pacific Sci.*, **15**, 358–369.

MACDONALD, G. A. and KATSURA, T. (1964): Chemical compositions of Hawaiian lavas. *J. Petrol.*, **5**, 82–133.

MAKIMOTO, H. (1978): Petrology of the Irisawai ultramafic complex in the Oshika district, Nagano Prefecture, central Japan —Petrography and chemical character of the Shiokawa peridotite mass— (in Japanese with English abstract). *J. Geol. Soc. Japan*, **84**, 317–329.

MARUYAMA, S. (1976): Chemical natures of the Sawadani greenstone complex in Chichibu belt, eastern Shikoku (in Japanese with English abstract). *J. Geol. Soc. Japan*, **82**, 183–197.

MATUDA, T. (1978): Discovery of the Middle-Late Triassic conodont genus Metapolygnathus from calcareous schist of the Sambagawa southern marginal belt in central Shikoku (in Japanese). *J. Geol. Soc. Japan*, **84**, 331–333.

McBIRNEY, A. R. (1963): Factors governing the nature of submarine volcanism. *Bull. Volcanol.*, **26**, 455–469.

MIYASHIRO, A. (1973): *Metamorphism and metamorphic belts.* George Allen & Unwin, London, 492 p.

——— (1975): Classification, characteristics, and origin of ophiolites. *J. Geol.*, **83**, 249–281.

MOSSMAN, D. J. (1973): Geology of the Greenhills ultramafic complex, Bluff Peninsula, Southland, New Zealand. *Geol. Soc. Amer. Bull.*, **84**, 39–62.

MUIR, I. D. and TILLEY, C. E. (1957): Contributions to the petrology of Hawaiian basalts. 1. The picrite-basalts of Mauna Loa and Kilauea. *Amer. J. Sci.*, **255**, 241–253.

MUIR, I. D. and TILLEY, C. E. (1963): Contributions to the petrology of Hawaiian basalts: II, The tholeiitic basalts of Mauna Loa and Kilauea. *Amer. J. Sci.*, **261**, 111–128.

MURATA, K. J. and RICHTER, D. H. (1966): Chemistry of lavas of the 1959–1960 eruption of Kilauea volcano, Hawaii. *U. S. Geol. Surv. Prof. Paper*, **537A**, 1–26.

MURRAY, C. G. (1972): Zoned ultramafic complexes of the Alaskan type: Feeder pipes of andesitic volcanoes. *Geol. Soc. Amer. Mem.*, **132**, 313–335.

NKAGAWA, C., SUYARI, K. and IWASAKI, M. (1972): Geological map of Tokushima Prefecture, scale 1: 150,000, and its explanatory text (Geology of Tokushima Prefecture) (in Japanese). Tokushima Pref.

NAKAJIMA, T., BANNO, S. and SUZUKI, T. (1977): Reactions leading to the disappearance of pumpellyite in low-grade metamorphic rocks of the Sanbagawa metamorphic belt in central Shikoku, Japan. *J. Petrol.*, **18**, 263–284.

NAKAMURA, Y. (1971): Petrology of the Toba ultramafic complex, Mie Prefecture, central Japan. *J. Fac. Sci. Univ. Tokyo*, Sec. II, **18**, 1–51.

——— and KUSHIRO, I. (1970): Compositional relations of coexisting orthopyroxene, pigeonite, and augite in a tholeiitic andesite from Hakone volcano. *Contrib. Mineral. Petrol.*, **26**, 265–275.

NAKAYAMA, I., KAJI, A., SHIODA, T. and IWASAKI, M. (1973): Finding of inverted pigeonite from the gabbro in the Mikabu zone at Kamiyama, eastern Shikoku, Japan. *Mem. Fac. Sci. Kyoto Univ.*, **40**, 27–33.

OGAWA, Y. (1974): Geologic structure of the Chichibu terrain in eastern Shikoku, Japan (in Japanese with English abstract). *J. Geol. Soc. Japan*, **80**, 439–455.

ONUKI, H. (1963): Petrology of the Hayachine ultramafic complex in the Kitakami mountainland, northern Japan. *Sci. Rept. Tohoku Univ.*, Ser. III, **8**, 241–296.

PEARCE, J. A. and CANN, J. R. (1973): Tectonic setting of basic volcanic rocks determined using trace element analyses. *Earth Planet. Sci. Lett*,. **19**, 290–300.

RIDLEY, W. I., RHODES, J. M., REID, A. M., JAKES, P., SHIH, C. and BASS, M. N. (1974): Basalts from Leg 6 of the Deep-Sea Drilling Project. *J. Petrol.*, **15**, 140–159.

RUCKMICK, J. C. and NOBLE, J. A. (1959): Origin of the ultramafic complex at Union Bay, southeastern Alaska. *Geol. Soc. Amer. Bull.*, **70**, 981–1018.

SAWAMURA, T., KATTO, J., KOJIMA, G. and SUYARI, K. (1961): Geological and mineral resources map of Kochi Prefecture, scale 1: 200,000, and its explanatory text (in Japanese). Kochi Pref.

SEKI, Y. (1958): Glaucophanitic regional metamorphism in the Kanto mountains, central Japan. *Jap. Jour. Geol. Geogr.*, **29**, 243–258.

SHIBATA, T. (1976): Phenocryst-bulk rock composition relations of abyssal tholeiites and their petrogenetic significance. *Geochim. Cosmochim. Acta*, **40**, 1407–1417.

SHIDO, F. and MIYASHIRO, A. (1971): Crystallization of abyssal tholeiites. *Contrib. Mineral. Petrol.*, **31**, 251–266.

SHIMIZU, D., IMOTO, N. and MUSASHINO, M. (1978): Permian and Triassic sedimentary history of the Honshu geosyncline in the Tamba belt, southwest Japan. *J. Phys. Earth*, **26**, suppl., S337–S344.

SHIRAKI, K., OHASHI, F. and KURODA, N. (1979): Chrome-spinels in a basanitic lava from Nanzaki volcano, Izu Peninsula (in Japanese with English abstract). *J. Japan. Assoc. Miner. Petrol. Econ. Geol.*, **74**, 114–121.

———, YUSA, Y., KURODA, N. and ISHIOKA, K. (1977): Chrome-spinels in some basalts from Guam, Mariana island arc (in Japanese with English abstract). *J. Geol. Soc. Japan*, **83**, 49–57.

SIGURDSSON, H. and SCHILLING, J.-G. (1976): Spinels in Mid-Atlantic Ridge basalts: chemistry and occurrence. *Earth Planet. Sci. Lett.*, **29**, 7–20.

SUGISAKI, R. (1977): Petrochemical features of the Mikabu green rocks (in Japanese with English abstract). In: K. HIDE (Editor), *The Sambagawa belt*, Hiroshima Univ. Press, Hiroshima, 37–47.

———, MIZUTANI, S., HATTORI, H., ADACHI, M. and TANAKA, T. (1972): Late Paleozoic geosynclinal basalt and tectonism in the Japanese Islands. *Tectonophysics*, **14**, 35–56.

SUYARI, K., BANDO, Y. and HADA, S. (1969): Structural studies on the Paleozoic system of the Chichibu terrain in eastern Shikoku (in Japanese with English abstract). *J. Sci., Univ. Tokushima*, **3**, 9–18.

———, KUWANO, Y. and ISHIDA, K. (1979): A preliminary study on the relationship between the Sambagawa belt and the Chichibu belt (in Japanese). *Studies on Late Mesozoic tectonism in Japan*, **1**, 39–49.

———, ——— and ——— (1980): Some problems on the Mikabu greenrocks (in Japanese). *Studies on Late Mesozoic tectonism in Japan*, **2**, 21–29.

SUZUKI, J. (1953): The hypabyssal rocks associated with ultrabasic rocks in Hokkaido, Japan. *Congr. Geol. Int., Sec. VI*, 131–137.

SUZUKI, M., MINAMI, A. and YOKOYAMA, S. (1977): Bulk chemical analysis of rocks by electron microprobe analyzer — with special referrence to the direct fusion method (abstract in Japanese). *Joint Meet. Soc. Mining Geol. Japan, Soc. Miner. Japan, and Japan. Assoc. Mineral. Petrol. Econ. Geol.*, preprint, p. 41.

SUZUKI, T. (1964a): The Mikabu green rocks in Shikoku (1) —Petrology and geology of the Mikabu green rocks in the district of Osugi, Kochi Prefecture— (in Japanese with English abstract). *Res. Rept. Kochi Univ.*, **13**, 93–102.

——— (1964b): Relation between the Sambagawa and Chichiba zone in the district of Agawa, Kochi Prefecture (in Japanese with English abstract). *J. Geol. Soc. Japan*, **70**, 339–347.

——— (1965): On the Kamiyakawa-Ikegawa tectonic line. *Geol. Rept. Hiroshima Univ.*, **14**, 293–306.

——— (1967): The Mikabu green rocks in Shikoku —with special reference to distribution and occurrence of agglomeratic rocks— (in Japanese with English abstract). *J. Geol. Soc. Japan*, **73**, 207–216.

——— (1977): The style of igneous activity of the Mikabu ophiolite (in Japanese with English abstract), In: K. HIDE (Editor), *The Sambagawa belt*, Hiroshima Univ. Press, Hiroshima, 23–36.

———, SUGISAKI, R. and TANAKA, T. (1971): Geosynclinal igneous activity of the Mikabu green rocks of Ōzu city, Ehime Prefecture (in Japanese with English abstract). *Mem. Geol. Soc. Japan*, **6**, 121–136.

———, KASHIMA, N., HADA, S. and UMEMURA, H. (1972): Geosynclinal volcanism of the Mikabu green-rocks in the Okuki area, western Shikoku, Japan. *J. Japan. Assoc. Mineral. Petrol. Econ. Geol.*, **67**, 177–192.

TAKEDA, K. (1976): Stratigraphy and geologic structure of the crystalline schists of the Sambagawa belt in the Higashiiya district, eastern Shikoku (in Japanese). *Jubilee Pub. Comm. Prof. G. KOJIMA's 60th Birthday*, 237–244.

———, TSUKUDA, E., TOKUDA, M. and HARA, I. (1977): Structural relationship between the Sambagawa and Chichibu belts (in Japanese with English abstract). In: K. HIDE (Editor), *The Sambagawa belt*, Hiroshima Univ. Press, Hiroshima, 107–151.

TANAKA, T. (1975): Geological significance of rare earth elements in Japanese geosynclinal basalts. *Contrib. Mineral. Petrol.*, **52**, 233–246.

——— (1977): Rare earth abundances in Japanese Paleozoic geosynclinal basalts and their geological significance (in Japanese with English abstract). *Bull. Geol. Surv. Japan*, **28**, 529–559.

———, SUGISAKI, R., SHIBATA, K. and KURASAWA, H. (1979): Strontium isotopes in Paleozoic geosynclinal basalt in Japan. *J. Geol. Soc. Japan*, **85**, 489–496.

TAZAKI, K. (1975): Chromian spinels in picrite basalt from Mineoka tectonic belt, Boso Peninsula, central Japan (in Japanese with English abstract). *J. Geol. Soc. Japan*, **81**, 399–406.

——— and INOMATA, M. (1974): Phlogopites and coexisting pargasites in wehrlite from the northern Kanto mountains, central Japan. *Papers Inst. Thermal Spring Res., Okayama Univ.*, **43**, 1–13.

THAYER, T. P. (1976): The Canyon Mountain Complex, Oregon, and some problems of ophiolites. In: R. G. COLEMAN and W. P. IRWIN (Editors), *North American ophiolites*, Oregon Dept. Geol. Mineral. Indust. Bull., **95**, 93–105.

THOMPSON, R. N. (1973): Titanian chromite and chromian titanomagnetite from a Snake River Plain basalt, a terrestrial analogue to lunar spinels. *Amer. Mineral.*, **58**, 826–830.

TILLEY, C. E. (1960): Differentiation of Hawaiian basalts: some variants in lava suites of dated Kilauean eruptions. *J. Petrol.*, **1**, 47–55.

TSUKUDA, E. (1976): A study on structural relationship between the Sambagawa belt and the Chichibu belt — in the case of district from Ikegawa-cho, Kochi Prefecture to Mikawa-mura, Ehime Prefecture (in Japanese). *Abst. Program*, 1976 *Annual Meet. Geol. Soc. Japan*, p. 288.

UCHIDA, N. (1967): Chemical compositions of basic tuffs from the Mikabu and Mamba Formations (in Japanese). *Seikei Ronso*, **6**, 206–220.

ULMER, G. C. (1974): Alteration of chromite during serpentinization in the Pennsylvanian-Maryland district. *Amer. Mineral.*, **59**, 1236–1241.

VALLANCE, T. G. (1960): Concerning spilites. *Linnaean Soc. N. S. Wales Proc.*, **85**, 8–52.

WAGER, L. R. (1960): The major element variation of the layered series of the Skaergaard intrusion and a reestimation of the average compostion of the hidden layered series and of the successive residual magmas. *J. Petrol.*, **1**, 364–398.

——— and BROWN, G. M. (1968): *Layered igneous rocks*. Oliver and Boyd, London, 588 p.

WALKER, F. (1953): The pegmatitic differentiates of basic sheets. *Amer. J. Sci.*, **251**, 41–60.

WALKER, D., KIRKPATRICK, R. J., LONGHI, J. and HAYS, J. F. (1976): Crystallization history of lunar picritic basalt sample 12002: Phase-equilibria and cooling-rate studies. *Geol. Soc. Amer. Bull.*, **87**, 646–656.

WALKER, K. R., WARE, N. G. and LOVERING, J. F. (1973): Compositional variations in the pyroxenes of the differentiated Palisades sill, New Jersey. *Geol. Soc. Amer. Bull.*, **84**, 89–110.

WATANABE, T., KAWACHI, Y. and YUASA, M. (1978): Relict clinopyroxenes in the Mikabu greenstones, Oshika and Kosetokyo districts, Nagano Prefecture, central Japan. *Jour. Fac. Sci., Hokkaido Univ., Ser.* IV, **18**, 509–520.

WILKINSON, J. F. G. (1961): Some aspects of the calciferous amphiboles, oxyhornblende, kaersutite, and barkevikite. *Amer. Mineral.*, **46**, 340–354.

Kenji TAKEDA

INSTITUTE OF GEOLOGY AND MINERALOGY
FACULTY OF SCIENCE, HIROSHIMA UNIVERSITY,
HIROSHIMA, 730 JAPAN
Present address:
INSTITUTE OF EARTH SCIENCE,
FACULTY OF EDUCATION, YAMAGUCHI UNIVERSITY,
YAMAGUCHI, 753 JAPAN

EXPLANATION OF PLATE XXI

Fig. 1. Elongate pillow lava, Kashio, Higashiiya area.
Fig. 2. Hyalocalastic breccia, Kubokage, Higashiiya area.
Fig. 3. Volcanic breccia, Nagoro, Higashiiya area. Note the fragments of basalt with a variety of fabric.
Fig. 4. Diabase dikes occurring in ellipsoidal form, intruded into hyaloclastic sandstone, Nagoro, Higashiiya area.
Fig. 5. A band of plagiogranite occurring in weakly laminated ferrogabbro of the Jizoji gabbro sill (Akikawa section). Note the development of micro-pegmatite with width of 5–10 mm on the upper and lower fringes of the band.
Fig. 6. Ophiolitic breccia including clasts of basalt, diabase, gabbro and plagiogranite, Higashi-ishihara, Jizoji area.

EXPLANATION OF PLATE XXII

Fig. 1. Aphyric basalt (T715) (Group I basalt). Intersecting blades of clinopyroxene displaying skeletal crystal form with interstitial chlorite and sheaths of tremolite. Accessories: calcite, leucoxene and opaque matters. Plane polarized light.
Fig. 2. Aphyric basalt (T2606) (Group I basalt). Small equant grains of clinopyroxene and glass altered to aggregates of chlorite and minor amounts of fibrous tremolite and leucoxene. Crossed polars.
Fig. 3. Variolitic basalt (Hp–1) (Group II basalt). Brown spherulitic aggregates of clinopyroxene and albite. Swallow-tailed clinopyroxene often forms a core of the spherulitic aggregates. Crossed polars.
Fig. 4. Clinopyroxene porphyritic basalt (MD–1) (Group III basalt). Clinopyroxene phenocrysts (C) are embedded in a groundmass composed of clinopyroxene, plagioclase altered to albite, chlorite and dark mesostasis. Crossed polars.
Fig. 5. Weakly laminated ferrogabbro (J918). Cloudy, tabular plagioclase laths (P) exhibit a weak igneous lamination. Clinopyroxene (C), brown and bluish-green amphiboles (H) and ilmenite (I) are interstices between the plagioclase laths. Crossed polars.
Fig. 6. Plagiogranite (J910). Granophyric intergrowth of quartz (Q) and throughly pumpellyized plagioclase (P) is well displayed. Accessories: apatite, calcite and pyrite. Crossed polars.
Fig. 7. Clinopyroxene-hornblende peridotite (T2). Poikilitic brown hornblende (H) encloses crystals of olivine altered to serpentine (S), clinopyroxene (C) and chromian spinel (Cr). Crossed polars.
Fig. 8. Stilpnomelane-chlorite albitite (T309). Porphyritic albite crystals distorted are set in a fine-grained groundmass composed mostly of albite with stilpnomelane and chlorite. Crossed polars.

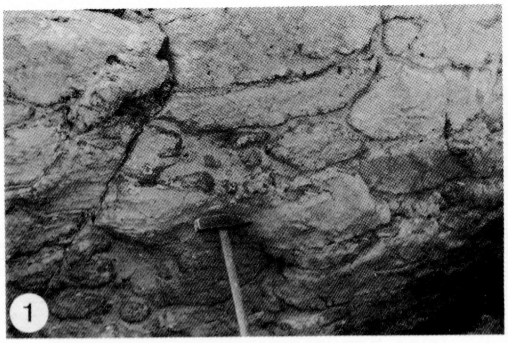
1


2


3


4

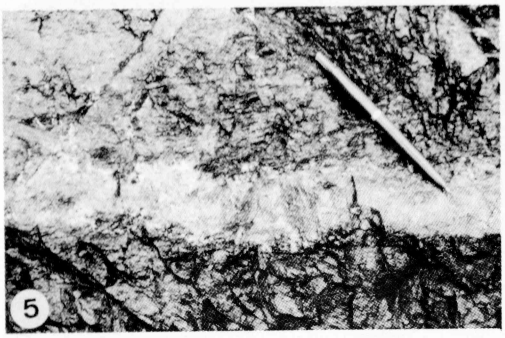
5

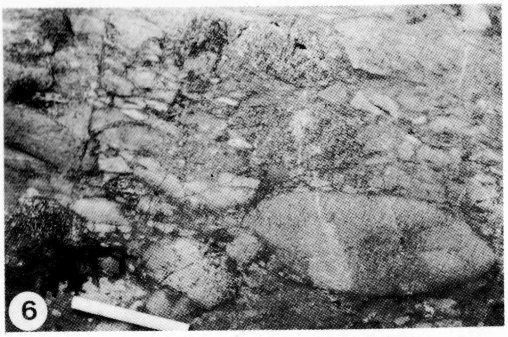
6

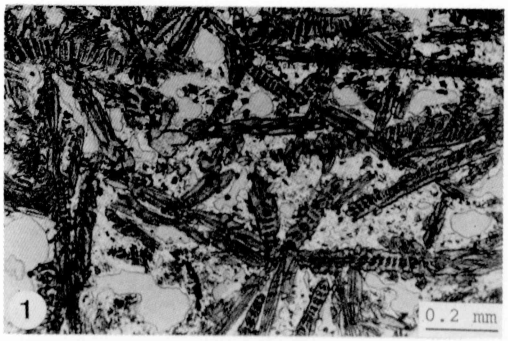
1
0.2 mm

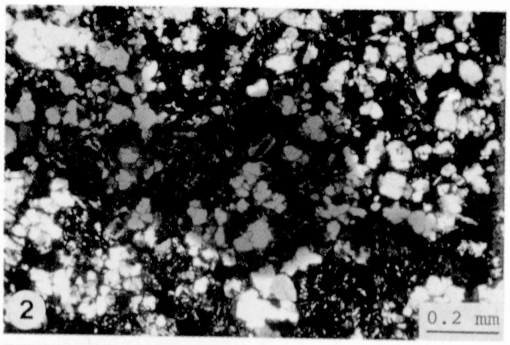
2
0.2 mm


3
0.2 mm

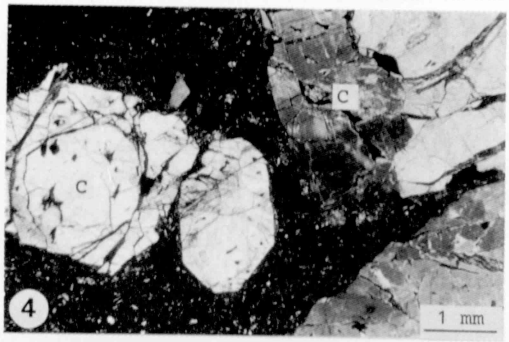
C
C
4
1 mm

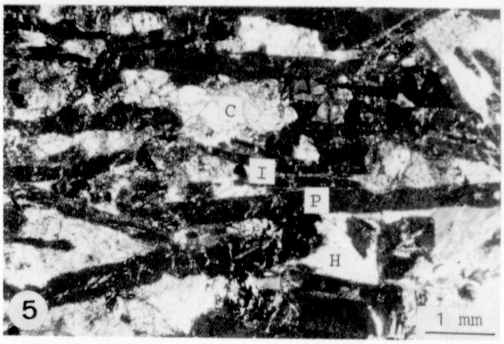
C
I
P
H
5
1 mm

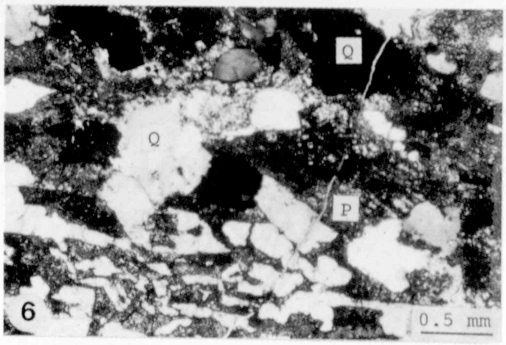
Q
Q
P
6
0.5 mm

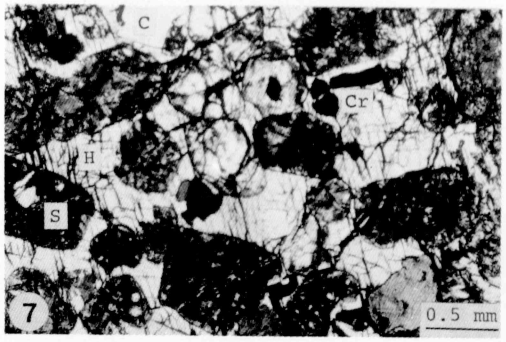
C
Cr
H
S
7
0.5 mm


8
0.5 mm